DEVELOPMENT OF THERMAL INSULATING AND LIGHT WEIGHT ROOFING MATERIALS USING FLY ASH-CEMENT COMPOSITES

G.L Madhushani Ariyadasa

Degree of Master of Science

Department of Materials Science and Engineering

University of Moratuwa

Sri Lanka

July 2019

DEVELOPMENT OF THERMAL INSULATING AND LIGHT WEIGHT ROOFING MATERIALS USING FLY ASH-CEMENT COMPOSITES

G.L Madhushani Ariyadasa

Thesis submitted in partial fulfillment of the requirements for the

degree Master of Science in Materials Science & Engineering

Department of Materials Science and Engineering

University of Moratuwa

Sri Lanka

July 2019

DECLARATION

I declare that this is my own work and this thesis does not incorporate without acknowledgement any material previously submitted for a Degree or Diploma in any other University or institute of higher learning and to the best of my knowledge and belief it does not contain any material previously published or written by another person except where the acknowledgement is made in the text.

Also, I hereby grant to University of Moratuwa the non-exclusive right to reproduce and distribute my thesis, in whole or in part in print, electronic or other medium. I retain the right to use this content in whole or part in future works (such as articles or books).

Signature: Date:

The above candidate has carried out research for the Master's thesis under my supervision.

Name of the supervisor:

Signature of the supervisor: Date:

Abstract

This thesis is focused on developing an alternative roofing material for asbestos fibre cement sheets. Coal Fly ash (CFA) was selcted as the main matrix modifier, which was collected from the electrostatic precipitator in Lakvijaya power plant, Norochcholai, Sri Lanka. The study is aimed at extracting low-density particles from CFA, called "cenospheres". Dry sieving and sink-float methods were adopted to take low-density fractions. Four types of CFA fractions were used in the study which were the unprocessed CFA, the CFA below 75 μm particle size, the CFA below 45μm particle size and the CFA particles extracted from wet separation method. CFA fractions were characterized with respect to morphology, particle size, particle density and chemical composition. The flexural strength and density variations were determined by casting mortar prisms, replacing 10-50% (by weight) of CFA from Ordinary Portland cement (OPC). Glass fibre reinforced fly ash cement (GFFC) roofing tiles were fabricated using size fractionated coal fly ash (CFA) which are the unprocessed CFA, the CFA particle sizes below 75μm and below 45μm. OPC was replaced by 30% (by weight) of each CFA fractions and those matrices were reinforced by Alkali Resistant glass fibres as 1% and 2% by weight. Physical, mechanical, durability and thermal properties were determined and those properties and the costs were compared with Calicut clay tiles, asbestos fibre cement corrugated sheet and non-asbestos fibre cement corrugated sheets. The spherical particle concentration increased with decreasing CFA particle size indicating those spherical particles in the finer fraction could be cenospheres due the relatively bigger spherical particle diameter and the low ratio of Si/Al compared to the unprocessed CFA. Sink-float method yielded the lowest density particles and it could be due to the presence of cenospheres and unburned carbon. The transverse strength was reduced with the decreasing CFA particle size .This could be due to the presence of cenospheres, low Ca content or less amorphous silica amount. All the compositions GFFC roofing tiles complied with the transverse strength requirements (230 N) as specified in the standard SLS 1189 Part 2. Highest value was observed in tile including 2% AR fibres with the unprocessed CFA (1650 N) and the lowest from tile incorporated with the CFA below 45μm (1470 N). The characteristic transverse strengths of GFFC roofing tiles is in comparable with Calicut clay tiles (1000-2000N) in Sri Lanka. The water absorption of GFFC roofing tiles did not comply with the requirement (maximum 10%) whereas the observed maximum value was 20%. Nevertheless, asbestos and non-asbestos roofing sheets have much higher values, which are 23% and 29%, respectively. The dry density of GFFC roofing tiles (1.63-1.68 g/cm^3) is comparable with the dry density of asbestos sheet, which is ≈1.65 g/cm^3. The long term durability of the GFCC roofing tile is in satisfactory level, it could due to the inclusion of CFA and AR glass fibres. GFFC roofing tiles can be considered as a good thermal insulator due to the high specific heat (1296 J/kg.K), low thermal (0.278 W/m.K) conductivity and diffusivity (1.31×10^{-7}m^2/s) compared with the asbestos, non-asbestos roofing sheets and Calicut clay tiles. However, Calicut clay tiles also offer good thermal comfort to dwellings, even though the thermal insulation is not depicted by k.c and α. This is because clay tiles have this natural system to gradually lower the air temperature through the process of evaporation. Hence, GFFC roofing tiles is a promising substitute for asbestos fibre cement roofing sheets using CFA in both unprocessed and sieved form due to the comparable strength, density, water absorption and durability. The cost for GFFC can be reduced by lowering the fibre content and replacing cement by ultrafine crushed rock particles.

Key words: coal fly ash, roofing tiles, thermal insulating, cement composites, glass fibres

ACKNOWLEDGMENTS

TABLE OF CONTENT

LIST OF FIGURES

LIST OF TABLES

LIST OF ABBREVIATIONS

PVC	: Polyvinyl chloride
CFA	: Coal fly ash
C-S-H	: Calcium Silcate Hydrates
PVA	: Polyvinyl alcohol
MCR	: Micro concrete roofing
NERD	: National Engineering Research and Development
XRF	: X-ray fluorescence
ICP-AES	: Inductively coupled plasma atomic emission spectroscopy
LOI	: Loss on ignition
XRD	: X-Ray diffraction
SEM	: Scanning electron microscopy
IFA	: Improved fly ash
ND	: Not detected
B	: Bituminous
SB	: Sub-bituminous
L	: Lignite
BDL	: Below detection level
BET	: Brunauer–Emmett–Teller
FACC	: Fly ash cenosphere containing cement composites
LWA	: Lightweight aggregate
SCM	: Supplementary cementitious materials
ULCC	: Ultra-lightweight cement composites
LWC	: Lightweight concrete
PE	: Polyethylene
AR	: Alkali resistant
OPC	: Ordinary Portland cement
ICP-MS	: Inductively coupled plasma mass spectrometry
FRC	: Fibre reinforced composites
SRI	: Solar refractive index
HVAC	: Heating, ventilation and air conditioning
EPA	: Environment protection authority

1 INTRODUCTION

1.1 Background

Roof is one of the vital parts in the house construction which shelters the dwellers from various climatic adversities. Apart from that, the roof gives an aesthetic value to the entire house. Roughly in a typical Sri Lankan residential house, the roof accounts 10-15% of the total cost depending on the roof structure and other variables.

Currently there are number roofing materials are being used by the Sri Lankans, which are asbestos fibre cement corrugated sheets, Calicut clay tiles, Galvanized Iron (GI) sheets, Zincalum, concrete slabs, pressed cement tiles, Polyvinyl chloride (PVC) roofing sheets, etc., Among them asbestos fibre cement corrugated sheets is the most popular roofing materials due its good strength, high roof covering per square feet, lightweight and cheaper prices. In 2015, the industry had a market share between 50-60 %.

The use of clay tiles is still drawing the highest interest among the people due to the aesthetic characteristic and good thermal comfort it provides. However, people are reluctant to use clay tiles nowadays because of easy breakage of tiles due to the loitering of monkeys or other impacts acting on the roof, having less roof covering per square meter and being denser than asbestos fibre cement sheets which necessitates to have more purlins with a good roof frame which ultimately escalates the cost associated with the roof structure. The market share of clay roofing tile industry began to shrink once the asbestos fibre cement sheets industry took over the market. In, 2015, the clay tile industry had a market share between 10-15% and was functioning approximately 200-300 clay roofing factories in Sri Lanka. The industry is faced by some challenges with respect to certain environment regulations regarding excavating clays and having high rejection rate at the production yard in the green stage of clay tiles.

There is a high tendency for concrete roof slabs because it saves space in confined areas. The use of pressed cement tiles is still not popular in Sri Lanka which could be due to the high cost and high weight associated with them. The use of PVC roofing

sheets also not popular in the country because of the tendency to undergo thermal fatigue due to heating and cooling. The distribution of roof covering materials in Sri Lanka in the year 2012 is shown in Figure *1.1*. [1]
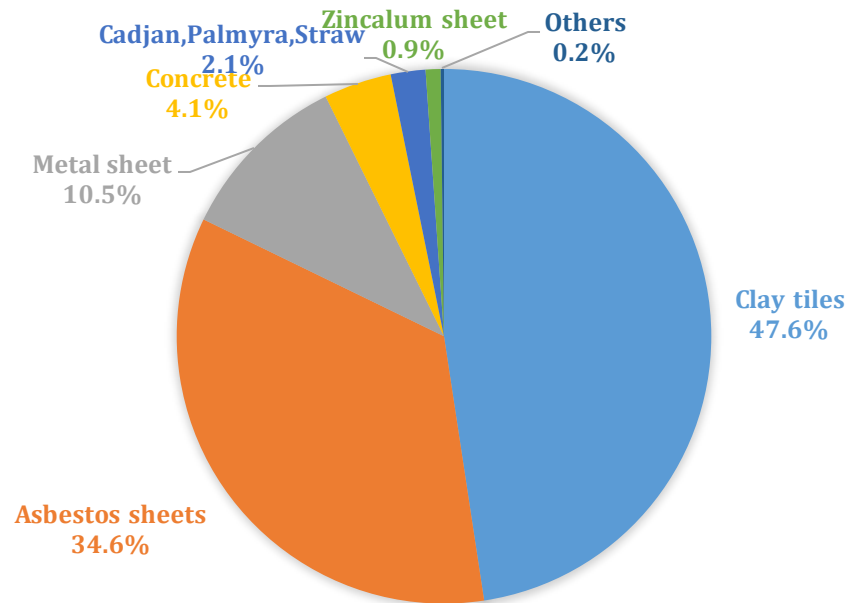
Figure 1.1: Roof covering distribution in Sri Lanka in the year 2012

The government of Sri Lanka in 2016 claimed that the importation and production of asbestos roofing sheets would be banned by 2018 [2]. The debate was that asbestos fibres get fibrillated from asbestos sheets during its service life and come into the airborne particles which would get inhaled by the dwellers causing health hazards. Even though, the decision was frozen, that momentum surged to take R & D initiatives to develop asbestos free roofing tiles/sheets.

This research is one such effort in developing an asbestos free roofing tile having comparable properties with asbestos fibre cement corrugated sheets. The properties which are mainly focused here are strength, density and thermal. The main matrix modifier used in the study is coal fly ash (CFA).

Lakvijaya thermal power plant, Norochcholai, (See *Figure 1.2*) which is the only thermal power plant in Sri Lanka produces 75 tons/day of bottom ash and 750 tons/day of CFA in the process of generating 300MW from. Presently, majority of CFA is taken by cement manufactures. But there is still a huge amount of CFA is dumped in the

open yard (See *Figure 1.3*) without any use leading to ground water pollution and other imbalances in ecological cycles due to its heavy metal constituents and low density particles.

Coal fly ash is a well-known pozzolan, a siliceous or silico-aluminous material that will, in finely divided form and in the presence of moisture, chemically react with calcium hydroxide at ordinary temperatures to form compounds having cementitious properties. The pozzolanic reaction between the calcium hydroxide and the amorphous silica in CFA, producing C-S-H, reduces the alkalinity and responsible of increasing the strength thereby improving the durability of the cement composite.

Cenospheres is one of the valuable components contained in CFA. Cenospheres are spherical particles with a hollow centre. The incorporation of cenospheres can be used to reduce the density. Specific gravity of cenospheres 0.2-0.9 whereas specific gravity of CFA is 2-4. The shells of cenospheres are made primarily of aluminosilicate phases that are thermally stable. The incorporation of cenospheres reduces the thermal conductivity. In solid as all atoms are bonded hence they cannot vibrate independently. When they vibrate they form waves and all the atoms vibrate in well-coordinated way. Due to such coordinated movement heat transfer is fast and efficient. In gas the atoms are not bonded. Hence when they are heated they gain energy and move randomly in the system. Hence transfer of energy from one atom to another atom is not efficient. Thereby, the heat transfer across a cenosphere compoent is poor due the solid shell and gaseous void.

This work seeks ways to take out this cenospheres component from CFA and incorporate that into the cementitious matrix to obtain lightweight and thermal insulation attributes. Development of fibres by our own as a reinforcement to resist in the alkali environment had not been studied here. Thereby, a fibre was purchased from the local market which is proven to be alkali resistant.

Finally, this work is aimed on utilizing CFA by fractionating low density particles (cenospheres) and partially replacing them by cement to develop glass fibre reinforced fly ash-cement roofing tiles which render lightweight, good thermal insulation along with acceptable mechanical properties complying with industry standards.

Figure 1.2: Lakvijaya thermal power plant located in Norochcholei, Sri Lanka (Source: web)

Figure 1.3: Coal fly ash is being dumped in the open yard at Lakvijaya power plant

1.2 Aim of research

The aim of this research is to fractionate low density particles (cenospheres) out from coal fly ash and incorporating them in a cementitous matrix to obtain lightweight and thermal insulation properties, which is reinforced by alkali resistant glass fibres to

fabricate a roofing tile with satisfied strength and durability complying with industry standards.

1.3 Objectives

1. To develop a cementitious matrix to obtain lightweight and thermal insulation for roofing applications.
2. To select a locally available fibre reinforcement which is compatible with the cementitious matrix which also delivers durability.
3. To develop a fibre reinforced cement based roofing tile which delivers good strength, lightweight, thermal insulation and good long-term durability.

1.4 Scope of the thesis

The thesis begins in Chapter 2 which provides a comprehensive literature review of the topics that concern the characterization of coal fly ash, coal fly ash added cementitious composites, the effects of coal fly ash morphology on cement based composites, properties of cenospheres and their effects on cement based composites.

Chapter 3 consists of characterization of size and density classified coal fly ash, the casting procedure of glass fibre reinforced fly ash-cement roofing tiles and the investigation of physical, mechanical and thermal properties of them.

Chapter 4 analyses the results and discusses the morphological properties of coal fly ash factions and their effects on the physical and thermal properties of glass fibre reinforced fly ash-cement roofing tiles. Further, cost calculation, and a mathematical model is developed between the fibre volume and the flexural strength of glass fibre reinforced fly ash-cement roofing tiles. Finally, the properties of glass fibre reinforced fly ash-cement roofing tiles compared with other available roofing materials in Sri Lanka.

Finally, Chapter 5 summarizes the data and comments on the suitability of the glass fibre reinforced cement-fly ash roofing materials and further developments required.

1.5   Chapter summary

Asbestos fibre cement corrugated sheet is the most popular roofing materials in Sri Lanka due to its good strength, high roof covering per square feet and cheapness. Calicut clay roofing tiles is the second most popular roofing material among house builders due to the aesthetic characteristic and good thermal comfort it provides. But to have a good roof structure with more perlins escalating the cost of the roofing is one of the reasons to decline the usage of Calicut clay tiles. This research is focused on developing a roofing materials having comparable properties with asbestos fibre cement corrugated sheets as an effort to introduce asbestos free roofing material after being claimed by the Sri Lankan government that the importation and production of asbestos roofing materials would be banned from 2018. The main properties looked in the study are strength, density and thermal. Coal fly ash was decided to use as the main matrix modifier due to its pozzolanic behavior which is having the capability of reducing the alkalinity of the pore solution and increasing the strength of the composite in the long run. Coal fly ash generated from Norochcholei power plant was used in the study because this waste was not satisfactorily utilized in the country leading to have huge piles of coal fly ash in the power plant's vicinity. The study seeks ways to fractionate one of the most valuable components of coal fly ash, which is called "cenospheres". Since they are hollow and spherical it has the ability to reduce the density and the thermal conductivity of the composite. The study is rather focused on developing the matrix than the fibre reinforcement. Hence, a fibre was chosen from the market which had proven to be alkali resistant. The final objective of the study is to develop a fibre reinforced cement based roofing tile which delivers good strength, lightweight, thermal insulation and good long-term durability complying with industrial standards.

2 LITERATURE SURVEY

2.1 Asbestos and non-asbestos fibre cement corrugated roofing sheets

In asbestos fibre cement corrugated sheets, Chrysotile ($Mg_3(Si_2O_5)(OH)_4$) fibre is used as the reinforcement. The matrix is comprised of cement and cellulose fibre pulp. Chrysotile is a mineral fibre which has a diameter in between 1-3μm with a length of 5-20μm. About 8-10% of Chrysotile fibre is used in fabricating a corrugated sheet which has a flexural strength of 5 kN/m. Normally, the asbestos fibre cement corrugated sheets is said to be durable for 50 years.

In commercially producing non-asbestos fibre cement corrugated sheets, Polyvinyl alcohol (PVA) is used as the reinforcement. PVA is an organic fibre ($(C_2H_4O)_n$) which has a diameter about 14μm and a length of 4-6mm. The matrix is contained of cement, bentonite, cellulose fibre pulp, microsilica (50%) and other materials such as fly ash. These corrugated sheets normally have a strength of 3.5 kN/m and said to be durable for 10-15 years [3]. One major problem associated with non-asbestos fibre cement sheets is high moisture movement, further, the ingredients need to be mixed perfectly in order to get desired properties whereas in asbestos fibre cement sheets, the mix can be varied up to a certain level with same properties intact. High shrinkage associate with non-asbestos fibre cement sheets can be avoided by adding calcium carbonate.

2.2 Micro concrete roofing (MCR) tiles/sheets R & D in Sri Lanka

In 2006, C Jayasinghe et al [4] investigated the MCR manufacturing process. Although the tile had been introduced to Sri Lanka by formulating SLS 1189 "Specification for concrete roofing semi-sheets, tiles and fittings" [5] [6] in 1999, it had not become popular among the house builders. Therefore, these researches carried out a comprehensive study on strength and durability aspects. The mix consisted of cement: sand: chips (4-6mm) in the ratios of 1:1:1.5. The cast roofing tile had a dimension of 600×600 mm with a thickness of 8 mm (See Figure *2.1*). The average braking load was 450 kg and the average water absorption was 8.63%. A roof angle beyond 22° was recommended to resist heavy rains. The strength and durability of MCR tiles were proven to be well above the specified limits in SLS 1189: Part 1 [5]. The cost and weight of MCR tiles were comparable with Calicut clay tiles. The cost of covering

material/m^2 for MCR tiles and Calicut clay tiles were respectively 320 LKR and 316 LKR, and the weight of covering material/m^2 were 45.60 kg and 40.50 kg respectively.
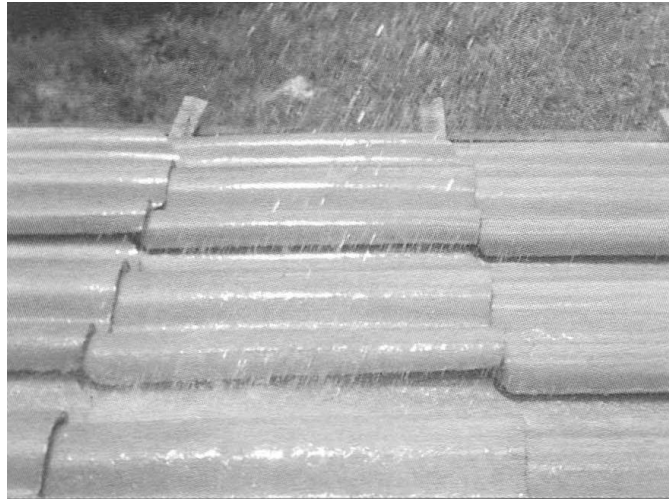
Figure 2.1: MCR tiles undergoing water spray test,
C. Jayasinghe et al [4]

J.A.C Chrishanthi et al [7] investigated manufacturing of MCR sheets and tiles at National Engineering Research and Development (NERD) Centre in 2010 as per SLS 1189: Part 1 [5]. They used a mix of cement and fine aggregate, fine aggregate as sand or quarry dust. Polypropylene (PP) net was sandwiched in between the cementitous mix. The sheet had a dimension of 910 × 670 mm (See Figure *2.2*) whereas for tiles it was 485 × 255 mm. The thickness was 8 mm. The sand and quarry dust incorporated sheets had flexural strengths of 1320 N and 1730 N, respectively. The recommended roof pitch was 20° and the estimated cost of tile was 47.00 Rs per Sq.ft. The cast MCR tiles and sheets complied the requirement stated in SLS 1189: Part 1 [5].

The main advantages of MCR tiles/sheets are they asbestos free, lighter than burnt clay tiles, good fire resistance, can be coloured and provide good water drainage. The main disadvantages are greater care need in transportation, susceptible for impact loads, greater supervision is needed at all stages of production and delivery. Further, there is tendency to crack on top of the corrugation in the green stage.

8

Figure 2.2: Manufacturing of MCR sheets at NERD
Centre, Sri Lanka, *J.A.C Chrishanthi et al [7]*

2.3   Coal fly ash added roofing tiles/sheets

Several researches were found on using CFA for the development of cement based
roofing materials.

Amitabh Tayal [8] obtained a patent in 2007 for a process for the manufacture of
asbestos fibre cement products comprising of fly ash, fibre, water and cement.
According to this invention he provided a composition for use for the manufacture of
asbestos fibre cement products comprising 8-11% by weight of asbestos fibre, 40-50%
by weight of cement, 25-35% by weight of fly ash and 0.1-0.2% by weight of an
additive or binder with or without 0-5% by weight of wood/paper pulp mixed with
each other in the form of a homogenous slurry. This invention is to overcome the
difficulties associated with the prior art which were inhomogeneous slurry formation
due to the mixing of fly ash with cement and the variation in the raw material
distribution in the sheet which affects process running and quality of the sheet. The
invention is a novel wet process and a novel composition for the manufacture of
asbestos fiber cement products and which obviates the disadvantages associated with
the prior art.

In 2006, Jagadesh Sunku [9] fabricated white Chrysotile asbestos fibre cement sheets
from Hatschek machine by replacing cement with low calcium fly ash. The fly ash

content varied from 10 – 40 % and cast sheets were tested after 10 days. Test result showed that the load bearing capacity of the sheets decreased with increasing fly ash content. At fly ash contents of 10% and 20%, the strengths of sheet decreased by 5-10% and 10-20% respectively but complied with the minimum requirement of 5000 N/m according to the Indian Standard IS 459:1992 [10], when tested as per the IS 5913: 1989 [11]. The strength of sheets cast with fly ash contents of 30 % and 40 % were below the minimum requirement.

Effect of utilisation of fly ash in micro concrete roofing (MCR) tiles was investigated by Sarthak Kuila [12], in which cement was replaced by fly ash. Both fly and pond ash were obtained from Parichha Thermal Power Plant, Jhansi, Uttar Pradesh and dry fly ash was obtained from Dadri Thermal Power Plant, Dadri, Uttar Pradesh. At the fly ash content of 4%, the strength of tiles increased by more than 25% compared with the standard composition followed during the study. Even with 16% of fly ash content, the tiles gave an improved breaking load. The tiles incorporated with the pond ash also delivered a similar effect on the tile properties. The study concluded that the strength development of the composites is similar in all the types of ash being used so that physical properties of the fly ashes being used had not affected upon them. A considerable variation of water absorption properties were not observed at lower fly ash contents. However, with increased addition of finer ash, the water absorption property of MCR tiles increased because the fine ash decreases the open pores by filling the interstitial spaces between the coarser aggregate and sand, delivering a more dense packing and lower water absorption.

G. Ramakrishna et al [13] studied on fly ash- based sisal fibre roofing sheets of the size of 250 x 500 x 6 mm. Those were cast manually as shown in *Figure 2.3* and the splitting strength due to direct and impact loads, were experimentally evaluated and compared with commercially available corrugated sheets. Cement: Sand ratio was 1:3 and cement was replaced by fly ash in three replacement levels (10%, 20% and 30% by weight). Six Sisal fibres (length of 20-30 mm) contents in the range of 0.25%- 2% by weight were considered. At the fly ash content of 20% and fibre content of 1.0%, the flexural and splitting loads of the composite delivered similar results with that of

the commercially available roofing sheet. The same mix also showed better performance in terms of energy absorption.

In 2015, Pardon K. Kuipa et al [14] investigated use of CFA in concrete roof tiles as shown in *Figure 2.4*. Results showed the possibility of substituting 20% of cement by CFA. This increased the overall tile strength by an average of 6.5% and reduced the process water demand by 7.5%. The water absorption of concrete tiles decreased with increasing CFA addition due to the packing effect of finer CFA particles and sealing of pores by pozzolanic reaction products. Further, the inclusion of CFA reduced the tile's efflorescence and bleeding as an improvement of the tile quality. Class F type of pulverized fly ash was used in the experiments.

(a) Spreading the Mortar (b) Dragging the Spread Mortar Over Corrugated Mould

(c) Creating and Finishing the Corrugations (d) Cast Corrugated Sheet in Wet State

(e) Finished Product with Base Frame
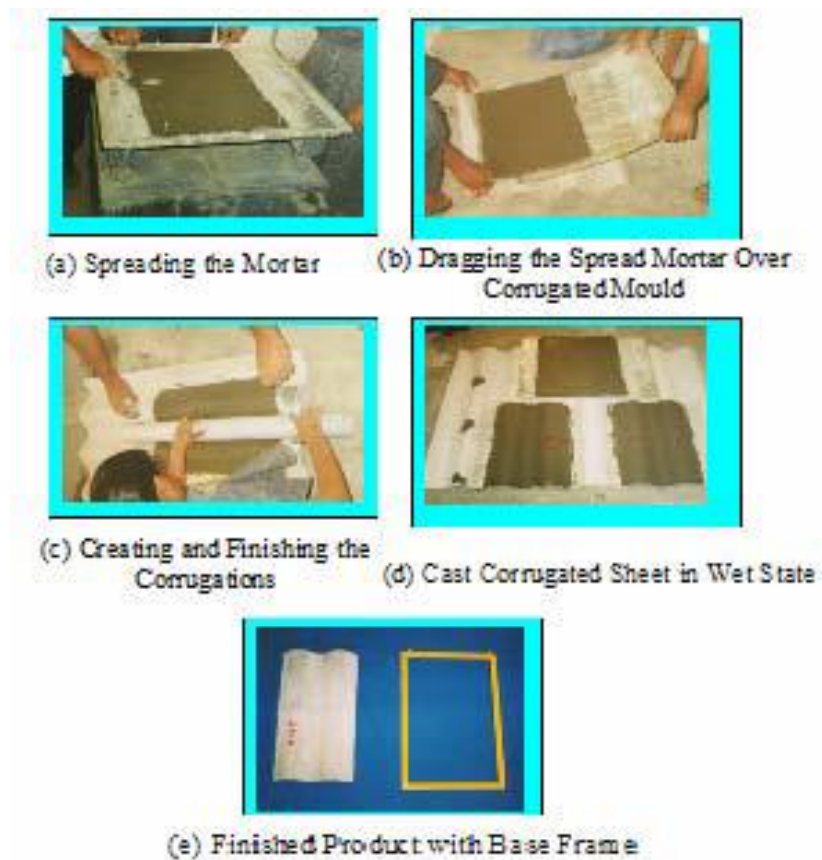
Figure 2.3: Fly ash-based sisal fibre roofing sheet. *G Ramakrishna et al [13]*

Figure 2.4: Concrete roof tile, *Pardon K Kuipa et al [14]*

2.4 Coal fly ash

Coal fly ash (CFA) is a byproduct generated during the combustion of pulverized coal in coal fired power stations. CFA is a fine particle produced at 1200-1700°C from the combustion of various inorganic and organic constituents (e.g., hydrocarbons and oxygen) of the feed coal. The noncombustible minerals related with the coal melt form small liquid droplets. The lighter droplets are carried away from the burning zone with the flue gases. They cool rapidly at the surface forming glassy spheres. In larger droplets, the inside cools more slowly which allows to form of some crystalline phases. These particles are called fly ash which can collect from the flue gases using mechanical and electrical precipitators or bag houses [15].

CFAs are considered as a complex anthropogenic materials due to the presence of the various components. It says that approximately 316 individual minerals and 188 mineral groups have been identified in different CFAs [16].

Though the utilization of CFA goes back to decades, CFA is still sent to land fill or stored in lagoons. It is expected that in 2012, 750 million tons of CFA are generated globally and of this only 20-50 % is utilised in applications other than land reclamation and restoration projects [16].

CFA is generally an impure silicate, containing varying amounts of alumina, iron oxides, alkaline earth and alkali oxides, but it also may contain smaller quantities of

many other elements including heavy and radioactive metals. Due to the presence of toxic heavy metals, disposal of CFA as landfill arises environmental concern due to the possibility of leaching. Besides the risks of air, soil, surface and ground water pollution as a result of CFA disposal, the fact that some of the harmful ingredients are usually highly enriched in respirable size (diameter < 10 μm) particles involves an additional health risks [17].

But CFA is regarded as an extremely attractive material due to the low price as well as being applicable for various purposes due to the complexities of their chemical, physical and mechanical properties. Hence, a significant amount of researches have been conducted in worldwide converting this waste material to economically viable products in order to lessen the environment impact.

The geotechnical properties of CFA (such as specific gravity, permeability, internal angular friction, and consolidation characteristics) make it suitable for use in construction of roads and embankments, structural fill etc. The pozzolanic properties of the ash makes it useful for the manufacture of cement, concrete and other building materials (bricks, blocks etc.). Having high percentages of certain oxide compounds in CFA, such as silica (60–65%), alumina (25–30%), magnetite, Fe_2O_3 (6–15%) [18] enables its use for the synthesis of zeolite, alum, and precipitated silica. The other important physicochemical characteristics of CFA, such as particle size , bulk density, porosity, water holding capacity, and surface area makes it suitable for use as an adsorbent.

Typically, all CFAs produced worldwide have similar qualitative composition but their chemical and physical properties vary widely, depending on the kind of the coal fired, boiler type, burning regime, and collector system setup.

Because of that an individual investigation of CFA from different power plants is crucial. Only a detailed study of the physical, chemical and morphological properties of particular fly ash would deliver an understanding of a potential environmental and health impacts associated with its disposal, and could help to estimate its significance as a material resource for different industrial applications.

2.4.1   Characterisation of coal fly ash

2.4.1.1   Chemistry

The properties of the parent coal and the techniques used for handling and storage affects the chemical properties of CFA largely. There are basically four types, or ranks, of coal, each vary in heating value, chemical composition, ash content, and geological origin. The four types (ranks) of coal are anthracite, bituminous, sub-bituminous and lignite. The handling technique could be dry or wet form. In addition, CFA is sometimes classified according to the type of coal from which the ash was derived. For the determination of major oxides commonly used techniques are X-ray fluorescence (XRF) and inductively coupled plasma atomic emission spectrometry (ICP-AES). ICP-AES and inductively coupled plasma mass spectrometry are used determine trace elements. To detect certain trace elements like mercury and selenium, it requires special atomic absorption spectrometric techniques. The principle components of CFA are silica, alumina, ferrous oxide and calcium oxide with varying amounts of carbon as measured by the Loss on Ignition (LOI) test [18] [19] [20]. In general CFAs have a bulk chemical composition (See Table *2-1*) containing a variety of metal oxides in the order $SiO_2 > Al_2O_3 > Fe_2O_3 > CaO > MgO > K_2O > Na_2O > TiO_2$ [16] [18] [19] [20]. However, there are significant differences in CFA composition within the regions itself [18] [19] [20].Lignite and sub-bituminous coal fly ash are categorized by higher concentrations of CaO and MgO and reduced percentages of SiO_2 and Fe_2O_3 as well as lower carbon content as compared with bituminous CFA [18] [19] [20]. There are only small amounts of anthracite coal fly ash since a very little amount of anthracite coal is burned in power plants.

Table *2-2* depicts the typical range of the chemical constituents of bituminous, lignite and sub-bituminous CFAs. As per the table, it is clear that lignite and sub-bituminous CFAs have a higher calcium oxide content and lower loss of ignition than fly ash from bituminous coals [18] [19]. Lignite and sub-bituminous CFAs may have a higher concentration of sulphate compounds than bituminous coal fly ash. Having contained of CaO less than 10% in bituminous and lignite CFAs often consist mainly of aluminosilicate glass and usually do not contain any crystalline compounds of calcium.

CFAs that contain more than 15% total CaO are composed of calcium aluminosilicate glass in addition to substantial proportions of crystalline calcium compounds including C_3A, C_4A_3S, CS, and CaO [19]. The CFA's chemical composition is usually the indicator in assessing its suitability as a cement replacement material. The American Society for Testing and Materials (ASTM) divide CFA into two classes: C and F. As shown in Table 2-3, Class F CFA has a combined percentage of SiO_2, Al_2O_3, and Fe_2O_3 greater than 70% whereas for Class C it is greater than 50%. It is sometimes believed that class C CFA is derived from lignite and sub-bituminous coals and class F CFA is derived from bituminous and anthracite coals.

The mineralogical distinction of CFA is also important to certain applications. Class F ash is regarded as a pozzolanic material. A pozzolan is a siliceous or silico-aluminous material that will, in finely divided form and in the presence of moisture, chemically react with $Ca(OH)_2$ at ordinary temperatures to form compounds having cementitious properties [15]. Due to the presence of high CaO in many of the lignite and sub-bituminous CFAs, have the capability to form cementitious products in the absence of $Ca(OH)_2$, but, they are not true pozzolans.

Table 2-1: Bulk chemical composition of CFA by region, *R.S Blisset [16]*

Component	Range (mass %)				
	Europe	US	China	India	Australia
SiO_2	28.5-59.7	37.8-58.5	35.6-57.2	50.2-59.7	48.8-66.0
Al_2O_3	12.5-35.6	19.1-28.6	18.8-55.0	14.0-32.4	17.0-27.8
Fe_2O_3	2.6-21.2	6.8-25.5	2.3-19.3	2.7-14.4	1.1-13.9
CaO	0.5-28.9	1.4-22.4	1.1-7.0	0.6-2.6	2.9-5.3
MgO	0.6-3.8	0.7-4.8	0.7-4.8	0.1-2.1	0.3-2.0
Na_2O	0.1-1.9	0.3-1.8	0.6-1.3	0.5-1.2	0.2-1.3
K_2O	0.4-4	0.9-2.6	0.8-0.9	0.8-4.7	1.1-2.9
P_2O_5	0.1-1.7	0.1-0.3	1.1-1.5	0.1-0.6	0.2-3.9
TiO_2	0.5-2.6	1.1-1.6	0.2-0.7	1.0-2.7	1.3-3.7
MnO	0.03-0.2	nd	nd	0.5-1.4	nd
SO_3	0.1-12.7	0.1-2.1	1.0-2.9	nd	0.1-0.6
LOI	0.8-32.8	0.2-11.0	nd	0.5-5.0	nd

Table 2-2: Bulk chemical composition of CFA by coal type, *R.S Blisset [16]*

Component (wt %)	Bituminous	Sub-bituminous	Lignite
SiO_2	20-60	40-60	15-45
Al_2O_3	5-35	20-30	10-25
Fe_2O_3	10-40	4-10	4-15
CaO	1-12	5-30	15-40
MgO	0-5	1-6	3-10
Na_2O	0-4	0-2	0-6
K_2O	0-3	0-4	0-4
SO_3	0-4	0-2	0-10
LOI	0-15	0-3	0-5

Table 2-3: Classification system of the US and European standards bodies for fly ash use in concrete, *R.S Blisset [16]*

ASTM C618 [21]				
Class	$SiO_2 + Al_2O_3 + Fe_2O_3$	SO_3	Moisture	LOI
C	> 50%	< 5 %	< 3 %	< 6 %
F	> 70%			< 12%
EN 450-1				
Class	$SiO_2 + Al_2O_3 + Fe_2O_3$	SO_3	Reactive Silica	LOI
A	> 70%	< 3%	> 25%	<5%
B				2-7%
C				4-9%

It is considered that CFA classification systems use for the cement replacement formulated by ASTM and the European standards are narrow, rather than based on performance. So they can be divisive because in practice since many class C ashes can meet the performance requirements of class F ashes.

CFAs comprise of many elements at concentrations of greater than 50 mg/kg. Some of these are environmentally hazardous. *Table 2-4* shows the concentrations of trace elements in 23 European CFAs. They are in wide agreement with the elemental composition of Australian CFAs analysed by Jankowski et al. It is clear that elements such as As, Cr, Pb, and Se are present in significant quantity. The leachability of the elements relates to the phase they are associated with and the pH that they are exposed to.

Table 2-4: Average trace element content in 23 European CFAs, *R.S Blisset [16]*

Element	Trace element composition (ppm)		
	25th Perc.	Median	75th Perce.
As	40	55	97
B	135	259	323
Ba	639	1302	1999
Be	6	8	12
Cd	1	2	2
Co	30	35	48
Cr	137	148	172
Cu	73	86	118
Ge	3	7	15
Hg	0.2	0.2	0.3
Li	150	185	252
Mo	7	11	13
Ni	87	96	144
Pb	59	80	109
Rb	50	108	147
Sb	4	4	8
Se	6	7	13
Sn	7	8	10
Sr	384	757	1647
Th	25	30	37
U	9	12	18
V	202	228	278
Zn	123	154	175

2.4.1.2 *Mineralogy*

Mineralogical composition is influenced by the type and source of fly ash. The X-ray diffraction (XRD) and infrared spectroscopy techniques are used to determine the crystalline phase in fly ashes.

In most CFAs, the phase and mineral composition includes the following: an inorganic constituent contained of amorphous and crystalline mineral matter; an organic constituent comprised of char materials; and a fluid constituent composed of liquid, gas, and gas–liquid inclusions. CFA encompasses of glass, mullite, quartz, char, hematite-magnetite, anhydrite-gypsum, feldspars, lime-portlandite, clay and mica minerals, cristobalite-tridymite, calcite-ankerite, corundum, jarosite, and some Ca and CaMg silicates, in the order of decreasing amounts.

The major phases of CFAs are mullite, quartz, and hematite. The mineralogy classification system divided four phase-mineral fly ash types which are Pozzolanic

(P), Inert (I), Active (A), and Mixed (M) which is based on the distinct behavior of (1) glass; (2) quartz+ mullite; and (3) the sum of any other mineral bearing phases such as Fe-Ca-Mg-K-Na-Ti-Mn oxyhydroxides, sulphates, carbonates, and silicates [16]. It is believed that, this CFA classification method would help to simplify the choice of application for each identical CFA composition. A quantitative determination of the major crystalline phases contained in the fly ashes was carried out by V.M Malhotra [20] et al using XRD technique. The results are shown in *Table 2-5*. X-ray diffraction patterns for a low and high-calcium fly ash are shown in implying the distinct difference of the mineralogy of the two ashes [15]. The presence of noncrystalline material (glass) is indicated by the broad hump in the diffraction pattern Figure *2.5* and its position replicates the composition of the glass. The data depicts that low- and high-calcium fly ashes have different chemical compositions and that the crystalline and glassy phases are also quite different. Low-calcium fly ash comprises mainly of aluminosilicate glass and crystalline quartz, mullite, hematite and magnetite. On the other hand, a number of reactive (hydraulic) crystalline phases present in high-calcium fly ash.

Table 2-5: Mineralogical composition of some selected fly ashes, *V.M Malhotra et al [20]*

Fly ash source	Type of coal[a]	Phase composition (%)					
		Glass	Quartz	Mullite	Magnetite	Hematite	LOI%
1	B	72.1	4.0	12.6	6.2	1.6	3.5
4	B	70.1	3.2	3.3	17.2	4.7	1.5
5	B	55.6	6.2	19.8	5.6	3.1	9.7
6	B	54.2	8.3	23.5	4.4	2.1	7.5
7	SB	90.2	2.9	6.1	-	-	0.8
8	SB	83.9	4.1	10.2	-	1.4	0.4
9	SB	79.8	8.7	11.5	-	-	0.8
10	L	94.5	4.6	-	-	-	0.9

[a] B: Bituminous; SB: Subbituminous; L:Lignite

The XRD pattern obtained by Annie S. Shoumkova et al [17], the fly ash observed has quite high amorphous halo, beside the main phase; quartz, the presence of small amounts of hematite, magnetite, gypsum, pyrite, ferrites and alumosilicates (mullite and silimanite) could be recognized in the sample (*Figure 2.6*), but the overlapping of

their characteristic picks complicates their identification. As the X-ray pattern gives low intensity magnetite lines, the researcher has not made an attempt to determine magnetite quantitatively from XRD data.
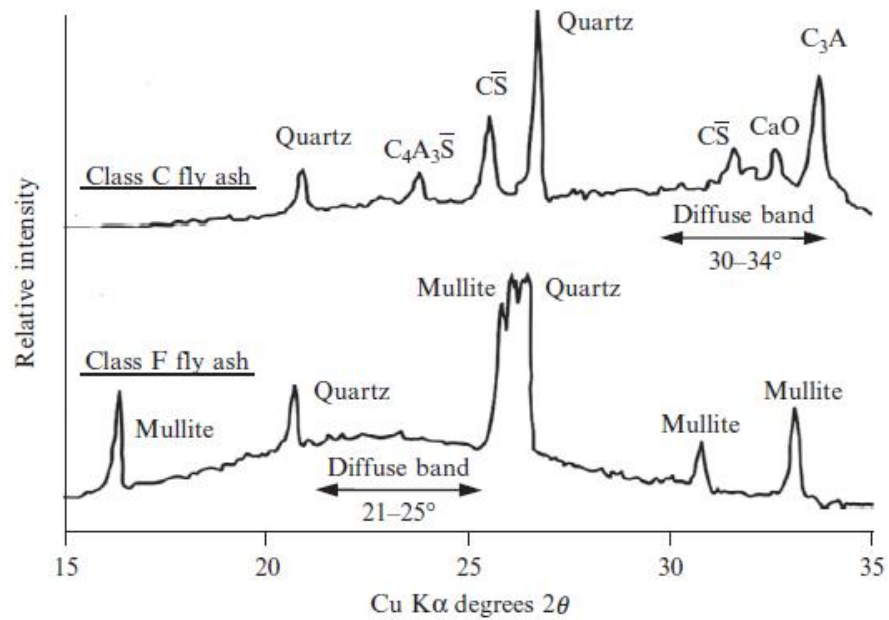
Figure 2.5: X-ray diffraction patterns for Class C and Class F Fly ash, *M Thomas et al [15]*
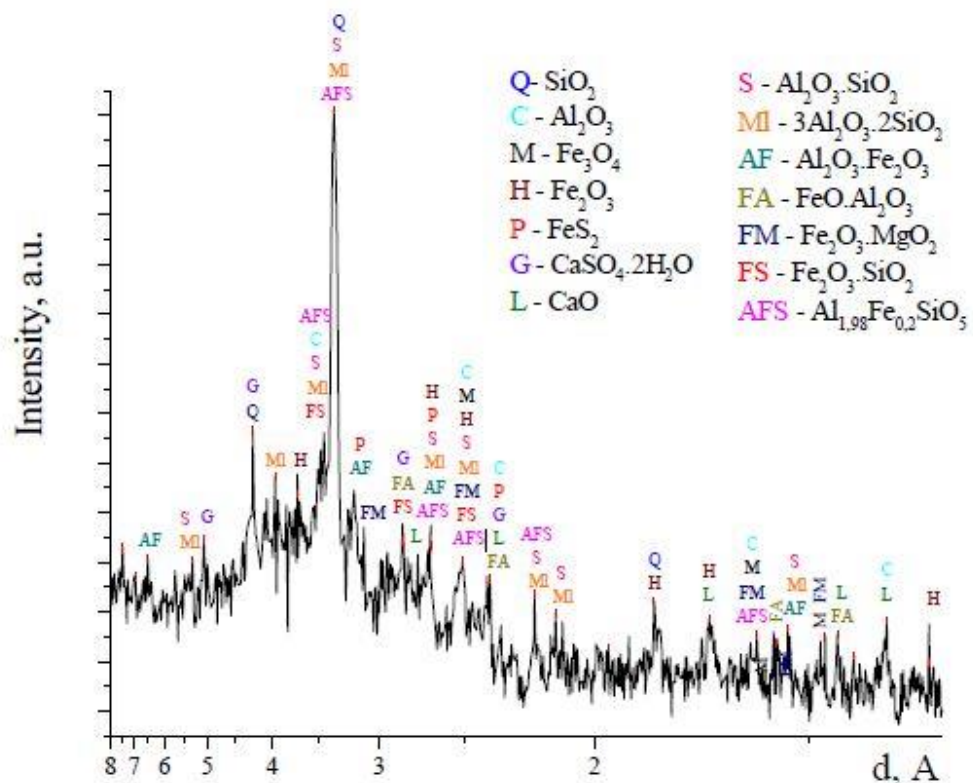
Figure 2.6: XRD pattern of the initial sample and the possible minerals, *Annie S. Shoumkova et al [17]*

2.4.1.3 Morphology

The combustion temperature and subsequent cooling rate control the morphology of CFA particles. It is revealed from the scanning electron microscopy (SEM) analysis that CFA comprises of solid spheres, hollow spheres (cenospheres) and irregular unburned carbon [16]. Mineral aggregates containing corundum, quartz and magnetite particles could also present.

Forming of fly ash particles is occurred in few steps. First the coal is converted into char. Then char is burnt out at much higher temperatures. The fine included minerals gradually reduce at the higher temperature and are released from within the char as it fragments. At this point the minerals decompose and convert to gases and eventually condense to form solid ash particles. Homogeneous condensation results in ash particles between 0.02 and 0.2 μm and fragmentation of included mineral matter results in the formation of particles between 0.2 and 10 μm. The excluded mineral matter undergoes a series of complex transformations to form predominantly spherical particles in the size range 10-90 μm.

R.S Blisset [16] examined five different fractions of CFA. They are cenospheres, enriched carbons, magnetic spheres, finely improved fly ash residue, coarsely improved fly ash residue.

Figure 2.7 displays the morphology of different CFA fractions. The lightweight fraction which is known as cenospheres; was originated from the two Greek words; ceno (meaning empty) and sphere. A large portion of the lightweight fraction is said to be formed by cenospheres. Since cenospheres are collected in a sink/float process, all particles less dense than water, despite being spherical or porous are collected and are considered to be ash cenosphere products. *Figure 2.7*a displays the typical appearance of a cenopshere.

Wet magnetic drum separator extracts the magnetic particles. The drum separator applies a medium intensity magnetic force over CFA slurry and lifts the magnetic fraction out. As shown in *Figure 2.7*c, the surface of the magnetic sphere is rougher

than that of the cenospheres. These magnetic spheres contain iron crystals set in a lattice of amorphous alumina and silica.

The morphology of the carbon enriched product is fully different with respect to the other ash fractions (*Figure 2.7*d). The carbon has a more irregular shape having a larger porous structure. But as opposite, the cenospheres, magnetic particles and fine ash are mainly spherical. An incomplete oxidation of the precursor coal is the reason for the formation of large porous carbon particles. The increase in porosity of the carbon, results to have a higher surface area relative to the inorganic matter contained in the CFA.

The two improved fly ash (IFA) residues are shown figures in *Figure 2.7*e and f. Basically, they are the remainders of the ash once the cenospheres, carbon, and magnetic fraction have been removed. Fractionating IFA through a hydrocyclone delivers two grades of product which are fine and coarse. The SEM images shows that the coarse IFA is more irregular in shape whereas the fine IFA is predominantly made up of spheres.

The Cenospheres is the most important value-added components of CFA. Due to its unique properties of sphericity and low density relative to water make them to be incorporated in a variety of different applications.
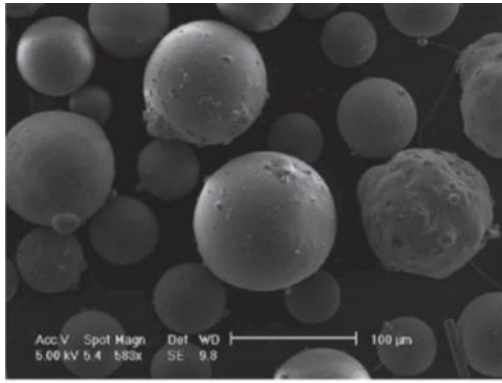
a.   Cenospheres
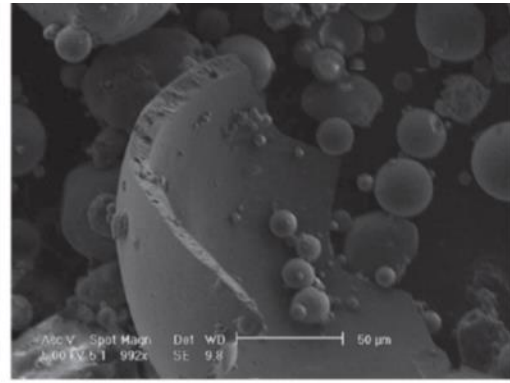
b.   Broken Cenospheres
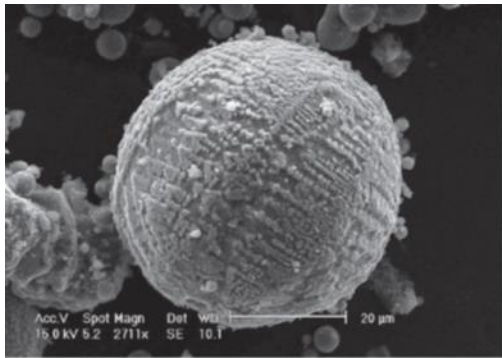
c. Magnetic sphere
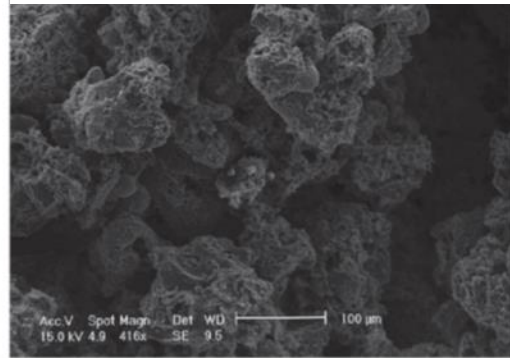
d. Carbon
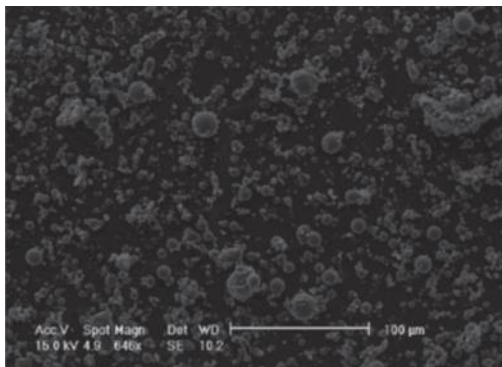
e. Fine improved fly ash residue
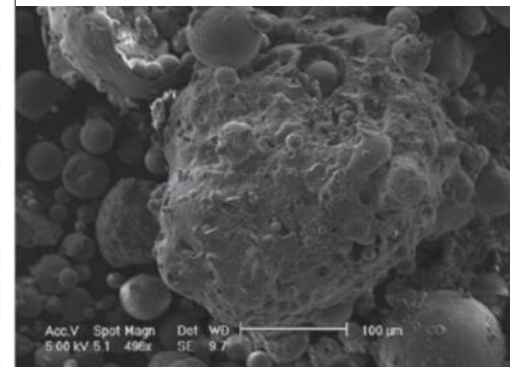
f. Coarse improved fly ash residue

Figure 2.7: SEM images of CFA fractions, *R.S Blisset [16]*

2.4.1.4 *Physical characteristics*

The most important physical properties of fly ash when using it as a cementitous material are particle size, fineness, specific surface area and specific gravity.

Particle size distribution

The particle size of spherical and rounded fly ashes varies from 1.0 to 150μm [15] [20] whereas the median particle size is in the range of 5 to 20 μm [18] [22]. Comparably,

22

the irregular and angular shapes particles are larger in size. The color of fly ash is dependent on the unburned carbon percentage hence the color would vary from tan to gray to black.

According to the experiment conducted by P.K Mehta [23] on the particle size distribution of several U.S fly ashes revealed that high-calcium fly ashes were finer than the low-calcium fly ashes. He found that it is due to the presence of larger amounts of alkali sulphates in high calcium fly ashes.

Sieve analysis is the simplest technique for the determination of particle size distribution and it could provide data on size distribution down to about 20–30 μm [24]. Nylon mesh sieves are better than metal meshes to sieve ashes to avoid possible contamination. The agglomeration of the particle can be reduced by gentle brushing. There are two types of sieving; which are wet sieving (with water) and dry sieving (with air). Since the wet sieving could possibly remove some of the trace elements from the ash, it affects to interpret the element partitioning with particle size for use in environmental studies. Air-based cyclone separators in a laboratory scale set up can be used provide data on size distribution down to 10–20 μm [24]. However, this separation technique is based on a combination of size and density (i.e., classification), and not on particle size alone. Thus, when the density of all the ash particles are the same, then the separation is inherently based on particle size. The air-based Bahco Aerodynamic classifier which is also constructed based on the classification principle can be used to obtain data for the particle sizes in the range of 4-100 μm [24].

The laser particle size analyzer is the popular instrument used for determination of the particle size distribution of fly ash. The instrument is based on the diffraction of laser light by ash particles suspended in a variety of fluids, including air, water, ethanol, and propanol. The diffraction intensity pattern is dependent on the particle size. A mathematical deconvolution of the diffraction pattern is then used to determine the particle size distribution, assuming that the shape of the particle is spherical. The refractive index of the ash which varies with the ash composition, shall also be taken into the consideration.

Fineness

The fineness of fly ash is an important characteristic as it correlates with the strength of concrete. Mostly particles above 45μm act as fine aggregates and the particles below

23

45μm contribute to the strength development in concrete. Wet and dry sieving methods and particle size distribution are used to characterize the fineness of fly ash.

Specific Surface area

The specific surface area of fly ash is the area of a unit of mass. Blaine specific surface-area technique is the most common method. It measures the resistance of compacted particles to an air flow. SLS 107: Part 2 "Specification for Ordinary Portland Cement Part2: Test Methods" [25] and ASTM C 204 "Standard Test Methods for Fineness of Hydraulic Cement by Air-Permeability Apparatus" [26] describe this method for the measurement of the surface area of Portland cement. The specific surface area of coal fly ash is generally in the range of 170-1000 m^2/kg [18] [20] [22].

Particle size analysis obtained by the laser particle size analyzer can also be used to determine the specific surface area of fly ash. The Brunaer-Emmett-Teller (BET) nitrogen adsorption technique is also a method for the determination of the specific surface of the particles, but the results obtained by this method are usually higher than the results obtained by Blaine's specific surface area technique or particle-size analysis.

Specific Gravity

The Le Chatelier flask is used to obtain the volume displacement of coal fly ash particles by which the specific gravity can be calculated. The true density of the particles can be determined using helium pycnometry. Many researchers used ASTM C 188 "Standard test method for density of hydraulic cement" [27] to find the specific gravity of fly ash. The specific gravity of fly ash usually ranges from 1.9 to 3.0 [15] [18] [20].

Comparisons of physical properties of fly ash from different sources are tabulated in *Table 2-6*.

Table 2-6: Comparison of physical properties of fly ash in different sources, *V.M Malhotra et al [20]*

Fly ash source	Type of coal[a]	Physical properties		
		Specific gravity (Le Chatelier method)	Fineness (% retained on 45µm test sieve by Dry sieving	Blaine specific surface area (m²/kg)
1	B	2.53	12.3	289
2	B	2.58	10.2	312
3	B	2.88	18.0	127
4	B	2.96	14.0	198
5	B	2.38	16.1	448
6	B	2.22	30.3	303
7	SB	1.90	26.4	215
8	SB	2.05	14.3	326
9	SB	2.11	33.0	240
10	L	2.38	18.8	286
11	L	2.53	2.5	581

2.5 Cenospheres

The word `cenosphere' originated from the two Greek words; which are kenos (hollow) and sphaira (sphere) [28] [29] [30]. Cenospheres are hollow, lightweight and inert spheres comprising of silica and alumina, are filled with air or gases [29].

When CFA is disposed in ponds or lagoons, these cenospheres particles float on water due to their hollow structure. Cenospheres and CFA have similar chemical composition though cenospheres tend to have a larger particle size [16] [31]. Normally, the cenospheres content in fly ash is about 1-2 wt. %. [29] [30] [32].

Superior properties of cenospheres include light weight, increased heat resistance, less water absorption, excellent mechanical strength, improved flow characteristics, good packing factor, reduced shrinkage, strength and good electrical properties [29] [30] [33] [34] [35] [36] [37].

The properties of the cenospheres incorporated composites depends largely on the physical properties of cenospheres such as diameter, particle size distribution, wall thickness, and shape [36] [37]. Cenospheres as a filler would increase the mechanical strength of the finished products if they are supposed to have thicker walls. The shape of ash cenospheres plays an important role as well. Basically, spherical particles have the lowest surface area to volume ratio, which necessitates to have less resin, binder,

and water to wet out the cenospheres' surface. Besides, spherical ash cenospheres reduce shrinkage, improve the workability and increase the ease of use as further advantages. Apart from the wall thickness and shape of cenospheres, the particle size distribution also affects the mechanical properties of the finished products.

The properties of cenospheres must be studied and understood in detail in order to recognize their effective areas of usage. This will enable to use cenospheres as a good replacement material of the expensive raw materials in the manufacturing industries.

Cenospheres can be used in wide range of applications in the construction industry. It can be incorporated as an additive to make light weight cements with reduced water release. Their spherical and hollow morphology, chemical characteristics, mechanical and energy-attenuating properties enable to be used with conventional cements to form lightweight workable cementing materials with a closed pore structure suitable for durable bridge decks, pavements, and highways. Furthermore, cenospheres can be used in applications wherein noise-proof barriers, in asphalt concrete matrices with adequate acoustic damping and as a freeze and thaw resistant. Apart from that, being light weight leads to ease in assembly minimizing the cost [30].

Cenospheres are not only limited to the incorporation of Portland cement based composites to produce lightweight cementitious products but also in geopolymers and magnesium oxychloride cements. In both the instances, cenospheres will lead to the reduction of density and thermal conductivity of the materials enabling for fire resistant construction applications [30].

2.5.1 Characterisation of cenospheres

2.5.1.1 Chemistry

The chemistry of cenospheres depends on the minerology of the parent coal and the combustion conditions leading to have varying chemistries from power plant to power.

Table 2-7 shows the typical oxide compositions of cenospheres which were indicated by different literatures. Accordingly, the main oxides present will decrease in the order of SiO_2, Al_2O_3 and Fe_2O_3.

N. Ranjbar et al [30] developed a ternary phase diagram (See *Figure 2.8*a) by taking the chemical analysis of 209 fly ashes and cenosphere specimens. The diagram is based

on the 'intersection' of their major oxides among these oxide groups: SiO_2 + Al_2O_3 + TiO_2; calcic: CaO + MgO+ Na_2O + K_2O+ (BaO); and ferric: Fe_2O_3 + MnO + P_2O_5 + SO_3. Fly ashes and cenospheres have plotted in the same diagram because both of them are by products during the coal combustion. As observed in *Figure 2.8*a, depending on the chemical composition of fly ash and cenospheres, they can be classified in subgroups: Sialic; Ferrocalsialic; Ferrosialic; Calsialic; Ferrocalcic and Calcic. This wide range of chemical compositions could be due to the inhomogeneous distribution of mineral contamination of the burnt coal.

As per the *Figure 2.8* , the chemical composition of fly ash and cenospheres are similar since the majority of samples are located in the Sialic and Ferrocalsialic area. N. Ranjbar et al [30] further stated that the chemical composition of fly ash and cenospheres are alike except fly ash being contained with remaining carbon, indicated by the higher LOI content. The results showed that Al and Si are the main elements of cenospheres.
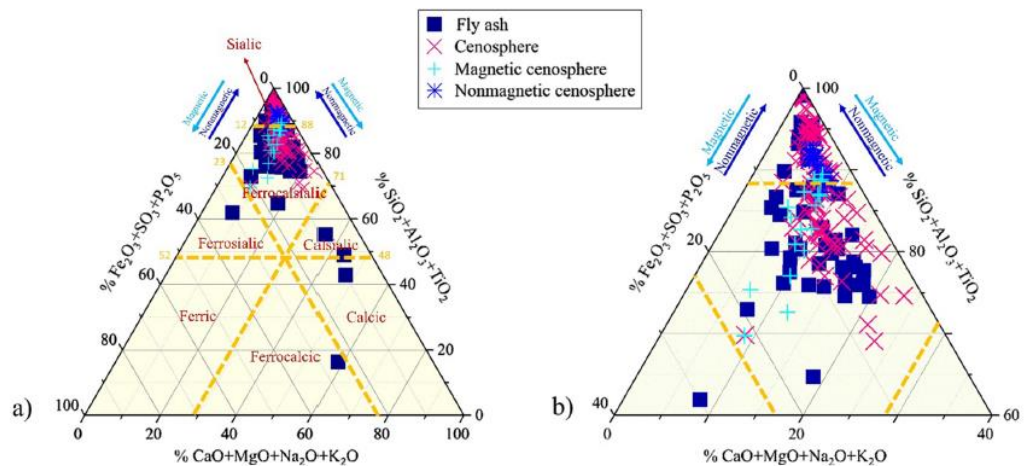
Figure 2.8: Ternary diagram presenting of the chemical composition of 209 fly ash and cenosphere samples. a) Full diagram; b) Magnification of the Sialic and Ferrcalsialic group*, N. Ranjbar et al [30]*

Table 2-7: Oxide composition (weight %) of Cenospheres analyzed by XRF taken from different literatures

Description		SiO$_2$	Al$_2$O$_3$	Fe$_2$O$_3$	CaO	SO$_3$	Na$_2$O	K$_2$O	P$_2$O$_5$	TiO$_2$	MgO	LOI
F. Blanco et al [38]		56	25	6.9	4.3		0.45	3.4		1.2	2.1	
P.K. Kolay et al [28]		52.53	30.01	7.53	1.15	0.02	0.02	1.98	0.45	1.79	0.32	4.2
P.K. Kolay et al [36]		38.4	15.5	25.4	3.73		0.99	3.1		0.56	0.99	0.95
I. Acar et al [29]		57.09	27.46	6.56	1.97	<0.01	0.31	3.89	0.11	1.13	2.38	1.68
		63.35	22.01	7.90	1.45	<0.01	0.79	1.95	0.16	0.91	2.31	2.15
U.S.Agrawal et al [39]	India	50-60	25-35	2.-8	1-6	0-1	0-1	1-3	0-1	1-5	0-1	
	China	40-65	15-35	2-8	1-6	0-1	0-2	1-3	0-1	1-5	0-1	
	Australia	45-60	25-30	5-10	1-6	0-1	0-1	0-3	0-1	1-5	0-1	
	USA	30-60	25-35	2-15	1-15	0-1	0-4	0-4	0-1	1-5	0-1	

2.5.1.2 *Mineralogy*

The mineralogy of cenospheres also varies from power plant to plant. According the XRD analysis [34] carried out by researchers, the main crystalline phases recognized by them in the cenospheres' shells are the mullite and/or quartz [29] [39] [32].As per the XRD diagram obtained by P.K. Kolay et al [28] (See *Figure 2.9*), alumina is the most predominant mineral present in cenospheres. Apart from that, presence of sillimanite, mullite, and magnetite can also be noticed.
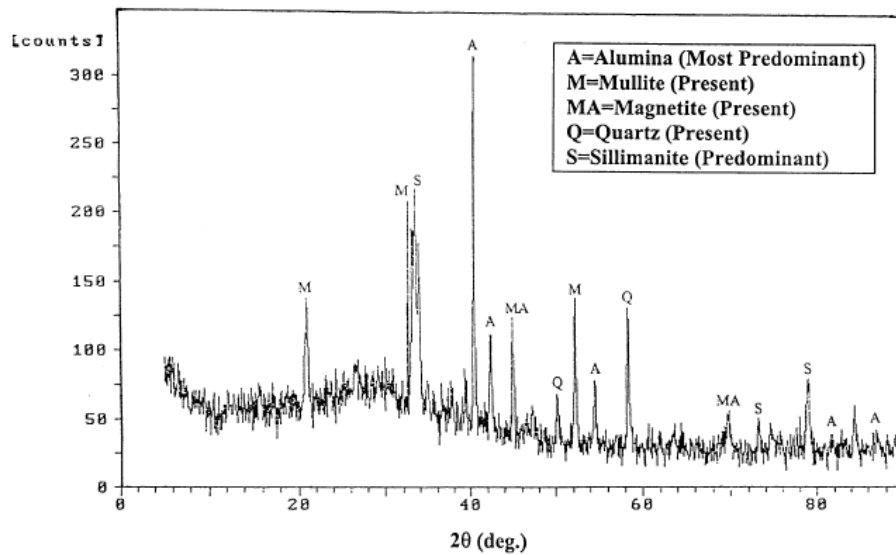
Figure 2.9: XRD pattern for the cenosphere sample examined by P.K Kolay et al *[28]*

As per the XRD pattern (See *Figure 2.10*) obtained by M. Zyrkowski et al [32], the crystalline phases present in the cenospheres, are quartz, mullite and calcite. According the *Figure 2.10,* the presence of an amorphous phase is indicated by the broad ovoid shape whereas the crystalline phases are depicted by the sharp peaks.

Si and Al are the main elements comprised in cenospheres, besides the presence of Fe, Na, Ti, K, Mg and Ca. All the elements are not present in their pure oxides but as a mixture of different crystalline and amorphous phase. The crystalline phases can be separated into mullite, cristobalite–quartz, K-feldspars, acid plagioclases and magnetite. Next to these, cenospheres are infused by quartz, lime and periclase [30].
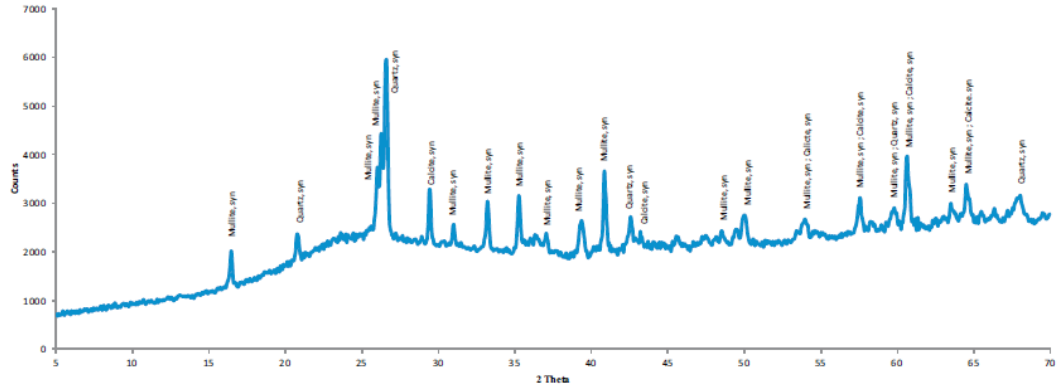
Figure 2.10: XRD pattern of cenosphere sample examined by M. Zyrkowski et al *[32]*

The skeleton of the cenosphere particles have been made of these groups of crystalline phases. Having a needlelike pattern skeleton structure provides a structural stability to cenospheres at high temperature and this skeleton is encapsulated by approximately 90 wt. % of an amorphous glass phase which provides a smooth surface. Since this layer consists of glass, it can be dissolved when it comes in contact with hydrofluoric acid. A schematic structure of cenosphere is shown in *Figure 2.11* by N. Ranjbar et al [30].
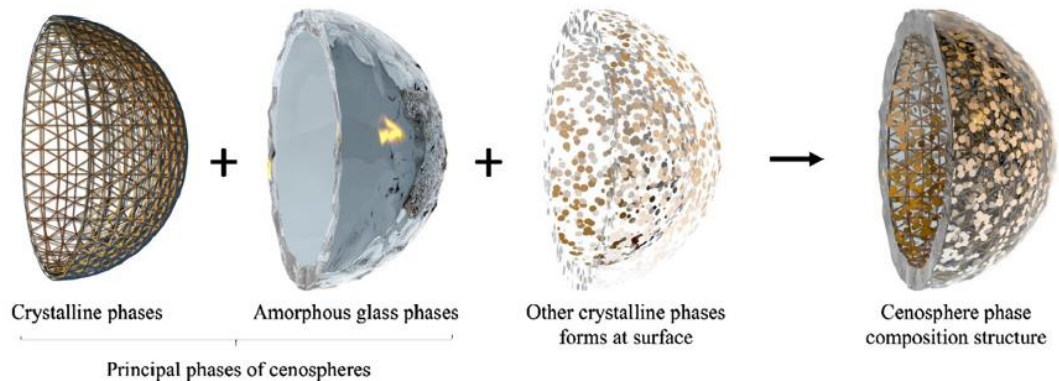
Figure 2.11: Schematic phase composition structure of a cenosphere, *N.Ranjbar et al [30]*

2.5.1.3 *Physical and morphological properties*

In general, the particle size of cenospheres lies in the range of 5-500μm and among them, the majority of cenospheres possess a diameter in between 20-250μm. Shell wall thickness is normally about 5-10% of their diameter and ranges in between 2-30μm. Bulk density of cenospheres varies from 200-500 kg/m^3 (much lower than that of water). Hence,

cenospheres can be easily separated and collected from fly ash in ash lagoons since cenospheres have low apparent density and float on the lagoons' surface. *Table 2-8* shows the physical properties of cenospheres taken from different literatures.

Table 2-8: Physical properties of cenospheres taken from different literatures

Particle size	Shell thickness	Apparent density	Bulk density	Specific surface area	Reference
10-400µm	0.5-40 µm	-	400-900 kg/m^3	-	Y. Wu et al. [40]
10-300µm	0.5-40 µm	0.67	375 kg/m^3	-	N. Barbare et al [33]
40-140µm	-	0.78	800 kg/m^3	457cm^2/g	P.K. Kolay et al [28]
5-500µm	0.25-50 µm	-	200-500 kg/m^3	-	I. Acar et al [29]
20-300µm	1-18 µm	0.4-0.72	250-700 kg/m^3	-	N. Ranjbar et al [30]
1-400 µm		2.48	400-800 kg/m^3	2.5-4.57m^2/g	A. Hanif et al [31]

The general belief is that ash cenospheres are normally hollow, having thin shells hence the cross-section of an ash cenosphere is a ring structure. Ling-ngee Ngu et al [37] characterized cenospheres taken from five Australian coal fired power stations. The study revealed that cenospheres can be both spherical and of a single-ring structure (*Figure 2.12*A) and nonspherical, irregular, and of a network structure (*Figure 2.12*B).

The SEM images (See Figure 2.12) taken by Ling-ngee Ngu et al [37], show that ash cenospheres of a single-ring structure are spherical whereas large ash cenosphere particles of a network structure have non-spherical and irregular shapes. This convey the fact that ash cenospheres of a single ring structure experienced complete melting whereas those of a network structure experienced incomplete melting and hence had high viscosities during combustion. Secondly, the authors showed that ash cenosphere particles of a network structure are dominantly in the large size fractions, particularly 150–250 µm and above 250 µm. Compared to an ash cenosphere particle of a single-ring structure, an ash cenosphere particle of similar size and a network structure would likely require bigger precursor ash-forming particles. Thirdly, the chemical analysis data indicated that the SiO_2/Al_2O_3 ratio of cenosphere decreased with increasing cenosphere size because a higher SiO_2/Al_2O_3 ratio indicates a lower ash sintering temperature. In other words, smaller ash cenospheres have lower sintering temperatures because of higher SiO_2/Al_2O_3 ratios which favors a ring structure.
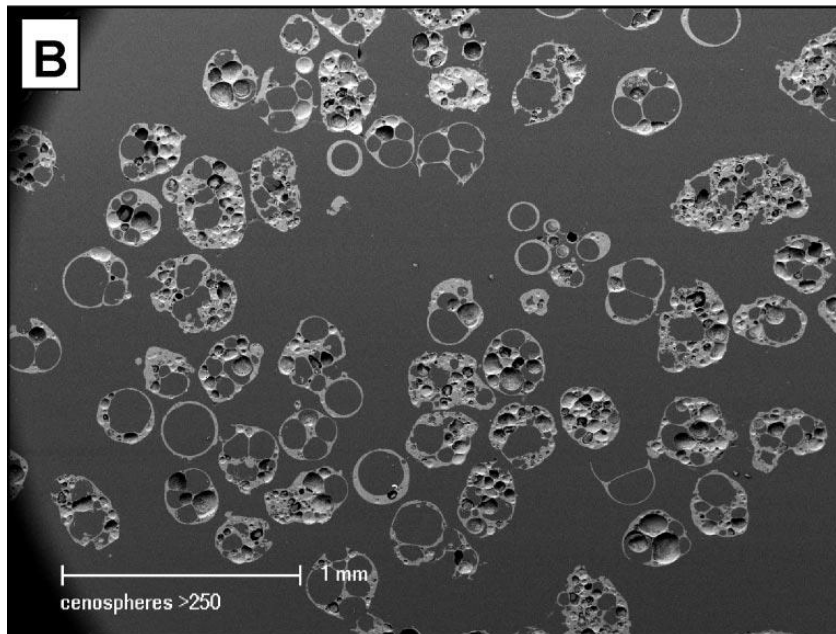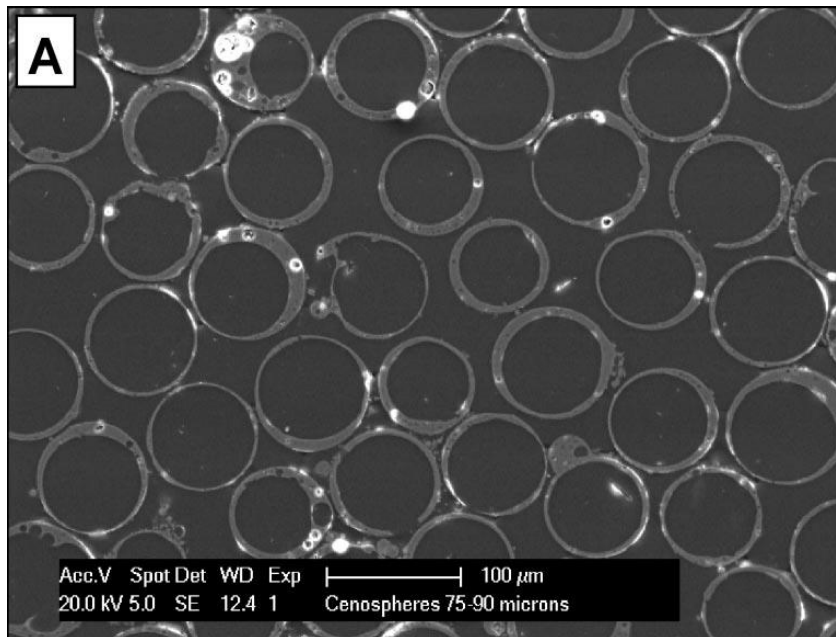
Figure 2.12: SEM images of the cross sectional views of cenospheres (A) spherical shape with single ring structure (B) non spherical shape with a network structure, *Ngu et al [37]*

2.5.1.4 Separation of cenospheres

There are two separation methods namely, wet and dry separation [19] [34] [36]. These two methods are schematically presented in *Figure 2.13* and *Figure 2.14*.
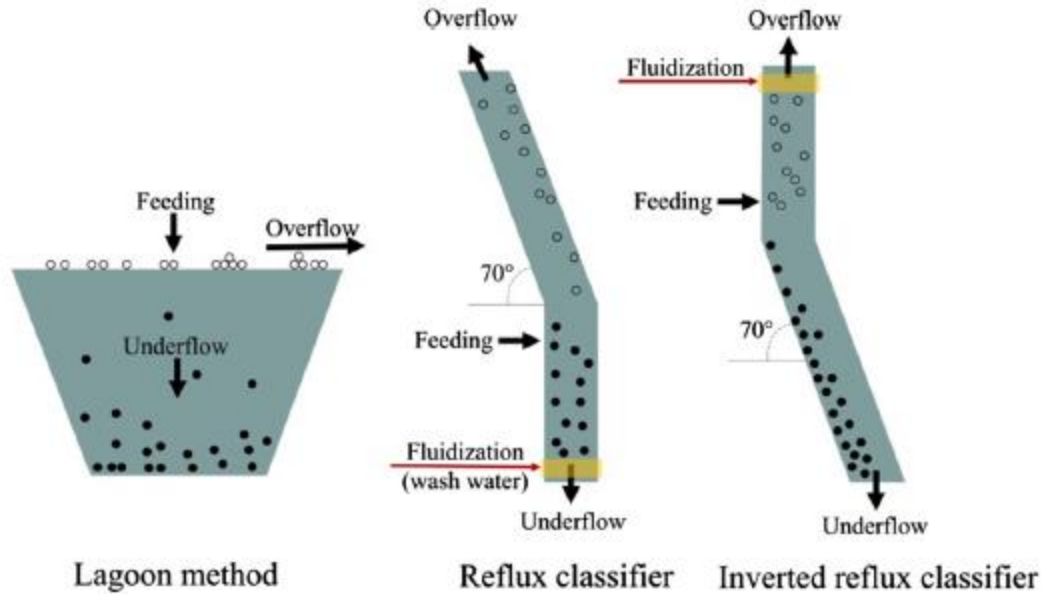
Figure 2.13: Schematic outline of some most often used wet separation methods, *N Ranjbar et al [30]*
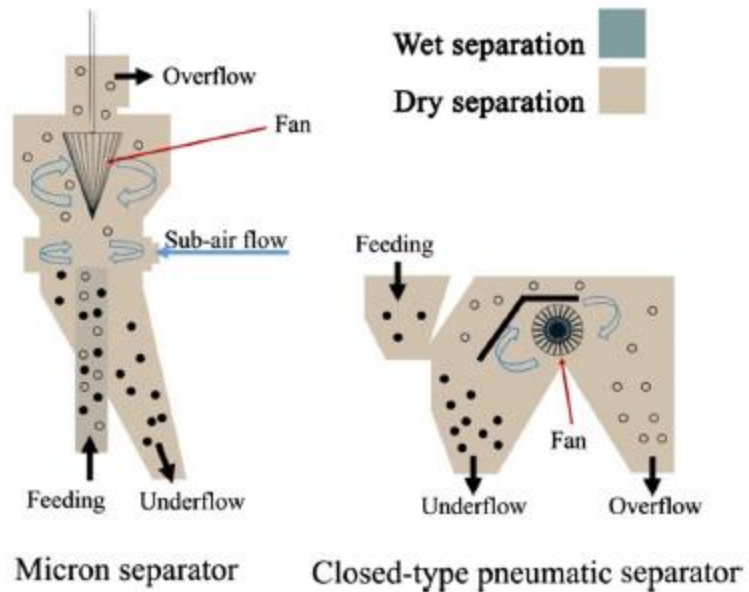
Figure 2.14: Schematic outline of some most often used dry separation methods, *N. Ranjbar et al [30]*

Wet separation

The flotation is the commonly used method which is followed by gravity and magnetic separation. In the gravity separation, cenospheres can be removed with the use of a liquid medium where floaters and sediments are divided. Water is the commonly used liquid medium. The cenospheres float on the surface of a fly ash suspension and are obtained by pond skimming. This method is popular because of its simplicity and common availability.

But, the efficiency of the gravity separation method depends on the following factors:

- Differences between the density of solid particles and the liquid medium, buoyancy forces,
- Feeding particle concentration,
- Porosity and texture of particles, (Ex: particles with smooth surface comes up faster compared to a rough surface due to lower interactions between surface and liquid and;
- Refinement cycles.

Liquid with different densities are used for different density classification. Distilled water with 1 g/cm^3 [41] , Lithium Metatungstate with 1.5 g/cm^3 [36] , Acetone with about 0.8 g/cm^3 [41] or combination of Carbon Tetrachloride, Dibromomethane and Di-iodomethan with 2.2 g/cm^3 [42] are some of the liquid mediums used for gravity separation.

Repeated stirring-settling procedure improves the recovery of floaters [36]. After the stirring-settling, a centrifuge can be used to increase the separation process. The degree of rotation and time period used in a centrifuge depends on the type of centrifuge, used liquid medium and fly ash quantity [28] [36] [42].

The major drawbacks in the wet separation method are the leachability of heavy metals to water, the unavailability of land and water for populous countries and the energy consumption required for drying before usage of separated CFA fractions. Minor drawback is the contamination of impurities of the cenospheres with the dense accumulation of fly ash particles on the surface of buoyant limiting the sinking of solid particles. Besides, fly ashes with a high calcium content have the affinity to form $Ca(OH)_2$

crystals on the surface of cenospheres. These crystals harden during drying of the cenospheres and limits the use for further application [36].

Dry separation

Dry separation is an alternative method used to overcome the drawbacks of wet separation. Dry methods are based on the separation of CFA particles in a gas stream or regular screening on appropriate sieves [43].

Dry separation method has several advantages over wet separation. They are; the chemical composition is unaffected, no water pollution and less energy consumption since drying is avoided and requires less space for equipment compared to wet separation. Air classifier is used to separate solid particles based on their difference in particle geometric or hydrodynamic/aerodynamic equivalent diameter and density.

There are five types of air classifiers which are gravitational, cascade, fluidized bed, inertial and centrifugal. Among them, only inertial and centrifugal air classifiers have the capability to separate particles with a micrometer size whereas the other classifiers can be used for particles with a millimeter size. The separation principle is based on the fact that the particles suspended in a flowing gas during which gravity and drag forces acting on the particle in opposite directions. Heavy particles with terminal settling velocity larger than the velocity of air move downwards against the air stream, while the light particles whose terminal settling velocity is smaller than the velocity of air rise along with the air stream to the top of the column [44]. The main drawback of dry separation method is its complexity of the preliminary setup and their mechanisms compared with the wet separation process.

2.5.2   Cenospheres incorporated cementitious composites

Cenospheres derived from coal fly ash can be used as a fine aggregate in the manufacture of lightweight concrete and as an additive to produce lightweight cements [34].

Compressive strength, flexural strength, tensile strength and thermal conductivity properties of fly ash cenospheres containing cement composites (FACC) can be illustrated below as extracted from the literature [31].

35

Density and compressive strength

It is found that FACC possess desirably a low density with satisfied higher strength as compared to normal concretes with conventional light weight aggregate (LWA). The density, mechanical properties and thermal conductivity of FACC as reported by several researchers are summarized in Table 2-9. The strength grades of FACC can be designed with the mixture proportioning, the water: binder ratio, the use of supplementary cementitious materials (SCMs) and admixtures.

The density of FACC decreases directly with the addition of cenospheres as a filler material but the resulting composites comply with the specifications for structural light-weight concrete. Besides, as elaborated by Yunpeng et al [40] and Jun-Yan et al [45], the incorporation of SCMs such as fly ash, silica fume and iron ore tailings into FACC deliver better mechanical strength and packing properties. Among the current researches on FACC, Liu et al. [46], Wu et al. [40] and Wang et al. [45] achieved the most promising results with specific strength (strength per unit weight) values of 40.14, 47.18, and 41.03 kpa/kg m^3, respectively. The resulting cementitious composites were named as ultra-lightweight cement composites (ULCC).

A method to design the mix proportions to attain a desired unit weight, compressive strength and workability was proposed by Wang et al. [45]. This method is based on the correlation between the spacing among spherical cenosphere particles (when packed together) and the water to binder (cement and SCM, if any) ratio to obtain the desired workability. The particle density and the particle size distribution have to be known to apply this method to achieve the expected unit weight and strength for the FACC. This is a useful method since it minimizes the laboratory trials required to achieve the target properties of fresh and hardened FACC.

Flexural and tensile strength

In general, the lightweight concrete (LWC) is more ''brittle'' than normal concrete which is same for FACC as well since it is an ultra-lightweight composite. Hence, the studies focused on fibre reinforcement FACC to improve its ductility and performance. The flexural strength of FACC as reported in the literature is summarized in Table 2-9.

Polyvinyl alcohol (PVA) fibers [47] [48] and polyethylene fibers (PE) [40], [49] have been used as reinforcements in the cenospheres incorporated cementitious matrix. At 2% of fibre volume of PVA which can be considered as a relatively higher volume fraction, led to noticeable strain hardening (up to 4.5% strain) with excellent multiple cracking under uniaxial tensile tests [48]. The results indicated that PVA fibers have good compatibility with FACC because of their hydrophilic nature and the presence of hydroxyl group (in the PVA fibers) resulting in strong chemical bonding.

Thermal conductivity

Thermal insulating behavior is one of the important properties delivers by LWAs because they provide greater air void content within the concrete. Since the thermal conductivity of air is much lower than that of the solid cement hydration products, the subsequent thermal conductivity of the concrete is also low. Previously researched LWAs in producing LWC and the corresponding thermal conductivity values obtained are provided in *Table 2-9*

The result shows that, the incorporation of cenospheres in concrete has led to lower the thermal conductivity significantly. However, the compressive strength of FACC concretes at the same unit weight, in comparison to other LWCs, is much higher which makes it more useful and beneficial over other LWAs. As an example, a thermal conductivity coefficient of 0.31 W/mK can be achieved with cenospheres with the composite density of 1196 kg/m^3 at 33 MPa compressive strength. This assess the beneficial effects of FACs quantitatively with respect to thermal conductivity and specific strength simultaneously.

Table 2-9: Density, mechanical properties and thermal conductivity of various FACC reported in literature (28 – day age).

Reference	Water/ Binder Ratio	Density (kg/m^3)	Compressive Strength (MPa)	Flexural Strength (MPa)	Thermal conductivity (W/mK)	Description
Hanif et al. [50]	-	1260-1612	30.38-55.92	5.38-9.29	-	1.0 wt% PVA fibers were used. Silica fume was used as SCM. 30–70% (by binder weight) of FAC was employed.
Blanco et al. [38]	0.30	1090-1510	5.04-33.03	2.09-5.05	0.36-0.46	Various granulometric fractions of FAC were incorporated to achieve a range of results. No micro-reinforcement was used.
Huang et al. [48]	0.26	1649-2001	44.3-48.1	-	0.278-0.370	Iron ore tailings and fly ash were used as SCM. PVA fibers were used.
Hanif et al [47]	0.70	1297	33.54	4.94	0.410	Silica fume was used to replace 10% of cement. PVA fibers were used.
Wu et al [40]	0.35-0.56	1196-1471	33.0-69.4	3.6-7.3	0.31-0.40	Silica fume was used to replace 8% of cement in binder. 38.3–51.6 vol% of FAC in the mixes were used. Polyethylene fibers were used.
Liu et al. [46]	0.35	1460	58.6	6.08	-	PVA fibers were used. Silica fume was used as SCM. Tests were conducted at various temperatures (values reported here are pertaining to room temperature conditions).
Losiewicz et al. [51]	1.2*	760-867	0.55-2.88	-	0.111-0.153	*refers to FAC/water ratio
Kannan et al [49]	0.45	-	46–55	-	-	FACs were used as cement replacement from 5% to 30% by weight.

2.6 Chapter summary

The main problem associated with commercially available non-asbestos fibre cement corrugated roofing sheet is its high moisture movement and shorten lifespan compared with asbestos fibre cement corrugated sheets. MCR tiles/sheets is one of the substitutes for asbestos fibre cement roofing sheets introduced to Sri Lanka in 1999. The cost and the weight of MCR tile is comparable with Calicut clay tile but denser than asbestos fibre cement sheets. Many studies have shown a maximum replacement of 20% coal fly ash from cement in fabricating MCR tiles or fibre reinforced corrugated tiles/sheets. Main oxide presented in CFAs are descend in the order of $SiO_2 > Al_2O_3 > Fe_2O_3 > CaO > MgO$, in general. Trace heavy metal elements could be As, Be, B, Cd, Co, Pb, Mn, Hg. Particle size of CFA ranges in between 1μm-300μm and specific gravity in between 2-4. The major phases of CFAs are mullite, quartz, and hematite. The main components comprised of CFA are cenospheres, enriched carbon, magnetic spheres, fine improved coal fly ash and coarse improved coal fly ash. Among them, the lightest component is cenospheres due to its hollow structure (857-1282 kg/m^3). Cenospheres are spherical, hollow smooth and larger in diameter (20-250μm). It has a needle-like pattern skeleton structure which is encapsulated by approximately 90 wt. % of an amorphous glass phase which provides a smooth surface. Chemical composition of CFA and cenospheres are alike except coal fly ash being contained with remaining carbon. Enriched carbon has larger porous structure and more irregular and has a density around 1970 kg/m^3. Magnetic particles are also spherical but has a rough surface having the highest density (3470kg/m^3) due to the relative high atomic weight of Fe compared with Si and Al. Fine IFA fraction is the it is predominantly made up of spheres which also has a high density (2330 kg/m^3) due to the enrichment of trace heavy metals. Coarse IFA is more irregular in shape having a density about 2190 kg/m^3. Use of centrifugal air classifiers is the most efficient way of recovering cenospheres, apart from that wet separation is also being used. Screening from appropriate sieve is also a way of extracting cenospheres but not that popular. Studies have shown that incorporation of cenospheres into the cementitious matrix could substantially reduce the density and the thermal conductivity along with reduced strength which is a detrimental effect. The brittleness associated being lightweight has been overcome by fibre reinforcement.

3 EXPERIMENTAL PROCEDURE

3.1 Materials and characterization

3.1.1 Particle size distribution

Coal Fly Ash (CFA) (See *Figure 3.1*) was collected from the electrostatic precipitator at Lakvijaya coal power plant, Norochcholai, Sri Lanka.
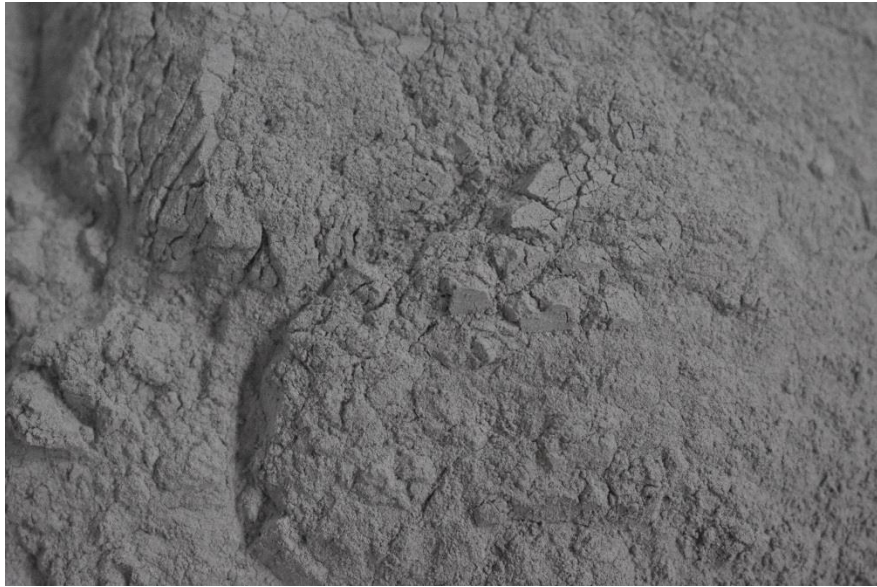
Figure 3.1: Coal fly ash

Particle size distribution of the CFA sample was obtained as per BS 1377 Part 2:1990 "Methods of test for soils for civil engineering purposes. Classification tests" [52].

CFA was analysed by Laser Diffraction technique using Malvern Zetasizer Nano ZS to determine the finest particles. The equipment has a measurable range of particle size of 0.6 nm – 6 µm. The test procedure includes of dispersing a small amount of CFA in deionized water and sonication for a minute. Then the sample was allowed to stand and settle. The readings were taken after 30 minutes and 60 minutes, for the samples carefully withdrawn from the middle part of the suspension. This test was carried out at Sri Lanka Institute of Nano Technology.

3.1.2 Materials

CFA fractions

CFA was dry sieved using 75µm sieve and the fraction passed through it was collected (See *Figure 3.2*). Similarly, another sample of CFA was dry sieved from 45µm size and the passed fraction was obtained. Thereby 3 fractions of CFA samples were used for the experiment, namely the unprocessed CFA, the CFA below 75µm sieve and the CFA below 45µm sieve.

Figure 3.2: Dry sieving of CFA

The wet separation technique was used to extract the low density fraction of CFA using Acetone (density 0.791 g/ml) as the liquid medium with repeated stirring-settling was carried out to improve the recovery potential of low density particles by adopting the methods described by L.M. Manocha et al [41] and P.K. Kolay et al [36].

For the wet separation procedure, initially a 60g of CFA was taken into a 500ml beaker. Acetone was poured into the beaker until the acetone level was 1cm above from the CFA level. The beaker was tightly sealed and it was shaken at 175 rpm for 45 minutes in an orbit shaker. After that it was allowed to settle for 15 minutes and again it was shaken for 60 minutes. Next, it was allowed to settle for 16 hours. Then the acetone siphoned with an aid of syringe and the siphoned liquid was discharged to a petri dish and allowed acetone evaporate.

(a) Sealed beakers consist of CFA in acetone solution are being shaken in

(b)After shaking, allowing CFA to settle for 16 hours

(c)Acetone is siphoned by a syringe

(d)The uppermost CFA layer (1 mm from the top) is scraping out

(e)Once the uppermost layer is completely scraped off

Figure 3.3: Extraction of low density particles from coal fly ash

Meantime the CFA with acetone in the beaker was also allowed acetone to evaporate till the CFA becomes slightly harden. Then the uppermost CFA layer (1mm depth) was

carefully scraped off to the same petri dish. The extracted CFA particles were oven dried at 110°C until constant weight is achieved. These steps are explained in Figure *3.3*.

Alkali resistant (AR) glass fibres

Commercially available AR glass fibres were used in this study (See *Figure 3.4)*. The technical characteristics of chopped strands given by the manufacturer is shown in *Table 3-1*.

Figure 3.4: Alkali resistant glass fibres

Table 3-1: Technical characteristics of AR glass fibres

Characteristics	Testing method	Standard value	Average test value
Glass density (g/cm^3)	ISO 1889:1997	2.78	2.65
Filament diameter (μm)	ISO:1996	15±2.3	15.5
Chopped length (mm)	N/A	12±1.5	12.1
Loss on Ignition (%)	ISO 1887:1980	1.9±0.3	1.77
Moisture (%)	ISO 3344:1977	<0.2	0.18
Zirconia (%)	N/A	14.5+0.5/-0.3	14.8

The chemical composition as provided by the manufacturer is given *Table 3-2*.

Table 3-2: Chemical composition of AR glass fibres

Composition (%)	ZrO$_2$	SiO$_2$	TiO$_2$	Na$_2$O	CaO	K$_2$O	AlO$_3$	Fe$_2$O$_3$
	16.5	56.7	5.87	12.8	4.89	2.49	0.39	0.26

3.1.3 Chemical composition

Elemental compositions of each CFA fractions (the unprocessed CFA, the CFA below 75 μm particle size, the CFA below 45μm particle size and the CFA particles extracted from wet separation method) were analysed by X-Ray Fluorescence (XRF) method using HORIBA Scientific XGT- 5200 X- ray Analytical Microscope from Sri Lanka Institute of Nano Technology. The equipment has the capability to detect elements only from 11Na to 92U. Samples were pasted on the sample stage using double tapes. Six different places of the samples were analysed and the average was reported. But the percentage values are not accurate for lighter elements. And also the element percentage values are calculated by the machine itself relative to the total detected elements present in each spot. Therefore, the total detected elements percentage values are added up to 100%.

The loss on ignitions were measured as described in BS EN 450-1: 2012 "Fly ash for concrete. Definition, specifications and conformity criteria" [53].

3.1.4 Scanning Electron Microscopic (SEM) analysis

The morphology of each CFA fractions (the unprocessed CFA, the CFA below 75 μm particle size, the CFA below 45μm particle size and the CFA particles extracted from wet separation method) were observed using Leo 1420 VP Scanning Electron Microscopy from Industrial Technological Institute, Colombo.

3.1.5 Particle density

Particle density of each CFA fractions were measured as per SLS 1144: Part 2:1996 "Specification for ready-mixed concrete Part 2: Test methods" [54] by displacement of a non-reactive liquid in a density bottle.

Following weight measurements were taken to density calculation.

m_1 -   Mass of empty bottle (g)

m_2 -   Mass of bottle with water (g)

m_3 -   Mass of bottle with kerosene (g)

m_4 -   Mass of bottle with kerosene & fly ash (g)

m_5 -   Mass of bottle with fly ash (g)

Hence, the density is given by the equation 1.

$$\text{Density } (kg/m^3) = \frac{(m_5 - m_1) \times (m_3 - m_1)}{(m_5 + m_3 - m_4 - m_1) \times (m_2 - m_1)} \times 1000 \qquad \text{Eq.1}$$

Two separate determinations were made on different portions of the sample of CFA. If two results differ by more than 30kg/m^3, the results were discarded and made two fresh determinations.

3.2   Casting and testing of coal fly ash-cement mortar prisms

3.2.1   Flexural strength

Mortar prisms (size: 40×40×160 mm) were cast for the flexural strength test as per the procedure given in SLS 107: Part 2 "Specification for Ordinary Portland Cement: Test Methods" [25]. Ordinary Portland Cement (OPC) was partially replaced by CFA fractions (the unprocessed CFA, the CFA below 75µm, the CFA below 45µm and the extracted CFA particles from wet separation) in 10%, 20%, 30%, 40% and 50% (by weight) and the water: cement ratio was 0.47. Prisms were cured in water for 28 days and tested for three-point bending test as indicated in SLS 107: Part 2 [25].

3.2.2   Density

The apparent density of fly ash-cement mortar prisms was measured from the broken specimen after the flexural strength.

Specimens were immersed in water for at least 24 hours.
Mass was determined of the saturated specimens suspended in water (A).
Specimens were removed from water and quickly removed the excess water from surfaces. Immediately determined the mass in air (B).
Specimens were oven dried in a ventilated oven which was maintained at a temperature of 100 °C ±5°C for 24 hours. Specimens were allowed to cool to room temperature after removing them from oven and determined the mass(C).

Mass was measured in grams and the balances had the accuracy to within 0.1% of the specimen mass.

Calculations were made as per the equations 2 and 3 as follows.

$$\text{Apparent density/cm}^3 = \frac{C}{B-A} \qquad \text{Eq.2}$$

$$\text{Water absorption, } \% = \frac{B-C}{c} \times 10 \qquad \text{Eq.3}$$

3.3 Casting and testing of glass fibre reinforced fly ash-cement roofing tiles

3.3.1 Casting procedure

Matrix

Only 30% of cement replacement by CFA fractions (which are the unprocessed CFA, the CFA below 75µm and the CFA below 45µm) was adopted to cast glass fibre reinforced fly ash-cement roofing tiles. The 30% replacement was considered as the optimum CFA content with respect to the satisfied strength and density suitable for casting roofing tiles as obtained by the literatures. The extracted CFA particles from wet separation was excluded in casting tiles because it is difficult to extract a large amount. AR glass fibres were added and premixed in 1% and 2% (≈1% and 2% by volume) by total weight of the cement and fly ash dry mix. However, because the fibres reduce the workability, only up to about 2% fibres by volume can be introduced in the mix by premix method [55]. An unreinforced cement composite containing 30% of the unprocessed CFA was cast. Mix proportions are given in *Table 3-3*.

Processing

The mix was produced using an electric mixer having 50Hz frequency. The fibres were dry mixed with CFA for 60s for homogenization. Then 85% from the total water added into to the mix and it was mixed well, followed by the addition of cement into the running mixture. Later, remaining 15% of water was added and thoroughly mixed until a uniform consistency was obtained. The total mixing time was 3 minutes starting from addition of initial water. After that, the remaining lumps were scraped down around adhered to the container within 30 s and mixed again for another 2.5 mins.

For the production of glass fibre reinforced fly ash-cement corrugated tiles, a plastic sheet was placed on the vibrating table having a frequency of 60Hz and the mix was spread on it followed by vibration for 0.45s-60s. The green mix was carefully moved on a mould so that it takes the corrugated shape of the mould. Then the mould was stacked for 24 hours. Thereafter, the tile was removed from the mould and stacked vertically in the water. Curing was done continuously for 14 days prior to the performance of laboratory tests. Then tiles were conditioned for another 14 days in normal environment. Casting procedure is shown in *Figure 3.5*.

The corrugated tile has a length, width and thickness of 490×250×8 mm. Tests were carried out as per SLS 1189: Part 2:1999 [6] "Specification for concrete roofing semi-sheets, tiles and fittings-Test Methods". 10 tiles were cast from each mix.

Table 3-3: Mix proportions of glass fibre reinforced fly ash-cement roofing tiles

Sample identification	Water: Cement ratio	Coal fly ash : Cement	Fibre % (by volume)	Coal fly ash fraction
A	0.47	7:3	0	The unprocessed CFA
BF1	0.47	7:3	1	The unprocessed CFA
CF1	0.47	7:3	1	The CFA below 75μm
DF1	0.47	7:3	1	The CFA below 45μm
BF2	0.48	7:3	2	The unprocessed CFA
CF2	0.48	7:3	2	The CFA below 75μm
DF2	0.48	7:3	2	The CFA below 45μm

(a) Mixing of raw materials

(b) Spreading the mix on the vibrating table

(c) Removal of frame once the levelling is done

(d) Green mix is carefully taking onto the mould
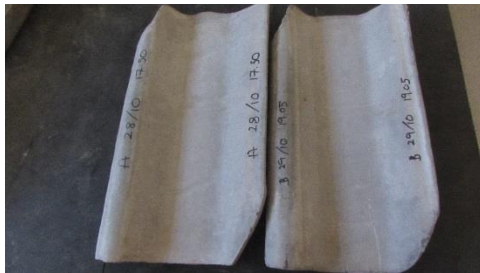
(e) Upper side of the finished tile

(f) Cross section of the finished tile

Figure 3.5: Casting procedure of glass fibre reinforced fly ash-cement roofing tiles

3.3.2 Dimensional properties

10 tiles were randomly selected. Hanging length and squarness, flatness, nib support, shape of overlapping ends and thickness were measured *(see Figure 3.6)* as per SLS 1189: Part 2:1999 [6]**.**

(a) Determination of hanging length and squareness

(b)Determination of flatness

(c)Assessment of nib support

(d)Assessment of shape of overlapping ends

Figure 3.6: Determination of dimensional properties of glass fibre reinforced fly ash-cement roofing tiles

3.3.3 Impermeability, "ring test" and "pore and crack" test

The above tests were performed (See *Figure 3.7*) as per SLS 1189: Part 2: 1999 "Specification for concrete roofing semi-sheets, tiles and fittings-Test methods" [6].

(a) Impermeability test

(b) Ring test

(c) Pore and crack test

Figure 3.7: Performing impermeability, "ring test", and "pore and crack test"

3.3.4 Characteristic transverse strength and Mass

Mass was weighed in each tile prior performing the transverse strength by using Universal tensile machine, type INSTRON UTM-HYD and model 600 DX-B1-C3-G1C. The loading rate was 800N/min. The testing arrangement is shown in *Figure 3.8*.

The maximum load of each tile was recorded to the nearest 10 N. The weight of the packing pieces was also included since it exceeded 5N.

Calculation were made to the nearest 10 N, using the following equations 4 and 5.

$$F_c = F - 1.64\,S_d \qquad \text{Eq.4} \quad ; \qquad \text{Where, } S_d = \sqrt{\sum \frac{(Fi - F)^2}{n-1}} \qquad \text{Eq.5}$$

n is the number of tiles tested;

Fi is the maximum load of tile;

F is the arithmetic mean of Fi values of the sample; and

F_c is the characteristic transverse strength
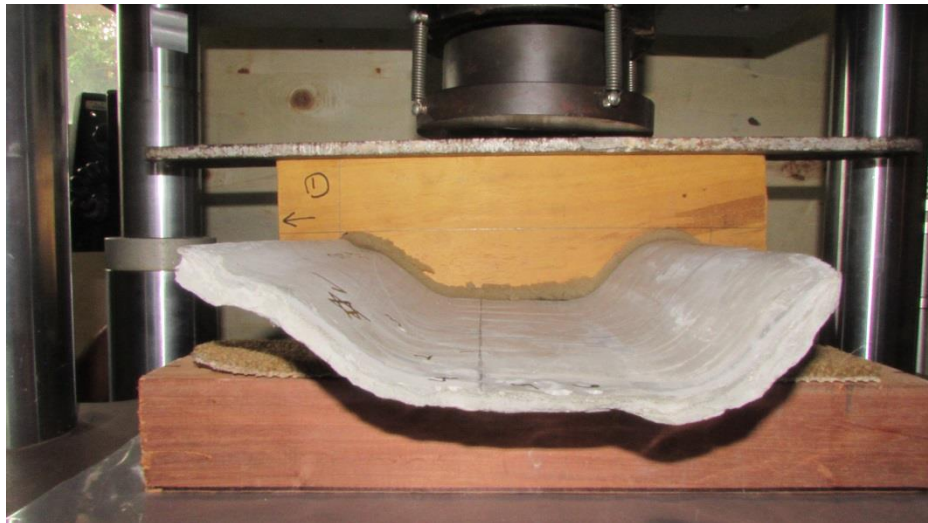
Figure 3.8: Testing arrangement for transverse strength

3.3.5 Water absorption and density

Water absorption and apparent density of glass fibre reinforced fly-ash cement roofing tiles were measure as per the same procedure indicted in section 3.2.2.

Tests method was adopted from ASTM C948-81 "Standard test method for dry and wet bulk density, water absorption, and apparent porosity of thin sections of glass-fiber reinforced concrete" [56] and ISO 10904:2011(E) "Fibre-cement corrugated sheets and fittings for roofing and cladding" [57]

3.3.6 Thermal properties

In this study, with respect to the thermal properties of roofing materials, thermal conductivity, specific heat and thermal diffusivity were considered.

3.3.6.1 Thermal conductivity

Thermal conductivity is defined as the property that characterizes the ability of a material to transfer heat [58]. It is defined by the following equation 6;

$$q = -k\frac{dT}{dx};$$
Eq.6

where q denotes the heat flux, or heat flow, per unit time per unit area (area being taken as that perpendicular to the flow direction), k is the thermal conductivity, and dT/dx is the temperature gradient through the conducting medium.

In this study, thermal conductivity was measured by the Lee's disk method. The apparatus consisted of two metal parts. The bottom plate and the top plate, both having the same diameter and thickness. The test sample was cut into the shape of the disc and then mounted on the bottom plate and the top plate was then placed on the test sample. Two thermometers were attached to the top and bottom plates to record the steady state temperature. The bottom plate was heated. To minimize the heat loss from the sides of the test sample, sides were covered from heat insulating gel.

When the heat flows from the bottom plate to the top plate through the sample for some time, the temperature recorded gradually become remain steady. At this stage;

Steady state temperature of top plate $: T2$

Steady state temperature of the bottom plate $: T1$

Specific heat of the metal plate $: C$

Mass of the metal plate $: m$

Thickness of the test sample $\qquad$: x

Cross sectional area of the test sample $\qquad$: $A\ (\frac{\pi D^2}{4})$

Thermal conductivity of the test sample $\qquad$: k

Once the steady state is achieved, the heating of the bottom plate is stopped and the top plate is suspended in air allowing both to cool down. Then the cooling curve of the bottom plate is recorded.

Assuming that the heat loss from the lateral of test sample is negligible, the steady state heat transfer (H) through the test sample by the conduction can be given by equation 7:

$$H = \frac{kA(T1-T2)}{x} \qquad \text{Eq.7}$$

The cooling law for the rate of heat loss from the bottom plate can be given by equation 8:

$$H = mC\left(\frac{dT}{dt}\right) \qquad \text{Eq.8}$$

When the system is in steady state, the rate of heat conduction through the bottom plate in-to the test sample must be equal to the rate of heat loss due to cooling (by air convection) from the top plate.

By equating the equations 7 and 8 at steady state, the thermal conductivity of the specimen can be calculated from the equation 9.

$$\frac{kA(T1-T2)}{x} = mC\left(\frac{dT}{dt}\right)$$

$$k = \frac{mCx\left(\frac{dT}{dt}\right)}{A(T1-T2)} \qquad \text{Eq.9}$$

The *Figure 3.9* shows performing the thermal conductivity test by the Lee's disk apparatus.
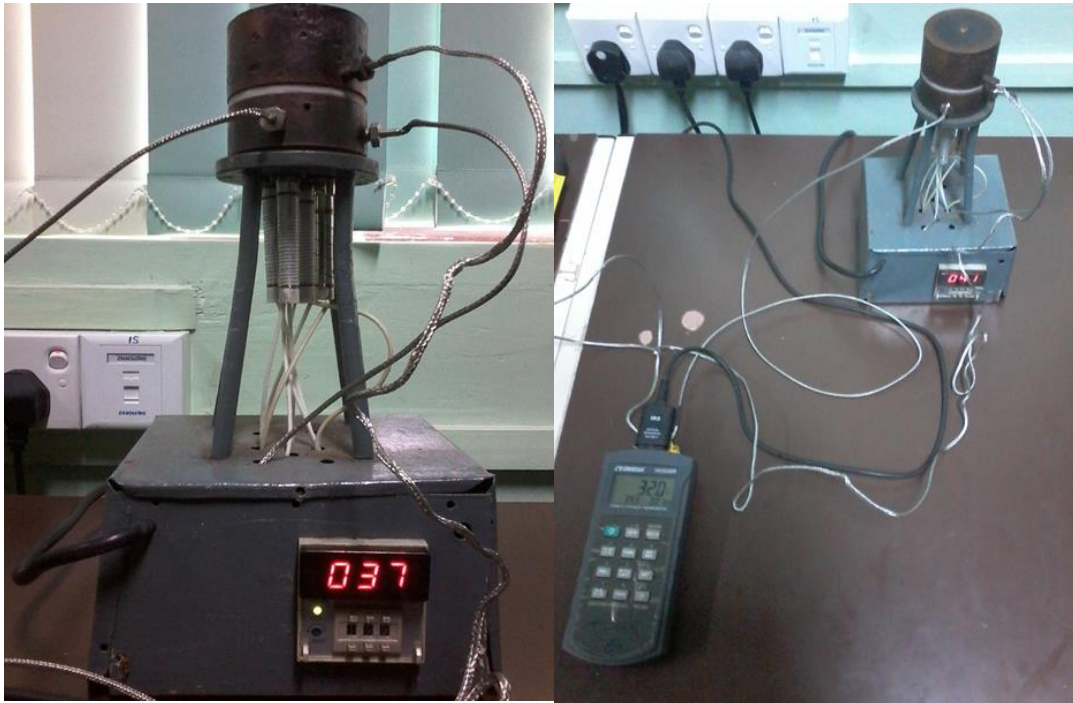
Figure 3.9: Thermal conductivity test by Lee's Disk method

3.3.6.2 Specific heat

Heat capacity indicates a material's ability to absorb heat from the external surroundings; it represents the amount of energy required to produce a unit temperature rise. It is usually expressed in J/kg·K in the metric system. Specific heat is applied in the calculation of heat transferred or absorbed by a system given by the equation 10;

$$q = mc\Delta T \qquad \text{Eq.10}$$

Where q: heat energy, m: mass, c: specific heat and ΔT: temperature change

The specific heat of different roofing materials were measured using a simple calorimeter. A calorimeter is a device used in calorimetry, the discipline that deals with the measurement of heat. Calorimetry includes the measurement of specific heat, latent heat and heat of reactions.

The general principle of all calorimeters is to isolate the system from the environment, so there is no heat loss to the environment. Although this adiabatic assumption is almost never achieved in real life, it allows us to formulate a simple formula to calculate the heat transfer within the components in the system. In the case of a two-component system, the

Second Law of Thermodynamics i.e. conservation of energy in a closed system tells us that the energy lost (q_1) by one component is equal to the energy gained (q_2) by the other component.

$$0 = q_1 + q_2$$

The actual measurement of the specific heat of the roofing tile involves heating a piece of tile to 110°C temperature in an oven for at least six hours to ensure a uniform temperature of the sample. The initial surface temperature of the sample was measured using a Non-contact infrared thermometer. The tile is then immediately immersed in water that has room temperature. Ideally, the heat given up by the tile is the same as the heat absorbed by water, container and stirrer. Hence the specific heat of the tile (C_{tile}) can be measured using the equation 11 when the system reached equilibrium temperature.

$$C_{tile} = \frac{m_{water} C_{water} (\Delta T)_{water} + m_{cont} C_{cont} (\Delta T)_{cont} + m_{stirer} C_{stirer} (\Delta T)_{stirer}}{m_{tile} (\Delta T)_{tile}} \qquad \text{Eq.11}$$

This temperature is determined by monitoring the temperature of water with the aid of data logger (See *Figure 3.11*). The water is continuously stirred before taking its temperature and an assumption is made that the temperature is uniform across the whole volume. Normally it takes 15 minutes to come to the equilibrium state. Samples were tested until the difference between the specific heat values of two samples is below 15 J/kg.K. Then the average of those two values were taken as the final result.

The simple calorimeter was assembled using a stainless steel container having an internal volume of 2.5 liters which was covered with polystyrene. The container is not fully filled with water so air is also present in the calorimeter. The experimental setup is elaborated in *Figure 3.10.*

Figure 3.10: Experimental set up of the calorimeter

Figure 3.11: Continuous stirring until the temperature of water becomes equilibrium which is monitored by a data logger

3.3.6.3 Thermal diffusivity

The thermal diffusivity of the roofing material is the ratio of its thermal conductivity to its heat capacity, and is expressed in m^2/s. It is given by the following equation 12; [59]

$$\alpha = \frac{k}{\rho c} \qquad \text{Eq.12}$$

3.3.7 Leaching properties

Leaching of heavy metals, namely Cd,Pb,Mn,Cr,Co,Hg,As,Be,Se,B,Mo,Sr and V from the glass fibre reinforced fly ash-cement roofing tiles and a non-asbestos fibre cement corrugates sheets available in the market were analysed by USEPA Method No 1311-Toxicity Characteristic Leaching Procedure [60].

The toxic elements which were leached from 10 g of sample into the extraction fluid I (pH<5) for a period of 18 hrs at 30 rpm were directly analyzed by Inductively Coupled Plasma Mass Spectrometry (ICP-MS) in order to determine the total characteristic leaching toxic elements. This test was carried out at Industrial Technological Institute Sri Lanka.

3.3.8 Durability test by Soak-dry method

Soak dry test is a durability test defined for fibre cement sheets in ISO 10904:2011(E) [57].

10 tiles underwent 50 soak-dry cycles by adopting the procedure given in ISO 10904:2011(E) [57].

The 50 soak-dry cycles is consisted of:

a) Immersion in water at ambient temperature for 18 h, and

b) Drying in a ventilated oven of 60 ±5°C and relative humidity of less than 20 percent for 6 h.

If necessary, an interval up to 72 h between cycles was allowed. During this interval, specimens shall be stored in immersed conditions. After 50 cycles, tiles were placed in a

laboratory atmosphere for 7 days. Transverse strength test was performed at the end of this period.

Calculation of results

The first lot of tile sample which underwent the normal transverse strength test is denoted by subscript 1. The second lot of tile sample which underwent the transverse strength after soak-dry test is denoted by subscript 2.

Mean transverse strength and standard deviation were calculated for each of the two lots. Let $\overline{X}_1$ and s_1 be the mean and transverse strength of lot 1, and $\overline{X}_2$ and s_2 be the mean and transverse strength of lot 2.

The lower estimation, L_2, of the mean breaking load of the lot 2 at the 95% confidence level is calculated by equation 13, and the upper estimation, L_1, of the mean breaking load at the 95% confidence level of the lot 1 is calculated according to equation 14.

$$L_2 = \overline{X}_2 - (0.953 \times s_2) \qquad \text{Eq.13}$$
$$L_1 = \overline{X}_1 - (0.953 \times s_1) \qquad \text{Eq.14}$$

The coefficient of 0.953 is related to a sampling size of 10 specimens, as defined in ISO 2602:1980 "Statistical interpretation of test results - Estimation of the mean - Confidence interval" [61], Table 1, for the unilateral level of confidence at 95%.

The ratio, R_L, as given in equation 15:

$$R_L = \frac{L_2}{L_1} \qquad \text{Eq.15}$$

As per ISO 10904:2011 [57], after 50 soak-dry cycles, R_L shall not be less than 0.70.

3.4 Chapter summary

Particle size distribution of unprocessed CFA was determined by the wet sieving and Laser diffraction methods. CFA was fractionated by sieving through 45μm and 75μm test sieves. Low density CFA particles were extracted by the sink-float method using acetone as the medium where the solution with CFA was shaken in an orbit shaker and allowing the mixture settle. Then, the uppermost layer was taken. Thereby, four types of CFA

fractions were experimented in the study, they are, the unprocessed CFA, the CFA below 75 µm particle size, the CFA below 45µm particle size and the CFA particles extracted from wet separation method. All the CFA fractions were characterised with respect to SEM to analyse the surface morphology, elemental composition via XRF and the particle density with use of density bottle. Coal fly ash-cement mortar prisms were cast adopting the casting procedure in SLS 107: Part 2 [25] by replacing OPC in the percentages of 10%, 20%, 30%, 40% and 50% by weight. The 28 days flexural strength and the density of mortar prisms were determined. Alkali resistant glass fibres were used as the reinforcement in casting roofing tiles. Glass fibre reinforced fly ash-cement roofing tiles were cast as per the specification on MCR tiles given in SLS 1189: Part 1 [5]. In casting tiles , three CFA fractions were used which are the unprocessed CFA, the CFA below 75 µm particle size, the CFA below 45µm. OPC was replaced by 30% of CFA and the fibre content varied by 1% and 2% by weight. An unreinforced tiles incorporating unprocessed CFA was able to cast. Dimensional properties, impermiability, ring, pore and crack tests, transverse strength, mass, water absorption and density of the tiles were determined as per SLS 1189: Part 2 [6]. Thermal conductivity of the tile was measured using the Lee's disc apparatus, specific heat was measured by fabricating a laboratory calorimeter. Thermal diffusivity was also calculated. The cost was calculated in fabricating glass fibre reinforced fly ash-cement roofing tiles. Strength, water absorption and density of Calicut clay tiles, asbestos fibre cement corrugated sheets and non-asbestos fibre cement corrugated sheets were determined as per SLS 2:1975 "Specification for clay roofing tiles" [62], SLS 9: Part 2: 2001 "Specification for asbestos-cement products; Part 2: Corrugated sheets [63] and ISO 10904:2011 (E) "Fibre-cement corrugated sheets and fittings for roofing and cladding" [57], respectively and those properties were compared with glass fibre reinforced fly ash-cement roofing tiles. Thermal properties and costs were also compared. Leaching properties, and the long term durability were determined by conducting 50 soak-dry cycles as indicated in ISO 10904:2011(E) [57]. Finally a numerical model was developed correlating the fibre content and the flexural strength of glass fibre reinforced fly ash cement roofing tiles.

4 RESULTS AND DISCUSSION

4.1 Particle size distribution of coal fly ash

The morphology of CFA particles is controlled primarily by the combustion temperature and subsequent cooling rate. The tested CFA sample has a particle size distribution of 2-200μm as obtained by the results from the wet sieving, hydrometer (See *Table 4-1*, and *Figure 4.1*) and laser diffraction. The reviews done out by V.M Malhotra et al [20] and M Aboustait et al [64] suggested a typical range of 1-150μm. The result shows that CFA has a quite inhomogeneous composition, containing very coarse and very fine particles as in agreement with the analysis carried out by S. Shoumkova et al [17] and M. Thomas et al [15].

Table 4-1: Wet sieving and hydrometer test results of CFA

Diameter (mm)	Percentage passing
0.3	100.00
0.212	99.89
0.15	96.54
0.063	58.31
0.05560	58.31
0.03986	55.84
0.02893	50.91
0.02085	47.21
0.01545	37.34
0.01159	31.17
0.00846	23.78
0.00623	15.24
0.00453	9.32
0.00324	6.85
0.00231	4.39
0.00133	3.39
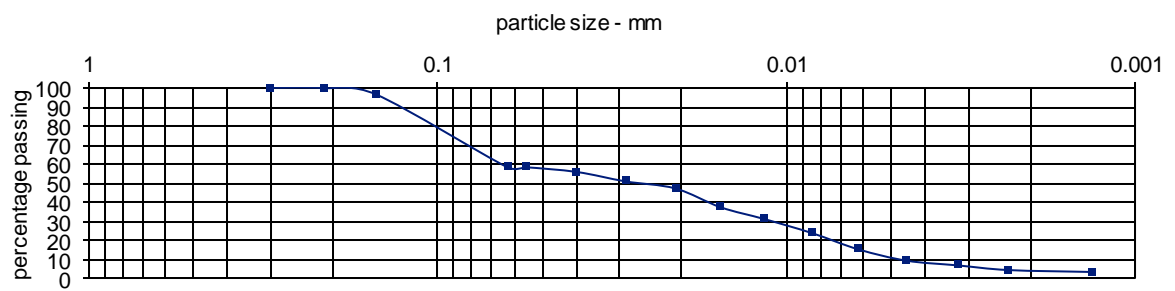
Figure 4.1*:* Particle size distribution of CFA

During the laser diffraction test, it was observed that the sample sedimentation rate was too high for CFA. Therefore, two samples were obtained after 30min and 60min sedimentation times in order to get the mean particle size. Due to the broad distribution of the particle sizes, a good quality test results could not be obtained by this technique. However, the averages of 3277nm and 2355nm were obtained after 30 minutes and 60 minutes sedimentation times, respectively. Hence, it can be said that the mean particle size of the tested CFA sample is 2 or 3μm. This result is closer with the median particle range obtained by M. Thomas et al [15], which is 5-20μm. The intensity (%) Vs Size (d.nm) are drawn in *Figure 4.2* and *Figure 4.3*.
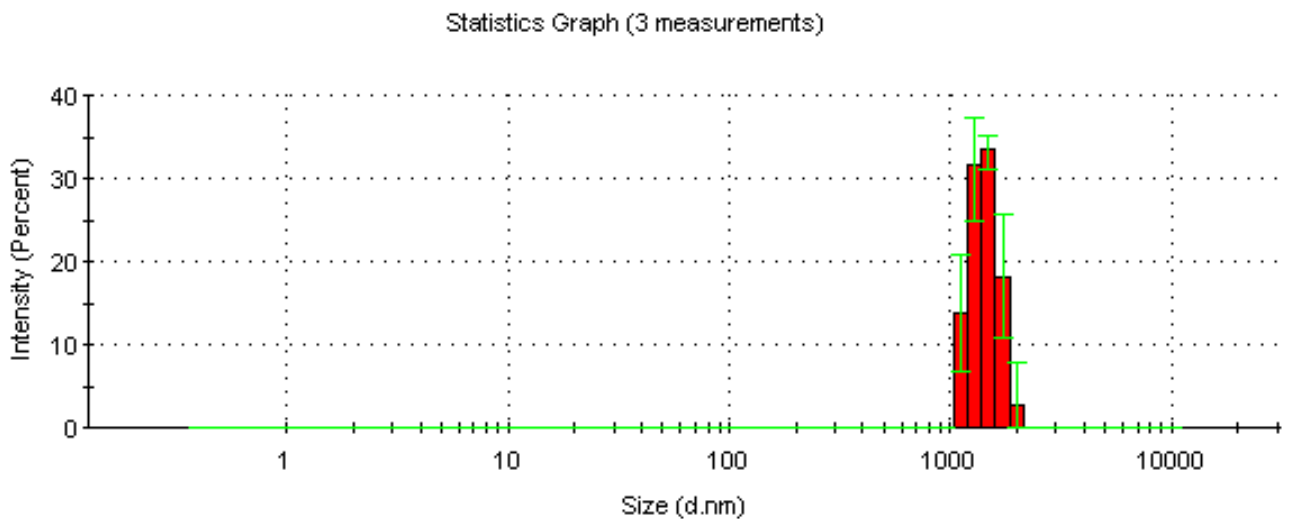
Figure 4.2: Statistics graph -laser diffraction test (after 30mins sedimentation time)
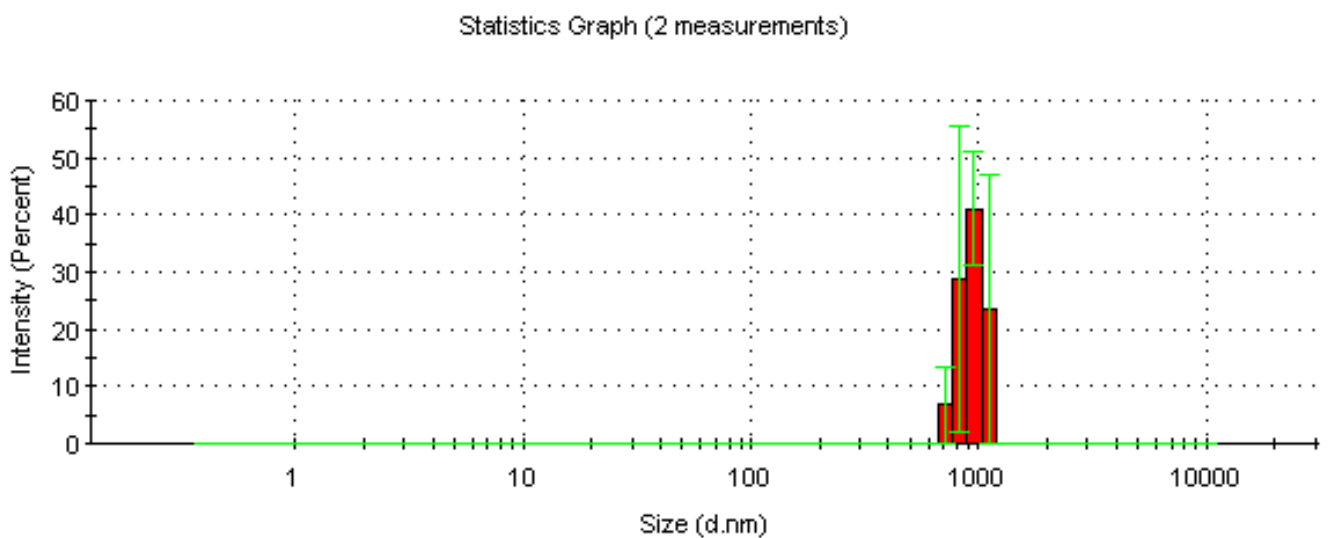
Figure 4.3: Statistics graph-laser diffraction test (after 60mins sedimentation time)

R.A Blisset et al [19] explained the coal fly ash particles formation in few steps where homogeneous condensation results in ash particles between 0.02 and 0.2 µm and fragmentation of included mineral matter results in the formation of particles between 0.2 and 10 µm. The excluded mineral matter undergoes a series of complex transformations to form predominantly spherical particles in the size range 10–90 µm.

4.2 Chemical composition

The unprocessed CFA has an elemental composition in the order Si> Al> P> Ca> S> Fe> Mg> Ti> K (See *Table 4-2*) while the typical coal fly ash oxide composition descend in the order of SiO_2> Al_2O_3> Fe_2O_3> CaO> MgO> K_2O [19] [22]. As described by R.S Blisset et al [19] the main reason for the variation between chemical compositions between different CFAs is due to the type of coal burned to produce it. However, the predominant elements present in this particular CFA sample is Si and Al. There is no significant difference in chemical composition among the four CFA fractions (the unprocessed CFA, the CFA below 75µm, the CFA below 45 µm and the CFA particles extracted from wet separation method) except the unburned carbon content given by LOI (See Table *4-2*). This particular CFA sample can be classified as Class F as described in ASTM C-618 "Standard specification for coal fly ash and raw or calcined natural pozzolan for use in concrete" [21], having a combined percentage of SiO_2 +Al_2O_3 +Fe_2O_3 above 70%. The chief difference between Class F and Class C fly ash is in the amount of calcium and the silica, alumina, and iron content in the ash. Due to the presence of high Al content in Class F fly ash compared with Class C fly ash, Class F has more amorphous alumino-silicate than Class C [18]. This amorphous content is reacted with the calcium hydroxide ($Ca(OH)_2$) produced during the cement hydration processes to form calcium-silicate-hydrates (C-S-H) gel and calcium aluminate-hydrates (C-A-H) gel [65].

Table 4-2: Chemical composition and particle density of CFA fractions

Elemental composition				
Element	Composition (%)			
	The unprocessed CFA	The CFA below 75µm particle size	The CFA below 45µm particle size	The CFA particles extracted from wet separation
Si	62.80	63.62	60.72	62.62
Al	29.20	28.29	32.71	32.28
P	2.30	3.00	2.70	2.30
Ca	4.11	3.55	3.52	3.02
S	1.34	0.81	1.59	1.25
Ti	0.32	0.30	0.29	0.30
Fe	0.45	0.29	0.22	0.31
K	0.17	0.18	0.17	0.16
LOI %	3.6	3.4	1.8	3.3
Si/Al	2.15	2.25	1.86	1.94
Physical properties				
Particle density (kg/m³)	2233	2455	2505	1805

4.3 Scanning electron microscopic analysis and particle density

The morphology of sieved CFA fractions studied by the SEM magnification is shown in Figure *4.4*. The examination of the morphology shows that the unprocessed CFA (See Figure *4.4(a)* and Figure *4.4(e)*) consists of spheres which could be solid or hollow (cenospheres) and irregular particles. According to the review paper written by R.A Blisset [16] on coal fly ash and its circular economy, the cenospheres, magnetic particles, and fine ash (fine improved fly ash residue(<45µm) and coarse improved fly ash residue (>45µm)) are primarily spherical in nature; in contrast the carbon is a larger porous structure exhibiting a more irregular shape.

As per the same author [16], cenospheres are enriched in SiO_2 and Al_2O_3 and contain the highest levels of mullite which is presumed to be in the form of fine crystalline needles within the skeletal wall of the cenosphere. The magnetic particles had a high level of Fe_2O_3 and are denser than the parent CFA but has a relatively low level of crystalline magnetite and hematite.

Carbon concentrate particles has a high level of organic material and can be observed to show a porous structure under SEM magnification. The residual ash fractions; fine improved and coarse improved are both largely amorphous aluminosilicates.

In this study, the spherical particle concentration increases with the decreasing CFA particle size. The unprocessed CFA (See Figure *4.4(a)* Figure *4.4(e)*) composes mostly of irregular shaped particles with a highly amorphous texture whereas the CFA below 75μm fraction (See Figure *4.4(b)* and Figure *4.4(f)*) consists of equal concentration of spherical particles with irregular particles. The CFA below 45μm (See Figure *4.4(c)* and Figure *4.4(g)*) consists mainly of spheres with a diameter in the range of 18-40μm. The CFA particles extracted from the wet separation method (See Figure *4.4(d)* and Figure *4.4(h)*) consists of relatively lager spheres (Max avg dia: 36μm) which is only second to the size of CFA particles below 45 μm (Max avg dia: 40μm).

The same pattern was observed in the study carried out by Jianglong Yu et al [66] on the characteristics of fly ash samples from two power stations (Eraring and Anshan) in Bulgaria in which, the SEM analysis showed that, most of the fine particles (<38.5μm) of both fly ash samples have round shape and are solid, indicating that they have experienced high temperatures and melting during coal combustion in boilers. Medium size particles (38.5-70μm) are also mostly round in shape and some particles are hollow. Large size fraction particles (>70μm) from Anshan fly ash are mostly irregular in shape, with some small particles either stick to the outer surface or inside the large cenospheres. The same correlation of finer the CFA higher the amount of spherical particles, has also shown by S. Shoumkova et al [17] by the characterization of CFA samples collected from Australia and China. As well as S.V. Vassilev et al [67] by examining fly ashes from eleven Bulgarian thermoelectric power stations.

These irregular particles present in the coarser fraction are unburned carbon because of the concentration of carbon content given by LOI is highest (3.6%) in the unprocessed CFA and subsequently decreasing in the order of the CFA below 75μm (3.4%), the CFA particles extracted from the wet separation method (3.3%) and the CFA below 45μm (1.8%) as shown in *Table 4-2*. This agrees with the suggestion given by James C. Hower et al [68] that dry sieving to remove unburned carbon because of the coarser fraction is

frequently contains as much as 50% of the total carbon present. Further, R.A Blisset et al [19] explained the irregular particles exceeding 90µm could be due to particle grouping in liquid and plastic states. Mutual germination of spheres, spheroids, debris, and other particles has also been suggested. The other possibility for particle sizes exceeding 90µm is that are made up of the organic constituent or the unburned coal (char) components. The coked and semi-coked are produced from the complete and partial melting of the various organic components, while the slightly changed particles are those which are exposed to temperatures no higher than 550 ℃. These slightly changed particles are typical for coarse-grained fractions over 100 µm in size. While the coked and semi-coked particles undergo melting and thus condense as spheres and spheroids, the coarser particles undergo incomplete oxidation, so they retain the irregularity of shape from the coal precursor [19].

The next question to answer is that in which CFA fraction (the unprocessed CFA, the CFA below 75µm, the CFA below 45µm and the CFA particles extracted from wet separation method) has the highest amount of cenospheres. This can be illustrated by three aspects which are the particle density with the morphology, particle size and the ratio of SiO_2/Al_2O_3.

I.   R.A Blissett [16] obtained the particle density of each CFA components as follows. Raw CFA: 2260-2300 kg/m^3, magnetic concentrate: 3470 kg/m^3, carbon concentrate: 1970 kg/m^3, fine improved fly ash residue: 2330 kg/m^3, coarse improved fly ash residue: 2190 kg/m^3 and cenospheres with densities of 857 and 1282 kg/m^3. Accordingly, the cenospheres are less dense than water and for this reason their collection methods are usually based on their ability to float. It also clear that the carbon is marginally less dense than the ash fractions, and the magnetite is much denser than the ash fractions. The high particle density of magnetite is due to the atomic weight of iron is heavier than both silicon and Aluminium.
The unique property of cenospheres is of its low particle density due to the thin walled hollow structure. The lowest particle density was observed in the CFA particles extracted from the wet separation method which is 1805 kg/m^3. Hence, it can be said that the low particle density of cenospheres has contributed to the overall particle density reduction in the said fraction.

In this study, in the sieved fractions, the spherical particle concentration increases in the order of the unprocessed CFA, the CFA below 75μm and the CFA below 45μm (See Figure *4.4*) while the particle density increases in the same order (2233, 2455 and 2505 kg/m^3) as shown in *Table 4-2*. The unburned carbon percentage also reduces in the same order as 3.6%, 3.4% and 1.8%.

The particle densities of all the CFA components may have contributed to the density of the unprocessed CFA but it can be said that, among them, carbon and coarse improved fly ash residue may have contributed majorly to the overall particle density reduction of the unprocessed CFA.

Highest particle density was observed in the CFA below 45μm fraction which consist of mainly spheres. These spheres could be cenospheres, magnetic spheres or fine improved fly ash residue. If they are magnetic spheres, the surface of the particle is much rougher and clear crystals can be observed which protrude from the surface. But as it can be seen in Figure *4.4* the observed spheres are smooth indicating that they could not be magnetic spheres. Thereby the increased particle density in the CFA below 45μm fraction could be due to the dense spheres or thick-walled cenospheres or fine improved fly ash residues. As per the literature [16] [66] fine improved fly ash residue is more denser due to the enrichment of some trace elements because the elements are volatilised in the combustion chamber and then condense on the surface of the CFAs. The smallest particles have the highest specific surface area and so are enriched preferentially on the smallest particles.

However, there exists a number of particles that may contribute to lower the particle density because they could be spongy or hollow, thick-walled or porous in nature.

Thereby, the particle density itself coal fly ash would be misleading to predict the presence of cenospheres without knowing the concentration of each CFA components in a particular CFA sample.

II.   S.V. Vassilev et al [61] said that the spheres could be dense and vesicular spheres, cenospheres and plerospheres while dermaspheres and ferrospheres are less common. The size of spheres is dominantly in the range 1-50μm. It may be why the spherical concentration was higher in the CFA below 45μm fraction in this study as well. The dense and vesicular spheres originate respectively from fully and partly degasificated

melts of various minerals. The cenospheres are thin-walled hollow spheres which are occasionally fragmented. They are larger (10-250 μm) than dense and vesicular spheres. In this study, the spherical diameter in the unprocessed CFA fraction is ranged approximately in 1-20μm while the CFA below 45μm fraction and the CFA extracted from wet separation method are ranged in 18-40μm and 3-36μm, respectively. Since the spherical particle diameter is bigger in the finer fraction than in the coarser fraction, the spheres in the finer fraction (< 45 μm) could be cenospheres

III. The chemical analysis carried out by Ling-ngee Ngu et al [37] indicated that the SiO_2/Al_2O_3 ratio of ash cenosphere decreases with increasing ash cenosphere size because a higher SiO_2/Al_2O_3 ratio indicates a lower ash sintering temperature. In other words, smaller ash cenospheres have lower sintering temperatures because of higher SiO_2/Al_2O_3 ratios. In the unprocessed CFA fraction and the CFA below 75μm fraction consist of comparably smaller spheres (Max avg dia: 20μm), have the SiO_2/Al_2O_3 ratios of 2.15 and 2.25 which are quite similar in values. The bigger spheres (Max avg dia: 40μm) consist in the CFA below 45μm fraction and the CFA particles extracted from the wet separation method, have the SiO_2/Al_2O_3 ratios of 1.86 and 1.94. This result correlates with what Ling-ngee et al concluded that bigger cenospheres have a low SiO_2/Al_2O_3 ratio.

So to conclude in which CFA fraction the cenospheres content is higher, again the three aspects are recapped. Aspect 1: With the relevant morphology and the lowest density, the CFA particles extracted from the wet separation may have the highest concentration of cenospheres. But the particle density itself may be misleading to interpret the highest cenospheres presence because there are other CFA components like unburned carbon which can also contribute to lower the density. Aspect 2: A larger spherical particle diameter (10-250μm) hints on the cenospheres presence. Hence, the spheres present in finer CFA (<45μm) and the CFA particles extracted from the wet separation method could be mainly cenospheres due to the larger spherical dimeters. Aspect 3: Lower ratio of SiO_2/Al_2O_3 gives a hint on ceneospheres presence. Hence, it can be said the finer CFA fraction (<45μm) and the CFA particles extracted from the wet separation method could be cenospheres.

The cenospheres could be identified by analysing the cross sectional view of particles by SEM. This can be achieved by monolayer pellet setting, controlled fine polishing, SEM, and image analysis as described by Ling-ngee Ngu et al [33]. The pellet specimen for SEM analysis is prepared by brushing a thin layer of epoxy resin on a finely polished epoxy pellet. The CFA sample of one of the narrow size fractions is then dispersed on the resin, in order to form a monolayer of ash particles on the pellet. After the resin solidified, ash particles within the monolayer is fixed and the contact points is aligned with the finely polished surface of the pellet.

4.4 Casting procedure of glass fibre reinforced fly ash-cement roofing tiles

In the premixing process, it was difficult to mix even at 2% (by volume) of fibre content. Increasing the mixing intensity to overcome such difficulties lead to have other adverse effects, such as fibre damage and separation of the strand into smaller units thus reducing the workability of the fresh mix. To increase the workability by going for higher W/C lead to poor dimensional stability of the green product. Therefore, mixing intensity and W/C ratios were carefully optimized.

When the green mix is carefully taken on to the corrugated mould, the corrugated areas tend to be thinning more than the perimeter. Therefore, when the tile is hardened the thickness of corrugated area is lesser than the perimeter.

4.5 Dimensional properties of glass fibre reinforced fly ash-cement roofing tiles

The dimensional properties comply with the requirements given in SLS 1189: Part 1:1999 "Specification for concrete roofing semi-sheets, tiles and fittings. Part 1: Requirements" [5] except hanging length because the nominal length of the mould used for casting tile was 490mm whereas the specification's nominal length is 500mm.The compliance of properties is shown in *Table 4-3*.
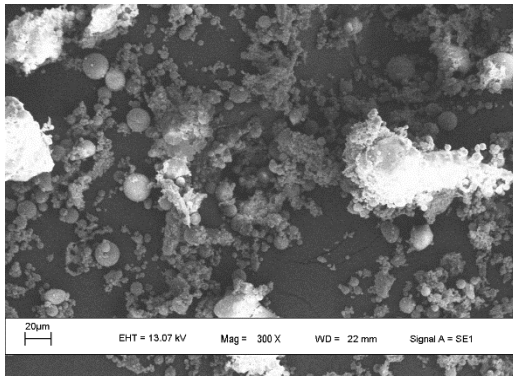
(a) Unprocessed CFA (300X)
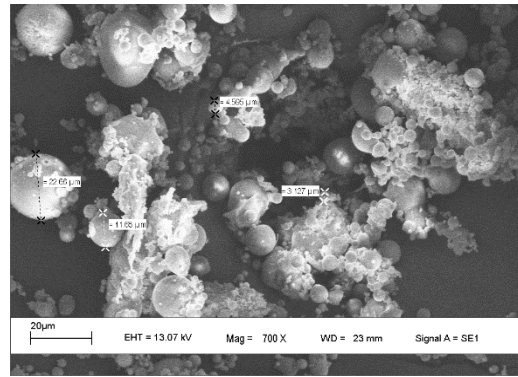
(e) Unprocessed CFA (700X)
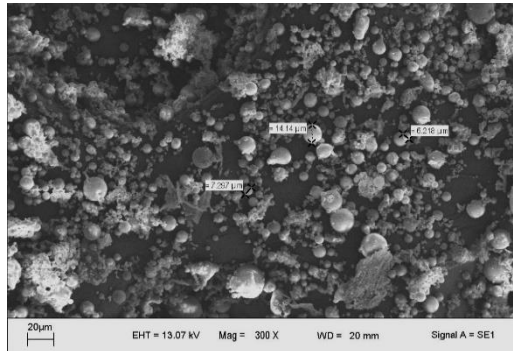
(b) CFA below 75μm size (300X)
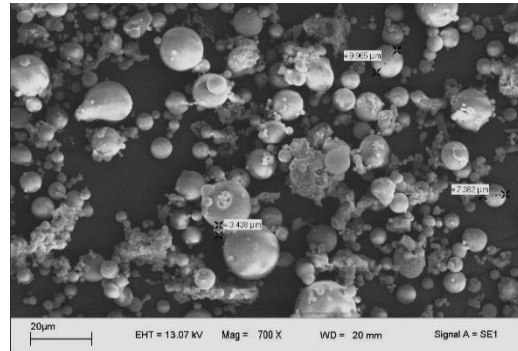
(f) CFA below 75μm size (700X)
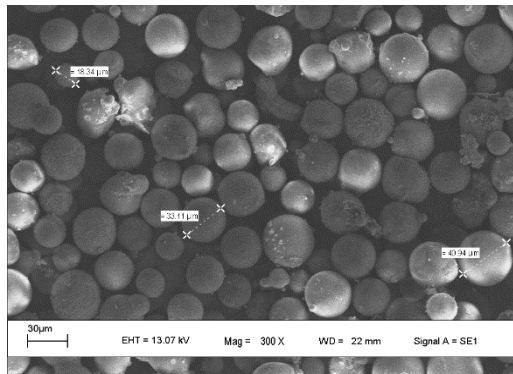
(c) CFA below 45μm size (300X)
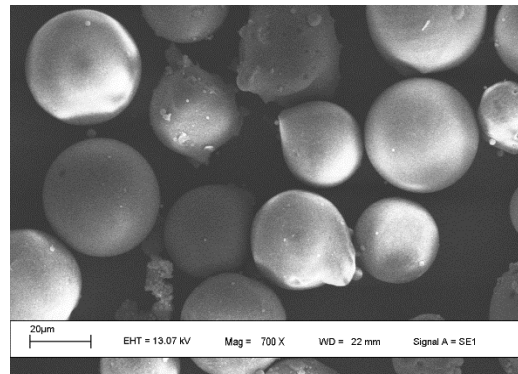
(g) CFA below 45μm size (700X)
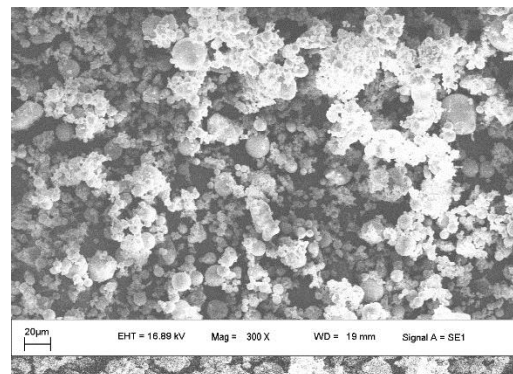
(d) CFA particles extracted from the wet separation method (300X)
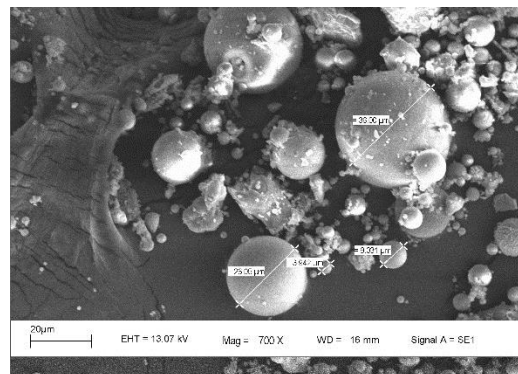
(h) CFA particles extracted from the wet separation method (700X)

Figure 4.4: SEM images of CFA fractions

Table 4-3: Dimensional properties

Property	Observed value	Specified value as per SLS 1189 [5]	Compliance
Hanging length	470±5mm	450±4 mm	See note [a]
Squareness	≤4 mm	≤4 mm	Pass
Thickness	8-9mm	6-9mm	Pass
Flatness	≤3mm	≤ 3mm	Pass
Nib support	Tile did not fall	Tile shall not fall	Pass
Shape of overlapping ends	≤3mm	≤3mm	Pass

[a] Nominal length of the mould was 490 mm , even though the standard nominal length is 500mm

4.6 Impermeability, "ring test" and "pore and crack" test of glass fibre reinforced fly ash-cement roofing tiles

During impermeability test, the water droplets did not form underside of the tile. During the "ring test", a clearing sound was produced. During "pore and crack" test defects such as surface pores deeper than 2mm, surface pores with a diameter greater than 5mm, more than three surface pores with a diameter greater than 2mm and visible cracks longer than 5mm did not observe.

Hence, the tiles are in compliance with the parameters of impermeability, "ring test" and "pore and crack" test

Table 4-4: Transverse strength, water absorption, density, mass and thermal conductivity of glass fibre reinforced fly ash-cement roofing tiles

Identification	Characteristic transverse strength(N)	Water absorption (%)	Density (g/cm^3)	Mass (kg)	Thermal conductivity (W/mk)
A	930	16	1.727	2.45±0.10	0.370
BF1	1450	21	1.625	2.30±0.20	0.310
CF1	1320	19	1.680	2.33±0.20	0.321
DF1	1240	18	1.684	2.33±0.20	0.338
BF2	1650	20	1.634	2.40±0.10	0.278
CF2	1580	20	1.651	2.45±0.10	0.325
DF2	1470	20	1.653	2.45±0.10	0.328

4.7 Strength of coal fly ash- cement composites

4.7.1 Flexural strength of coal fly ash-cement mortar prisms

The cast mortar prims having the dimensions of 40×40×160 mm are shown Figure *4.5*. The 28 days strength of those prisms are tabulated in

Table 4-5 and has graphically presented in Figure *4.6*.

Figure 4.5: Coal fly ash-cement mortar prisms

Table 4-5: Flexural strength of fly ash-cement mortar prisms (in Mpa)

Coal fly ash fraction	Coal fly ash content				
	10%	20%	30%	40%	50%
The unprocessed CFA	10.5	10.0	9.2	7.5	6.7
The CFA below 75μm particle size	9.4	9.0	8.1	7.0	6.0
The CFA below 45μm particle size	9.0	8.7	7.9	6.7	5.5
The CFA particles extracted from wet separation	8.5	8.0	6.0	4.2	3.5
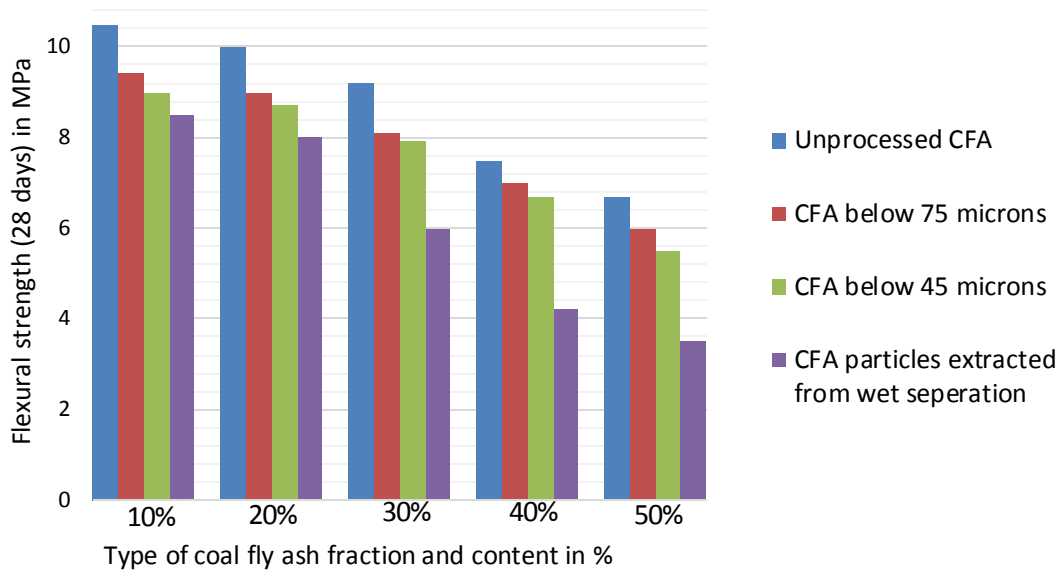
Figure 4.6: Flexural strength of coal fly-ash cement mortar prisms

Accordingly, with the increasing content of CFA (10% to 50%) regardless of the CFA fraction, the flexural strength decreased. Thereby, this particular CFA has acted as a filler rather than a binder. But for CFA added cementitious composites, 56 days strength has to be considered to obtain maximum strength development, because production of C-S-H is a slow process when amorphous silica in CFA is reacted with $Ca(OH)_2$

Further, with the decreasing CFA particle size the flexural strength decreased. In each set of CFA content, the highest flexural strength can be observed in the unprocessed CFA samples and lowest from the samples containing the CFA particles extracted from the wet separation method.

The reasons for strength variation of coal fly ash cementitious composites can be described by three aspects; which are the particle size of CFA, cenospheres content and the Ca content.

I. Firstly, when smaller the particle size of CFA higher the specific surface area which yields a high rate of reaction of coal fly ash. Hydration activity occurs on the surface of solid phases and through heterogeneous processes of diffusion and dissolution of materials in concentrated phases. Hence, smaller CFA shall contribute to the strength development. As expected, the study done by K. Erdoğdu et al [69] on the effect of

fly ash particle size on mortar strength, obtained higher compressive strength in the finer the size fraction used. But the results analyzed by V.M Malhotra et al [20] for the study carried out by Cabrera et al for 18 fly ash samples produced from bituminous coals by power stations in the United Kingdom, showed no relation between the 45μm sieve retention values and the 28d cube strengths of fly ash concretes. Wesche and vom Berg et al, also found no correlation between fineness and compressive strength of mortars at 7 or 28 d, from more than 340 tests on fly ashes from 14 sources, but found a minor correlation at 90 d. They believed that many fly ash related variables may influence strength development; poor correlation with particle size only indicate that particle size is not the dominant variables in fly ash reactivity. Why finer coal fly ash not contributing to the strength may be because the amount of amorphous silica could be lesser in the finer fraction. However, the researchers say thattTo establish a relationship with particle size, it is necessary either to limit all other variables to a minimum number or to perform multi variable experiment. Accordingly, coal fly ash used in this study, finer CFA does not contribute to the strength development.

II. Secondly, the presence of spheres in the finer fraction (<45μm) and the CFA particles extracted from the wet separation method which earlier predicted in section 4.3 as cenospheres may have contributed to lower the flexural strength. In the review carried out by Navid Ranjbar et al [30] , mentioned that incorporation of cenosphere reduces the density of the concrete and also reduces the mechanical properties.

III. Thirdly, the Ca content in the unprocessed CFA, the CFA below 75μm, the CFA below 45μm and the CFA particles extracted from the wet separation method are 4.11%, 3.55%, 3.52% and 3.02%, respectively. Hence, the Ca content in finer fractions (<45μm, <75μm) and the CFA particles extracted from the wet separation method are lower than the unprocessed CFA. Amir Fauzi el al [65] described that the high Ca fly ash consists of the glassy rich calcium-alumino-silicate and various kinds of crystalline phases which are not found in the low Ca fly ash. It is said that high Ca fly ash has higher reactivity compared to the low Ca fly ash which is due to the reaction of some crystalline content with the alkaline solution which has more reactive nature of calcium bearing glass. While, the low Ca fly ash consists of alumino-silicate glasses has various amounts of quartz, mullite, hematite and magnetite. These crystalline

phases are essentially passive. Hence, the low Ca content (in finer fractions and the CFA particles extracted from the wet separation method) could be another reason for the strength reduction in the composites.

4.7.2 Characteristic transverse strength of glass fibre reinforced fly-ash cement roofing tiles

For the fabrication of glass fibre reinforced fly ash-cement roofing tiles, an optimum CFA content of 30% was incorporated based on the literature data. Those are, in 2007, Amitabh Tayal [8] incorporated 25-35% by weight of fly ash for the manufacturing of asbestos fibre cement products. In 2006, Jagadesh Sunku [9] varied the fly ash content from 10%-40% to fabricate white Chrysotile asbestos fibre cement sheets. Sarthak Kuila [12] observed even at 16% of fly ash content an improved breaking load in micro concrete roofing tiles. G. Ramakrishna et al [13] obtained an optimum fly ash content of 20% for the production of fly ash- based sisal fibre roofing sheet. In 2015, Pardon K. Kuipa et al [14] investigated use of CFA in concrete roof tiles and results showed the possibility of substituting 20% of cement by fly ash.
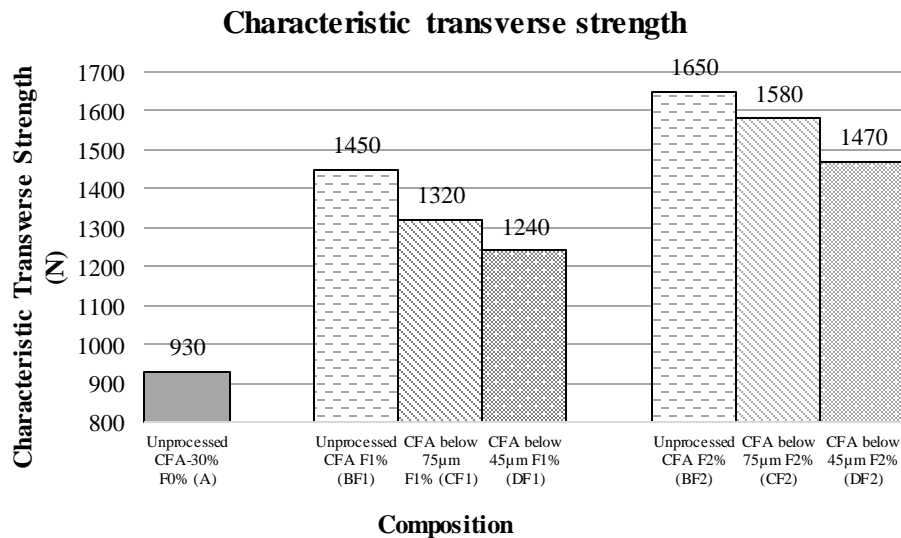
Figure 4.7: Characteristic transverse strength of glass fibre reinforced fly ash-cement roofing tiles

Plain, unreinforced cementitious materials are characterized by low tensile strengths, and low tensile strain capacities; that is, they are brittle materials [55]. Hence, to overcome this deficiency, fibre reinforcement was invented by scientists. In scientific aspect fibres

are not added to improve the strength, though modest increases in strength may occur [55]. But, the main role of fibre reinforcement is to control the cracking of fibre reinforced composite (FRC) and to alter the behavior of the material once the matrix has cracked, by bridging across these cracks and so providing some post-cracking ductility [55].

In this study, as shown in *Figure 4.7*, the transverse strength of the fibre reinforced tiles increased with increasing fibre volume. Kelly [70] has applied the following equations *(Eq.16 and Eq.17)* to describe the strength of the composite as a function of fibre volume, assuming efficiency factors of 1 for continuous and aligned fibres. The graph is shown in Figure *4.8*.

$$\sigma_{mu} = \sigma_{mu}{}^1 + n_l n_\theta \sigma_f{}^1 V_f \qquad \text{Eq.16 (for the lower fibre contents)}$$
$$\sigma_{cu} = n_l n_\theta \sigma_{fu} V_f \qquad \text{Eq.17 (for the higher fibre contents)}$$

Where,

$\sigma_{mu} = Stress\ in\ the\ matrix\ at\ first\ crack$
$\sigma_{mu}{}^1 = Tensile\ strength\ of\ the\ matrix\ in\ the\ absence\ of\ fibre$
$n_1 = Length\ efficiency\ factor\ of\ fibre$
$n_\theta = Orientation\ efficiency\ factor\ of\ fibre$
$\sigma_f{}^1 = Stress\ in\ the\ fibre\ at\ the\ first\ crack\ strain$
$V_f = Fibre\ volume\ content$
$\sigma_{cu} = Tensile\ strength\ of\ the\ composite\ (in\ the\ post\ cracking\ zone)$
$\sigma_{fu} = Tensile\ strength\ of\ the\ fibre$
$V_{f(crit)} = critical\ fibre\ volume\ content$

The fibres will contribute markedly to strength only when $V_f > V_{f\ (crit)}$. In this range, the mode of fracture is characterized by multiple cracking of the matrix. After first cracking, the load carried by the matrix is transferred to the fibres, which due to their sufficiently large volume can support this load without failure. Additional loading leads to more matrix cracking, which is still not accompanied by failure of the composite. In contrast, at $V_f < V_{f\ (crit)}$ the mode of failure will be by the propagation of a single crack, since there is an insufficient volume of fibres to support the load that was carried by the matrix as it cracked. As calculated by Arnon Bentur et al [55] , the critical fibre volume range for glass reinforced cements is 0.3% to 0.8%.
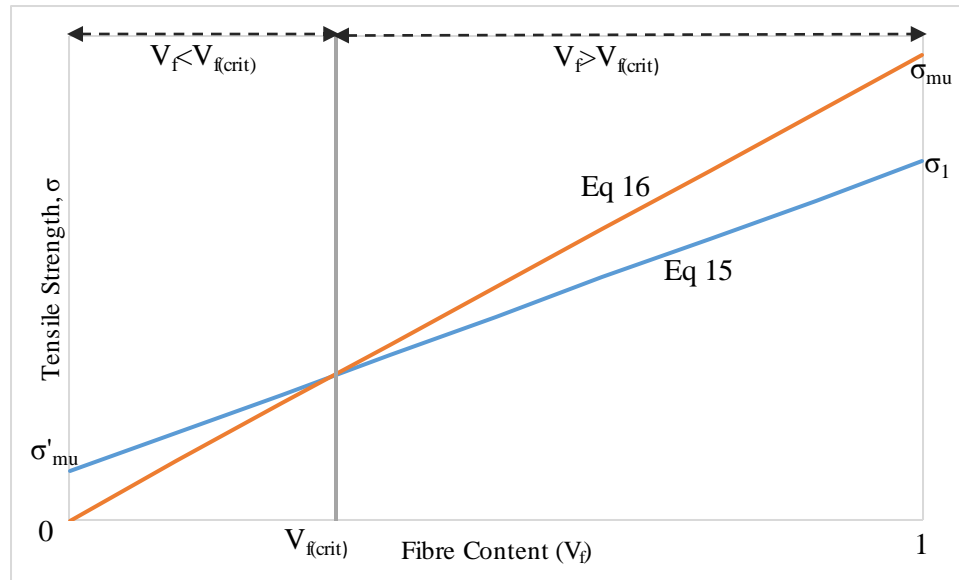
Figure 4.8: Relations between composite strength, σ_{cu}, and fibre volume content as predicted by Eqs 15 and 16, for continuous and aligned fibres (Kelly *[70]*).

If the orientation and length efficiency are taken into account, the critical fibre volumes will be considerably greater; increases by factors of about 3 or 6 are expected due to random orientation in two or three dimensions, respectively. Thus, in practice, the critical fibre volume is generally greater than 1-3%. This is in the range of the maximum fibre content that can be incorporated by conventional mixing procedures.

Further, with the decreasing CFA particle size transverse strength decreased. Highest characteristic transverse strength is observed in the unprocessed CFA sample which is 1650N and the lowest from the CFA below 45μm particle size sample which is 1240N. However, all the samples satisfy the strength requirement which is 230N.

The transverse strength reduction of the glass fibre reinforced fly ash-cement roofing tiles with respect to each CFA fraction is as same as described in section 4.7.1. Those influences are the particle size of CFA, cenospheres content and the Ca content.

A fracture surface of the glass fibre reinforced roofing tile is shown in *Figure 4.9*. Spherical particles and AR glass fibre being pulled out from the cement matrix can be observed.

Figure 4.9: Fracture surface of the AR glass fibre reinforced fly ash-cement composite

4.8 Density of fly ash-cement composites

4.8.1 Density of fly ash-cement mortar prisms

The apparent density of fly ash-cement mortar prisms is tabulated in Table *4-6* and has graphically presented in Figure *4.10*.

Table 4-6: Apparent density of fly ash-cement mortar prisms (in g/cm^3)

Coal fly ash fraction	Coal fly ash content				
	10%	20%	30%	40%	50%
The unprocessed CFA	1.743	1.572	1.468	1.350	1.288
The CFA below 75µm particle size	1.850	1.744	1.623	1.519	1.427
The CFA below 45µm particle size	1.920	1.810	1.700	1.599	1.510
The CFA particles extracted from wet separation	1.556	1.425	1.347	1.299	1.090
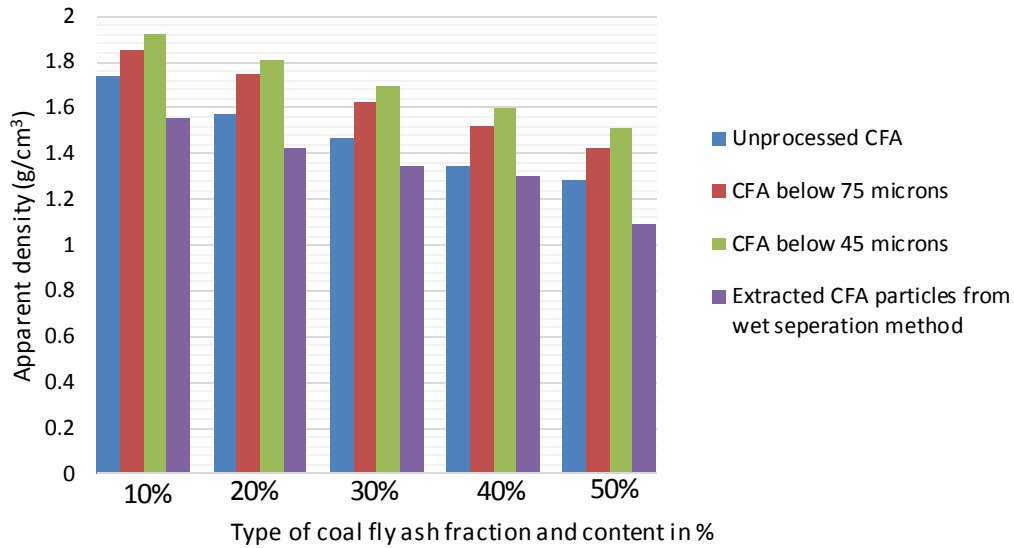
Figure 4.10: Apparent density of fly-ash cement mortar prisms

Accordingly, with the increasing content of CFA (10% to 50%) regardless of the fraction, the density is decreased. Because in particular CFA is a lightweight material.

The density reduction pattern of the composites are as similar with the pattern observed of the particle density reduction of each CFA fraction where the particle density descend in the order of the extracted CFA particles from the wet separation method> the unprocessed CFA> the CFA below 75µm> the CFA below 45µm. Thereby, the lightest composite was obtained from incorporating particles extracted from the wet separation method. As described in section 4.3, this particular CFA fraction may have consisted of cenospheres and unburned carbon which have majorly contributed to the overall particle density reduction. The particle densities of all the CFA components (cenospheres, magnetic spheres, unburned carbon, improved fly ash residues) may have contributed to the density of the unprocessed CFA but it can be said that, among them, carbon and coarse improved fly ash residue may have contributed majorly to the overall particle density reduction of the unprocessed CFA. Since, the finer fraction (<45µm) assumed to be solid or thin walled spheres may be the reason for the possession of higher particle density among all the other CFA fractions.

4.8.2 Density of glass fibre-reinforced fly ash cement roofing tiles

The density variation of the glass fibre reinforced fly ash-cement roofing tiles (See Figure *4.11)* are also as same as the density variation observed in the fly ash-cement mortar prisms where the density is increased with the decreasing particle size of CFA. But, the reinforced tiles are lighter than the unreinforced prisms because the AR glass fibres have also a similar density values like CFA which is 2.78 g/cm^3 which has contributed to the overall density reduction of the tiles. Compared to 1% fibre content, 2% fibre incorporated tiles delivered lower density due to the effect of the low density of AR glass fibres.

.
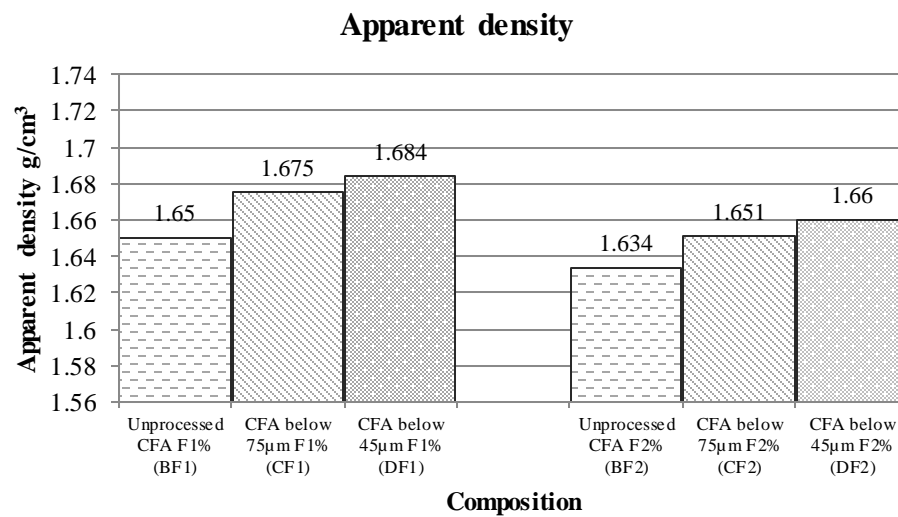
Apparent density

Figure 4.11: Apparent density of glass fibre reinforced fly ash-cement
roofing tiles

4.9 Water absorption

Inclusion of fibres increased the water absorption of glass fibre reinforced fly ash-cement roofing tiles (See *Table 4-4* and Figure *4.12).* It was expected to increase the water absorption with increased fibre due to the creation of interstitial voids between fibre-matrix interfaces. However, there is no significant difference in the water absorption in terms of fibre percentage. The glass fibre reinforced fly ash-cement roofing tiles did not comply with requirement for the water absorption as specified in SLS 1189: Part 1:1999 "Specification for concrete roofing semi-sheets, tiles and fittings. Part 1: Requirements" [5] which is less than or equal to 10%.

Water Absorption
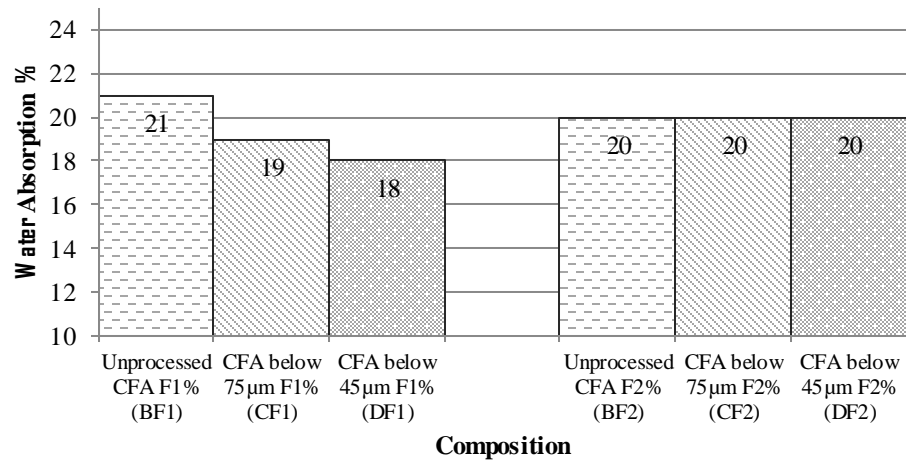
Figure 4.12: Water absorption of glass fibre reinforced fly ash-cement roofing tiles

4.10 Thermal properties

Table 4-7: Thermal properties of roofing materials

No	Roofing Material	Density (ρ) (kg/m^3)	Thermal conductivity (k) (W/mK)	Specific heat (c) (J/kg.K)	Thermal diffusivity (α) (m^2/s)
1	Calicut clay tile	1790	0.7106	973	4.08×10^{-7}
2	Asbestos fibre cement corrugated sheet	1645	0.4733	1482	1.94×10^{-7}
3	Non asbestos fibre cement corrugated sheet	1582	0.2135	1215	1.11×10^{-7}
4	**Glass fibre reinforced fly ash-cement roofing tile** (30% the unprocessed CFA with 2% fibre)	1634	0.2780	1296	1.31×10^{-7}

Thermal insulation is the easiest and most efficient way to limit global climate change and carbon emissions today. Thermal insulation reduces energy consumption of heating and cooling systems, reduces costs and adds comfort and hygiene [71].

This aims to investigate the thermal properties of the roofing materials with respect to the thermal conductivity k, specific heat c and thermal diffusivity α that describes heat transport through material. The test results are tabulated in Table *4-7*.

4.10.1.1 Thermal conductivity

Thermal conductivity k, is a measure of the rate at which energy is transferred by the diffusion process due to random molecular motion. It depicts of how readily a material can conduct heat. Hence, low thermal conductive materials give better thermal insulation.

Heat is transported in solid materials by both lattice vibration waves (phonons) and free electrons. A thermal conductivity is associated with each of these mechanisms, and the total conductivity is the sum of the two contributions, or [58]

$k = k_l + k_e$ where k_l and k_e represent the lattice vibration and electron thermal conductivities respectively; usually one or the other predominates [58].

Thermal conductivity is very sensitive to the microstructure of the material. It is strongly influenced by such factors as mineral composition, degree of crystallinity, impurities in the crystal structure, average grain size, grain orientation and porosity [72].

The thermal conductivity of insulating systems depends not only on the material's atomic and molecular structure but also on its surface radiative characteristics and porosity.

As per the test results (See Figure *4.13*), the lowest thermal conductivity was observed in non-asbestos fibre cement corrugated sheets and second in glass fibre reinforced fly ash-cement roofing tiles. Highest thermal conductivity value is possessed by Calicut clay tiles. Hence with respect to the thermal conductivity, non-asbestos fibre cement corrugated sheet is the better thermal insulator having low thermal conductivity amongst all. But the second best thermal insulator with regard to the thermal conductivity is the glass fibre reinforced fly ash-cement roofing tiles.
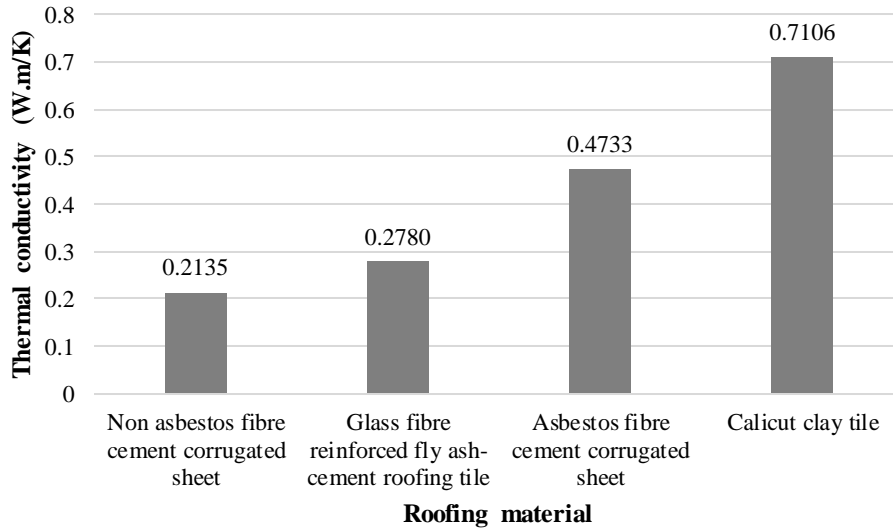
Figure 4.13: Comparison of thermal conductivity of different roofing materials

It is said that the thermal conductivity of crystalline silica is about 15 times that of amorphous [73]. In crystalline solids, crystals are made of atoms in an ordered and periodic array over a length scale much larger than the lattice constant. Vibration on one or a group of atoms will be transmitted as waves through the whole crystal. These lattice vibration waves carry energy and are responsible for thermal energy transport in crystalline solids. Unlike crystals, amorphous materials lack the translational symmetry and periodicity over a long distance [72] [74]. That is why the thermal conductivity of crystalline silica is higher than that of amorphous.

Additionally, several researchers [73] have reported that the thermal conductivity decreased due to the density decreasing of concrete. Lu-shu et al [73] experimentally formulated a correlation between the density and thermal conductivity, and reported that the thermal conductivity increased with increasing density. Thus, the presence of hollow structured spherical shaped cenospheres in CFA could reduce the density of the composites which ultimately helps in reducing the thermal conductivity of glass fibre reinforced fly ash-cement roofing tiles.

Hence, the reduction in thermal conductivity of the glass fibre reinforced fly ash-cement roofing tiles by means of CFA is probably related to the, the lower particle density, partly to the amorphous structure of CFA [75] and due to the presence of cenospheres in CFA.

Besides, ceramic materials are thermal insulators in as much as they lack large numbers of free electrons. Thus the phonons are primary responsible for thermal conduction and they are not as effective as free electrons in the transport of heat energy as a result of the inefficient phonon scattering by lattice imperfections [58].

Thermal Conductivity
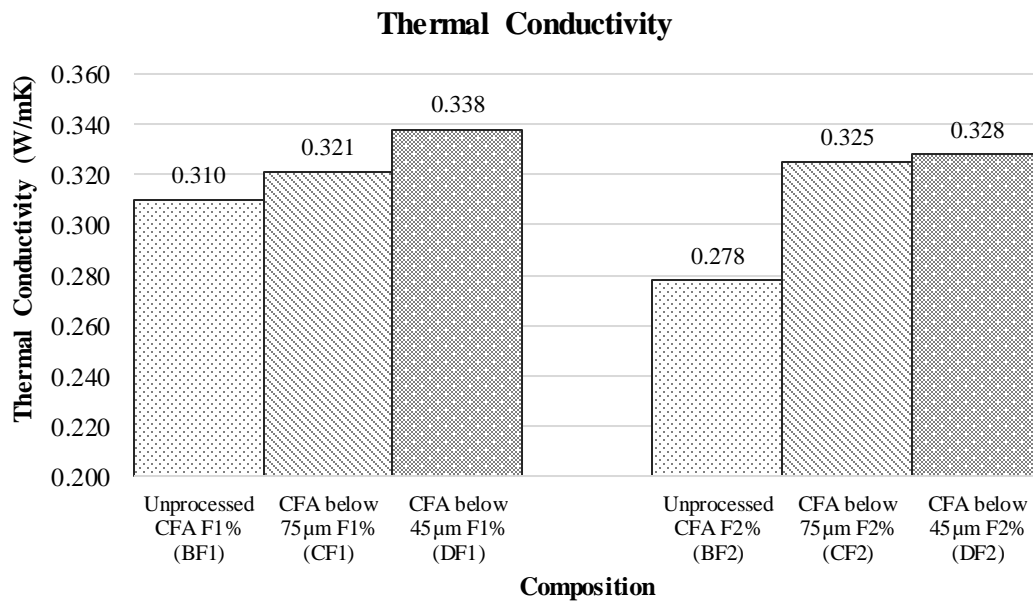
Figure 4.14: Thermal conductivity of glass fibre reinforced fly ash-cement roofing tiles

Further, the thermal conductivity of glass fibre reinforced fly ash-cement roofing tiles in 2% fibre content was lower compared to that of 1% fibre content (See Figure *4.14*). AR glass fibres typically have a chemical composition of 71% SiO_2. A typical inorganic glass consists of an amorphous silicon–oxygen network [55]. Hence, the increase of amorphous silica due to the addition of AR glass fibres may have led to the reduction of thermal conductivity.

4.10.1.2 Specific heat

The specific heat of water, stainless steel container and the Aluminum stirrer were taken as 4186 J/kg.K, 460 J/kg.K and 870 J/kg.K, respectively. Firstly, the specific heat and

density of a clay brick was measured and compared with literature to confirm the reliability of the fabricated calorimeter. The comparison of data confirmed that the used calorimeter provides reliable test results (See *Table 4-8*).

Table 4-8*:* Comparison of density and specific heat of clay brick

Material	Density (kg/m^3)	Specific heat (J/kg.K)	Reference
Clay brick	1920	835	[59]
	-	920	
Clay brick tested in the study	1819	956	This study

The specific heat capacity of a material is the amount of heat needed to raise the temperature of 1kg of the material by 1K (or by 1°C). A good insulator has a higher specific heat capacity because it takes time to absorb more heat before it actually heat up (temperature rising) to transfer the heat [59].

In solid materials, atoms are constantly vibrating at very high frequencies and with relatively small amplitudes. Then lattice waves are produced in a crystal by means of these atomic vibrations. These vibrational thermal energy for a material consists of a series of elastic waves having a range of distributions and frequencies [58].
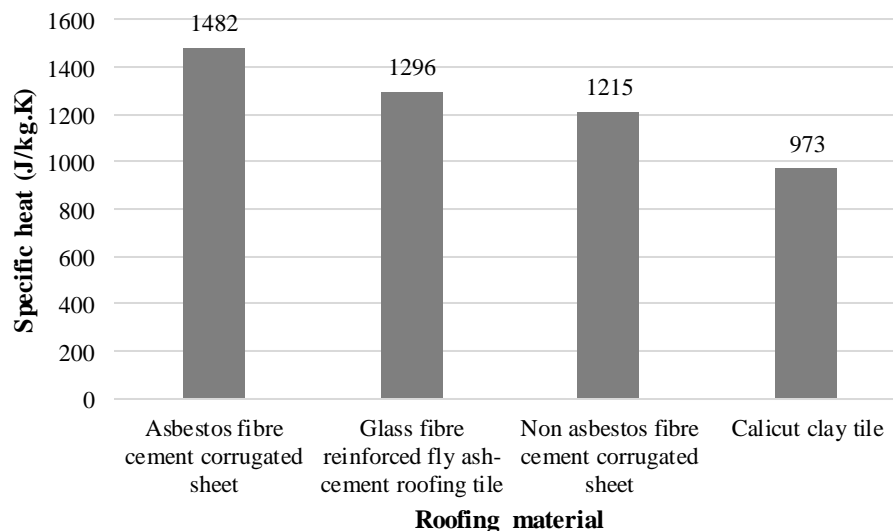
Figure 4.15: Comparison of specific heat of different roofing materials

As shown in Figure *4.15*, the highest specific heat was observed in asbestos fibre cement corrugated sheets and then in glass fibre reinforced fly ash-cement roofing tiles. Least in

Calicut clay tiles. Hence, with respect to the specific heat, asbestos fibre cement corrugated sheet is the better thermal insulator having higher specific heat among all. But the second best thermal insulator with regard to the specific heat is the glass fibre reinforced fly ash-cement roofing tiles. The comparably high specific heat of glass fiber reinforced fly ash-cement roofing tiles could be is due to higher specific heat carrying capacity of coal fly ash particles [76] [77].

4.10.1.3 Thermal diffusivity

Thermal Diffusivity measures the ability of a material to conduct thermal energy relative to its ability to store thermal energy. Insulators have low thermal diffusivity.
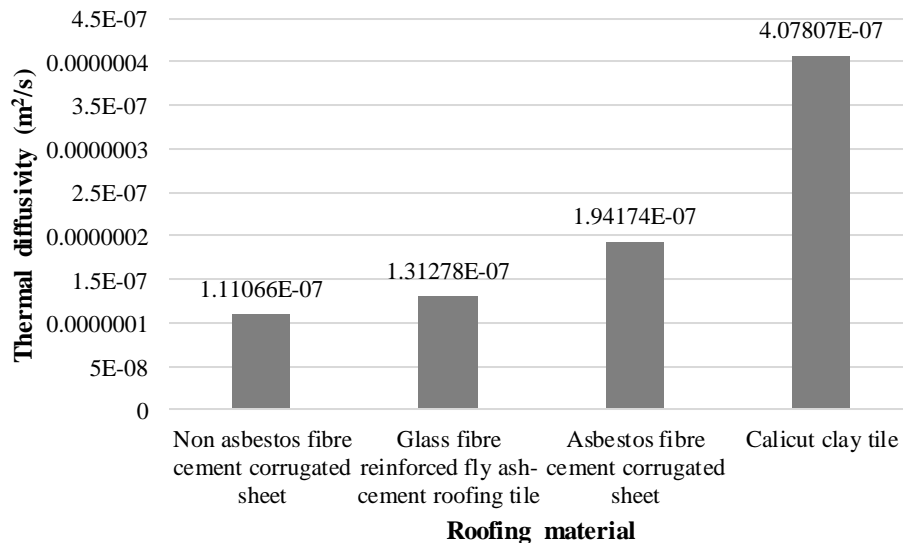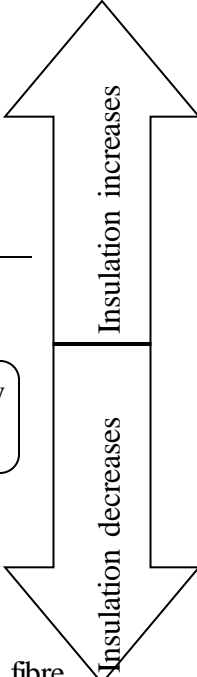
Figure 4.16: Comparison of thermal diffusivity of different roofing materials

As shown in Figure *4.16*, the lowest thermal diffusivity was observed in non-asbestos fibre cement corrugated sheets and then in glass fibre reinforced fly ash-cement roofing tiles. Highest in Calicut clay tiles. Hence, with respect to the thermal diffusivity, non-asbestos fibre cement corrugated sheet is the better thermal insulator having lower thermal diffusivity among all. But the second best thermal insulator with regard to the thermal diffusivity is the glass fibre reinforced fly ash-cement roofing tiles. This is may be due to low thermal conductivity, low thermal expansion and high specific heat capacity of the composite [76].

As a summary, the thermal insulation can be graphically demonstrated as follows

Thermal conductivity	Specific heat	Thermal diffusivity
1.Non asbestos fibre cement corrugated sheet	Asbestos fibre cement corrugated sheet	Non asbestos fibre cement corrugated sheet
2.Glass fibre reinforced fly ash-cement roofing tile	Glass fibre reinforced fly ash-cement roofing tile	Glass fibre reinforced fly ash-cement roofing tile
3.Asbestos fibre cement corrugated sheet	Non Asbestos fibre cement corrugated sheet	Asbestos fibre cement corrugated sheet
4.Calicut clay tile	Calicut clay tile	Calicut clay tile

Insulation increases

Insulation decreases

Considering the three thermal properties (k, c and α), it can be concluded that glass fibre reinforced fly ash-cement roofing tiles as a good thermal insulator due to the high specific heat, low thermal conductivity and diffusivity compared with the other roofing materials. But Calicut clay tiles also offer good thermal comfort to dwellings, even though the thermal insulation is not depicted by k.c and α. This is because clay tiles have this natural system to gradually lower the air temperature through the process of evaporation. Based on the 'bio air-conditioning', the porous surface acts as a heat exchange; it absorbs water from the inside and sends it to the outer surface. On contact with air, the water evaporates [78]

Thermal insulation is one of the easiest and most efficient way to limit global climate change and carbon emissions today. When used appropriately, savings of up to 50% can be achieved [71], and higher energy efficiency is possible with higher levels of insulation. Thermal insulation reduces energy consumption of heating and cooling systems, reduces costs and adds comfort and hygiene.

In commercial aspect, the thermal performance of a roofing material is determined by Solar reflectance and Thermal emittance which are graphically represented in Figure *4.17*. Solar reflectance is the ability of a roof to reflect the solar energy and accompanying heat, preventing it from entering the attic space. The higher the solar reflectance index (SRI) value, the less additional heat will seep in [79].
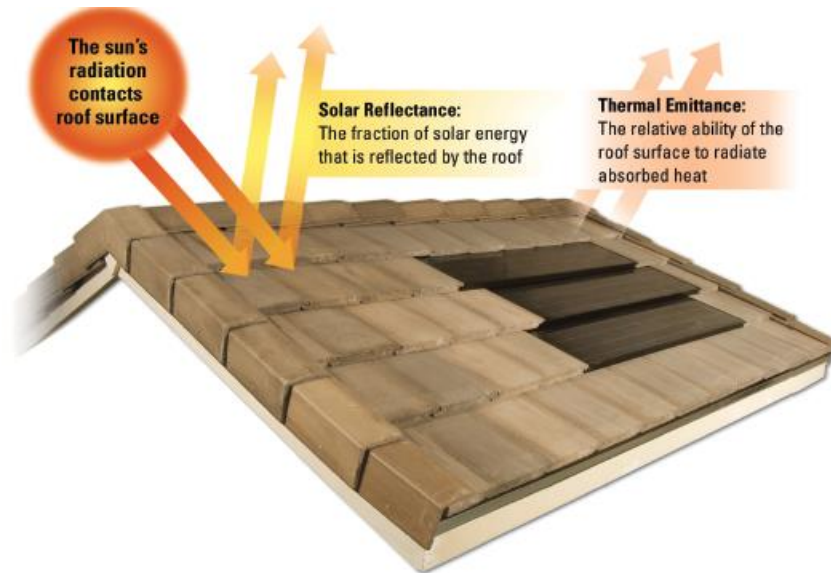
Figure 4.17*:* Solar reflectance and thermal emittance in graphical representation *[79]*

SRI values vary depending on the desired color, reflective coating and roof angle. SRI value is greater for lighter colors hence lesser the heat transferred into the building. A roof with a high SRI value is more economical to operate since less heat will be absorbed into the building through the roof which reduces the requirement for air conditioning and refrigeration in the building.

Roofing materials with high thermal emittance values are also more economical to operate because they reduce the loads of the Heating, ventilation and air conditioning (HVAC) systems.

4.11 Leaching properties

Leaching of heavy metals were compared with the glass fibre reinforced roofing tile with the composition of 30% of the unprocessed CFA with 2% of AR glass fibres, with commercially available non-asbestos fibre cement corrugated sheets. The reason for taking this particular composition was that is comprised of maximum amount of fibre content (2%) used along with the unprocessed CFA where maximum amount of chemical constituents are present. The results are tabulated in Table *4-9*

According to the results, only a fewer number of heavy metals have been leached from glass fibre reinforced fly ash-cement roofing tile sample compared with the non-asbestos fibre cement corrugated roofing. However, the leaching amount of Cr from glass fibre

reinforced fly ash-cement roofing tile surpassed the limit specified by Environment Protection Authority (EPA) of USA [80]. Since the chemical composition of the unprocessed CFA and AR glass fibre do not indicate any Cr content, this element must have come from cement or water used for the production of tiles. The leaching of As from non-asbestos fibre cement corrugated roofing sample has surpassed the limiting value. The health effects indicated by EPA, higher Cr consumption in drinking water would lead to allergic dermatitis and As would lead to skin damage or problems with circulatory systems, and may have increased risk of getting cancer. However, commercially available non-asbestos fibre roofing and the tiles in this research possess some leaching constituents.

Table 4-9: Leaching of heavy metals comparison

Test/unit (mg/L)	Limit of detection	Glass fibre reinforced fly ash-cement roofing tiles	Non-asbestos fibre cement corrugated roofing sheets	EPA (Maximum contaminant level for drinking water) [80]
Cd	0.02	Not detected	Not detected	0.005
Pb	0.01	Not detected	Not detected	0.000
Mn	0.01	Not detected	0.55	-
Cr	-	**0.25**	0.04	**0.1**
Co	0.01	Not detected	0.02	-
Hg	0.001	Not detected	Not detected	0.002
As	0.001	Not detected	**0.09**	**0.01**
Be	0.01	Not detected	Not detected	0.004
Se	-	0.002	0.04	0.05
B	1	Not detected	5.1	-
Mo	-	0.07	0.01	-
Sr	-	6.6	0.93	-
V	-	0.02	0.11	-

4.12 Durability test by Soak-dry method

Soak dry test is an indication of the long term durability of a roofing material. Many of the long-term performance problems of fibre reinforced cement composites are rather induced by volume changes in the material, due to temperature and humidity changes. Volume changes which are induced in natural exposure due to wetting and drying may cause internal damage due to micro cracking [55]. Damage of this kind might be expected to be greater for testing under restrained conditions where internal stresses of greater magnitude are expected to occur as the result of the restrained volume changes [55].

The soak dry test performed as per ISO 10904:2011 "Fibre-cement corrugated sheets and fittings for roofing and cladding" [57] ; the value shall not be less than 0.70 after 50 soak-dry cycles. The calculated value for glass fibre reinforced fly ash-cement roofing tile is 0.75. Thereby, the durability of the tile is satisfied.

This improvement of long term durability has been due to the fibre reinforcement by Alkali resistant glass fibre and the matrix modification by the inclusion of CFA.

Degradation of fibres by chemical attack can result from two types of processes [55]:

i. direct attack by the cementitious matrix due to reactions with the highly alkaline pore water (pH>13) or

ii. attack by external agents which penetrate through the cementitious matrix into the fibre

As described by Arnon et al [55] alkaline degradation has been known to occur in glass fibres. Beyond 24 h or so, the pore solution is dominated by sodium (Na^+) and potassium (K^+) ions, which originate principally from the OPC, together with hydroxyl ions (OH^-) to maintain electro neutrality [15]. The concentration of hydroxyl ions increases with the alkali content of the OPC and is generally in the range of pH 13.3–14.0. Exposure of the E-glass fibres to this high alkalinity leads to a rapid deterioration process which involves strength and weight losses, and reduction in the filament diameter. This process can be attributed to breaking of the Si−O−Si bonds in the glass network, by the OH− ions which are highly concentrated in the alkaline pore solution:

$$-\overset{|}{\underset{|}{Si}}-O-\overset{|}{\underset{||}{Si}} \quad +O\bar{H} \rightarrow \overset{|}{\underset{|}{Si}}-OH + SiO^- \text{(in-solution)}$$
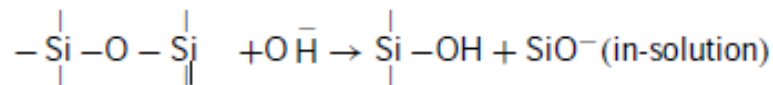
To overcome this the durability problem, alkali resistant glass fibre were developed by scientists by the incorporation of ~16% ZrO_2 in the glass composition. The Zr-O bonds, in contrast to Si-O bonds, are only slightly attacked by the OH− ions, and thus the incorporation of ZrO_2 as part of the network imparts stability to the glass structure in the alkaline environment, that is, considerably reduces the network breakdown.

89

This can be either the result of an overall improvement in the stability of the glass network when ZrO$_2$ is present, or the formation of a ZrO$_2$-rich protective surface layer as some SiO$_2$ is broken down and extracted. The undissolved ZrO$_2$- rich layer thus formed remains on the glass and may serve as a diffusion barrier to reduce the rate of further attack. Microanalysis of the AR glass surface has confirmed the formation of a ZrO$_2$-rich layer after ageing in a cement paste while bulk analysis did not show any appreciable change in the ZrO$_2$/SiO$_2$ ratio. As a more complex characteristics of the surface layer, involves interactions with the Ca in the pore solution: the Ca/Si and Zr/Si ratios of the surface layer increase with time and there is some evidence for the formation of calcium silicate hydrogel which may bear some similarity to the hydration product of cement.

Primary chemical reactions during cement hydration are as follows [81];

$$2(3CaO.SiO_2) + 6H_2O \rightarrow 3CaO.2SiO_2.3H_2O + 3Ca(OH)_2$$

$$2(2CaO.SiO_2) + 4H_2O \rightarrow 3CaO.2SiO_2.3H_2O + Ca(OH)_2$$

$$3CaO.Al_2O_3 + 12H_2O + Ca(OH)_2 \rightarrow 3CaO.Al_2O_3.Fe_2O_3.12H_2O$$

$$4CaO.Al_2O_3.Fe_2O_3 + 10H_2O + 2Ca(OH)_2 \rightarrow 6CaO.Al_2O_3.Fe_2O_3.12H_2O$$
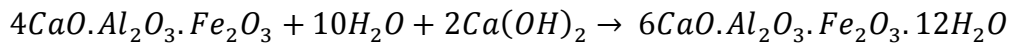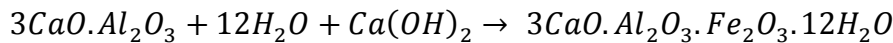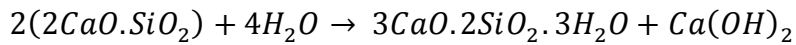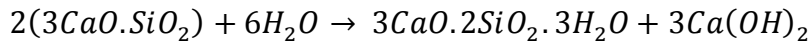
C-S-H ($3CaO.2SiO_2.3H_2O$) is the principal cementing compound in produced in the hydration and is largely responsible for providing strength and other desirable properties [15]. But weaker calcium hydroxide does not contribute to strength.

In ordinary Portland cement, the amorphous silica content is not enough to transform all the calcium hydroxide present into C–S–H gel. This excess of calcium hydroxide is desirable for steel-reinforced concretes but increased alkalinity of the medium is a drawback durability in fiber cement composites, thus necessitating calcium hydroxide to be reduced or removed from the medium [82]. Hence, the addition pozzolanic compounds like CFA comprised of amorphous silica, to the cement paste promotes the transformation of calcium hydroxide into C–S–H gel. This reduces the alkalinity and increases the strength thereby improving the durability of the cement composite [15] [82].

The pozzolanic reaction between the calcium hydroxide and the amorphous silica in CFA, producing C-S-H is as follows;

$$Ca(OH)_2 + SiO_2 + H_2O \rightarrow CaO.2SiO_2.3H_2O$$
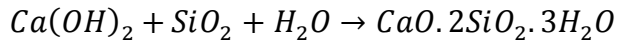
4.13 Cost calculation for the production of glass fibre reinforced fly ash-cement roofing tiles

The actual cost incurred during the production of glass fibre reinforced fly ash-cement roofing tiles was calculated. For that, cost for electricity (mixing and vibration), cost for materials (cement and AR glass fibre) and human capital (to cast tiles) were taken into account. The cost of the tile is 117 Rs per Sq.ft. The cost breakdown is elaborated as follows.

Cost calculation for glass fibre reinforced fly ash-cement roofing tiles

In making 35 tiles

1. **Energy cost**

Power consumption of the electric mixer	0.85	kW
Mixing time for 5 tiles	7/60	h
Mixing time for 35 tiles	49/60	h
No of units consumed by electric mixer	0.69417	kWh
Energy cost for mixing (on domestic rate base)	**1.32**	**Rs**
Power consumption of the vibrating table	0.24	kW
Vibrating table operating time for 1 tile	1/60	h
Vibrating table operating time for 35 tiles	35/60	h
No of units consumed by vibrating table	0.14	kWh
Energy cost for vibration (on domestic rate base)	**0.27**	**Rs**
Total energy cost (Mixing & vibration)	**1.58**	**Rs**

2. **Materials cost**

No of cement bags required for 35 tiles	1	bag
Unit cost for cement	910	Rs/bag
Cost for cement	910	Rs
Cost of coal fly ash	0	Rs

Glass fibre required for 35 tiles	1.4	kg
Unit cost for glass fibre	1450	Rs/kg
Cost for glass fibres	2175	Rs
Total materials cost (cement & glass fibre)	**3085**	**Rs**

3. <u>Labour cost</u>

Labour involvement	2	labours
Time involvement to make 35 tiles	2	hours
Unit cost of labour (For half a day)	500	Rs
Total labour cost	**1000**	**Rs**

4. <u>Total cost</u>

Total energy cost (mixing & vibration)	1.58	Rs
Total materials cost	3085.00	Rs
Total labour cost	1000.00	Rs
Cost for 35 tiles	4086.58	Rs
Cost per tile	**116.76**	**Rs**

	9 tiles for 8.2482 Sq.ft	
	1.1 tiles per Sq.ft	
Cost of covering per Sq.ft	**116.76**	**Rs**

The cost comparison between different roof coverings is tabulated in Table *4-10*. Accordingly, the most costly roof covering is the AR glass fibre reinforced roofing tile in this study which could be unappealing in the commercial aspect. It was noted during the cost calculation that a 53% of cost comes from the AR glass fibre component.

Table 4-10: Cost comparison of different roof coverings available in Sri Lanka

No	Description	Unit	Cost of the covering material	Reference
1	Calicut tile pattern roof covering	Sq.ft	75.00	[7]
2	Asbestos fibre cement corrugated sheet roof covering	Sq.ft	57.00	
3	Zn/Alum (0.47 thick) pattern roof covering	Sq.ft	96.00	
4	Glass fibre reinforced fly ash-cement roof covering	Sq.ft	117.00	This study

4.14 Empirical relationships for the flexural strength of fibre reinforced cement composites

For conditions of equal elastic strain in fibers and matrix, the tensile strength of a composite, σ_c, containing uniaxial continuous fibers can be expressed by the law of mixtures as [55] [83] in equation 18;

$$\sigma_c = \sigma_m V_m + \sigma_f V_f \qquad \text{Eq 18}$$

where $V_f + V_m = 1$

Hence,

$$\sigma_c = \sigma_m \left(1 - V_f\right) + \sigma_f V_f \qquad \text{Eq.19}$$

where σ_m and σ_f is the tensile stresses of the matrix and fibres and V_m and V_f are the volume fractions of the matrix and the fibre.

The critical fibre length, l_c, can be defined as the minimum fibre length required for the build-up of a stress (or load) in the fibre which is equal to its strength (or failure load). From equilibrium considerations, the average tensile stress (σ_f) of the fibre can be written as;

$$\sigma_f = 2\tau \frac{l}{d} \qquad \text{Eq 20}$$

where τ is average interfacial bond stress, "l" and "d" are length and the diameter of the fibre.

It is assumed that the fibres are distributed uniformly and oriented in any direction with equal probability, the effective fibre-volume fraction is 41% of the nominal volume fraction [84]. Thus equation 19 can be re written as;

$$\sigma_c = \sigma_m \left(1 - V_f\right) + 0.41 \sigma_f V_f \qquad \text{Eq 21}$$

From Eq 20 and 21, the equation 22 can be deduced.

$$\sigma_c = \sigma_m \left(1 - V_f\right) + 0.82 \tau V_f \frac{l}{d} \qquad \text{Eq 22}$$

The equation 22 can be rewritten as equation 23 where researchers [[55] [83] [85] [86] [84] [87]] have accepted the empirical relationship between the tensile strength/flexural strength and fibre volume for a composite containing randomly oriented fibers which fail by pull-out as,

$$\sigma_c = A\sigma_m \left(1 - V_f\right) + BV_f \frac{l}{d} \qquad \text{Eq.23}$$

where l/d is the aspect ratio of the fibre and A and B are constants whose values vary depending on the composite.

However some researchers [55] has questioned the validity of the equation 23, since the cracked matrix cannot provide any contribution to strength.

To determine constants A and B, the same equation 23 is converted into Y= mX+C type to come up with the equation as 24 and then a graph has to be plotted against σ_c and V_f. Hence by substituting the values for gradient and intercept for (Equation 25 and 26) obtained after plotting the graph, A and B constants can be determined. However, the relationship is claimed to be applicable for both flexural and indirect tensile strengths of fibre concrete up to fibre aspect ratios of 150 [86] but the l/d ratio of the alkali resistant glass fibre used in this study is 800.

$$\sigma_c = \left(-A\sigma_m + B\frac{l}{d}\right)V_f + A\sigma_m \qquad \text{Eq.24}$$

Thus, the gradient of the graph, $\qquad m = -A\sigma_m + B\frac{l}{d} \qquad$ Eq.25

Intercept of the graph, $\qquad\qquad C = A\sigma_m \qquad\qquad$ Eq.26

However, in this study the above empirical relationship cannot be directly used in predicting the flexural strength of the glass fibre reinforced fly-ash cement roofing tiles beacause (a) the flexural strength values are not in Mpa (b) not having at least three fibre content values to plot the graph (c) σ_m is unknown for unreinforced composites incorporated with the CFA below 75μm and the CFA below 45 μm fractions due to cracking of the composites after casting.

Hence, mortar prisms in the dimensions of 40×40×160 mm were cast incorporating fibre in the percentages of 0% 1%, 2% and 3% with the same water: cement ratio as used to cast glass fibre reinforced fly ash-cement roofing tiles with the unprocessed CFA, the CFA below 75μm and the CFA below 45μm.

Thereby, A and B constants were calculated for each CFA fractions by plotting graphs for each and mathematical relationships were developed. The flexural strength results are tabulated in *Table 4-11*.

Table 4-11: Flexural strength values of glass fibre reinforced fly-ash cement mortar prisms

Sample ID	W/C ratio	CFA fraction	Fibre content, V_f (%)	Flexural strength, σ_c (N/mm^2)	Standard deviation
B	0.46		0	8.9	0.5642
BF1	0.47	The unprocessed	1	9.3	0.4512
BF2	0.49	CFA 30%	2	10.3	0.5514
BF3	0.50		3	12.1	0.6231
C	0.46		0	8.1	0.4489
CF1	0.47	The CFA below	1	8.5	0.4128
CF2	0.49	75 μm 30%	2	10.2	0.5874
CF3	0.50		3	12.2	0.5423
D	0.46		0	7.9	0.3998
DF1	0.47	The CFA below	1	8.2	0.4526
DF2	0.49	45 μm 30%	2	9.7	0.4781
DF3	0.50		3	11.5	0.4432

The graphs plotted against σ_c vs V_f for each CFA fractions and their obtained equations are indicated in Figure *4.18*.

Flexural strength Vs Fibre content of fibre reinforced mortar prisms with 30% of CFA fractions
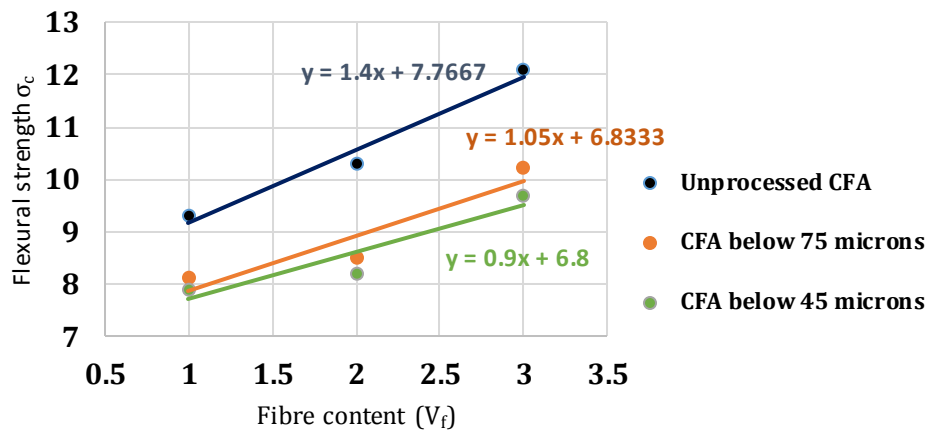
Figure 4.18: Flexural strength Vs Fibre content of mortar prisms with different CFA fractions

The following example elaborates in determining A & B constants for the the unprocessed CFA incorporated mortar prisms.

$y = 1.4x + 7.7667$ Eq 27   (See Figure *4.18*)

$c = 7.7667$ (From Eq *27*)

Since $= A\sigma_m$,

$A = \dfrac{7.7667}{8.9} = \mathbf{0.8727}$ (where σ_m= 8.9 Mpa, See Table *4-11*)

$m = 1.4;$ (From Eq *27*)

Since $m = -A\sigma_m + B\dfrac{l}{d}$

$1.4 = -0.8727 \times 8.9 + B \times 800$ (Where l/d= 800)

$\boldsymbol{B = 0.0115}$

By substituting A & B values for equation 23, the empirical relationship identical for flexural strength of the AR glass fibre reinforced mortar prisms incorporated with the the unprocessed CFA is given by;

$$\sigma_c = 0.8727\sigma_m(1 - V_f) + 0.0115V_f\frac{l}{d} \qquad \text{Eq 28; (where A= 0.8727 and B=0.0115)}$$

Likewise, other identical relationships for the AR glass fibre reinforced mortar prisms incorporated the CFA below 75μm and the CFA below 45μm are given can be given in equation 29 and 30.

For The CFA below 75μm;

$$\sigma_c = 0.8436\sigma_m(1 - V_f) + 0.00985V_f\frac{l}{d} \qquad \text{Eq 29; (where A=0.8436 and B=0.00985)}$$

For The The CFA below 45μm;

$$\sigma_c = 0.8608\sigma_m(1 - V_f) + 0.00963V_f\frac{l}{d} \qquad \text{Eq 30; (where A=0.8608 and B 0.00963)}$$

Essentially, the above equations do not predict the strength of corrugated tiles other than mortar prisms because the equation gives composite strength in Megapascals whereas the strength of the glass fibre reinforced fly ash-cement roofing tiles is defined in Newtons. But A, B constants and l/d ratio will remain the same even for the equation developed for glass fibre reinforced fly ash-cement roofing tiles if the matrix strength (σ_m) in Mpa can be found by experiments.

Since the σ_m in Newton is known for the unreinforced roofing tile consisted of the the unprocessed CFA, an empirical relationship was developed (See equation 31) by trial and error method by taking the same A and B value obtained for the mortar prism contained with the unprocessed CFA. To develop the equation 31, the tile geometry, the strength contribution from the cracked matrix, fibre being used in bundles and the allowable maximum aspect ratio (150) were considered.

$$F_c = \left[AF_m(1 - V_f) + BV_f\frac{l}{d}\left(\frac{L}{150}\right)^2 \right]\left[\frac{34V_f}{150}\frac{l}{d}\right] \qquad \text{Eq 31}$$

Where; $F_c = Composite\ load$; $F_m = Matrix\ load,$ $L = Length\ of\ tile$ and $A\ and\ B\ are\ constants.$

The Eq 31 was validated for the glass fibre reinforced fly ash-cement corrugated tiles incorporated with the the unprocessed CFA. For which A=0.8727, B=0.0115, F_m=930N l/d= 800 and L=470mm

Table 4-12: Validating the empirical relationship for the glass fibre reinforced fly ash-cement roofing tiles with the unprocessed CFA

Fibre percentage (%)	Actual strength (N)	Strength obtained from the empirical relationship (Eq 31) (N)	Variation (%)
1	1450	1459	+0.6%
2	1650	1699	+2.94%

Hence, it can be said that the equation 31 can be used to predict the maximum flexural load of the glass fibre reinforced fly ash-cement roofing tiles incorporated with the the unprocessed CFA with the variation of (+1.77%)

4.15 Chapter summary

Coal fly ash particles has a quite inhomogeneous composition, containing very coarse and very fine particles ranging from 2-200μm levels. The elemental composition descend in the order of Si> Al> Fe> Ca> Mg> K. If these elements were presented in oxide forms, this particular CFA falls into Class F, having combined percentage of SiO_2 +Al_2O_3 +Fe2O3 above 70%.

The examination of the morphology showed that the unprocessed CFA consisted of spheres which could be solid or hollow (cenospheres) and irregular particles. Those spheres could be the cenospheres, magnetic particles, and fine ash (fine improved fly ash residue (<45μm) and coarse improved fly ash residue (>45μm)). The magnetic particles has a high level of Fe_2O_3 and are denser than the parent CFA. Carbon concentrate particles has a high level of organic material and they have a porous structure under SEM magnification. The residual ash fractions; fine improved and coarse improved are both largely amorphous aluminosilicates.

In the sieved fractions, the spherical particle concentration increased in the order of the unprocessed CFA, the CFA below 75μm and the CFA below 45μm and the particle

density increased in the same order (2233, 2455 and 2505 kg/m^3). Unburned carbon percentage also reduced in the same order as 3.6%, 3.4% and 1.8%.

The particle densities of all the CFA components may have contributed to the density of the unprocessed CFA but it can be said that, among them, carbon and coarse improved fly ash residue may have contributed majorly to the overall particle density reduction of the unprocessed CFA.

Highest particle density was observed in the CFA below 45μm fraction which consist of mainly spheres. The increased particle density in the CFA below 45μm fraction could be due to the dense spheres or thick-walled cenospheres or fine improved fly ash residues. The fine improved fly ash residue is denser due to the enrichment of some trace elements.

The lowest particle density was observed in the CFA particles extracted from the wet separation method which is 1805 kg/m^3. That fraction also has an unburned carbon amount of 3.3% and bigger spherical particles. Hence, the low particle densities of unburned carbon and cenospheres may have contributed to the overall particle density reduction in the said fraction.

The larger spherical particle diameter (10-250μm) hints on the cenospheres presence in finer CFA (<45μm) and the CFA particles extracted from the wet separation method. Further, lower ratio of SiO_2/Al_2O_3 gives a hint on the cenospheres presence in the finer CFA fraction (<45μm) and the CFA particles extracted from the wet separation method could be cenospheres.

Further, with the decreasing CFA particle size the strength decreased. In each set of CFA content, the highest flexural strength can be observed in the unprocessed CFA samples and lowest from the samples containing The CFA particles extracted from the wet separation method.

The reasons for strength variation of coal fly ash cementitious composites can be described by three aspects; which are the particle size of CFA, cenospheres content and the Ca content. Accordingly, coal fly ash used in this study, finer CFA did not contribute to the strength development may be due to the low concentration of amorphous silica. The

presence of spheres in the finer fraction (<45μm) and in the CFA particles extracted from the wet separation method which earlier predicted as cenospheres may have contributed to lower the flexural strength. Furthermore, the low Ca content (in finer fractions and the CFA particles extracted from the wet separation method) could be another reason for the strength reduction in the respective composites.

In this study, all the compositions of glass fibre reinforced fly ash-cement roofing tiles complied with the minimum transverse strength requirement of 230 N as specified in the standard SLS 1189 : Part 1: "Specification for concrete roofing semi-sheets, tiles and fittings. Part 1: Requirements" [5]. Highest value was observed in tiles incorporated with the unprocessed CFA and the lowest from tiles incorporated with the CFA below 45μm. The characteristic transverse strength of glass fibre reinforced fly ash-cement roofing tiles is in comparable with Calicut clay tiles (1000-2000N) in Sri Lanka.

The physical properties compared with Calicut clay tiles, asbestos fibre cement corrugated sheet and non-asbestos fibre cement corrugated sheet is shown Table *4-13*.

Table 4-13: Comparison of different roofing materials in Sri Lanka

Roofing Material	Density on oven dry basis (kg/m^3)	Average transverse strength	Water absorption
Calicut clay tile	1790	1.66 (kN)	18%
Asbestos fibre cement corrugated sheet	1645	5.64 (kN/m)	23%
Non asbestos fibre cement corrugated sheet	1582	2.39 (kN/m)	29%
Glass fibre reinforced fly ash-cement roofing tile (The unprocessed CFA 30% + AR-glass fibre 2%)	**1625**	**1.65 (kN)**	**20%**

The density of glass fibre reinforced fly ash-cement roofing tile is comparable with the density of asbestos fibre cement corrugated sheets. The density was ranged in between 1.63-1.68g/cm^3.The lowest average dry density was observed in glass fibre reinforced fly ash-cement roofing tile consisted of unprocessed CFA whereas the density of tiles consisted of CFA below 75μm particle size and CFA below 45μm particle size were closer

in values. The dry density of the glass fibre reinforced fly ash-cement roofing tile is in comparable with the dry density of asbestos fibre cement corrugated sheets ($\approx$1.65g/cm^3).

High water absorption was observed in all the compositions of glass fibre reinforced fly ash-cement roofing tiles which is around 20%. But the water absorption of asbestos fibre cement corrugated sheets and non-asbestos fibre cement corrugated sheets have much higher values which are 23% and 29%, respectively.

Thermal properties were compared with glass fibre reinforced fly ash-cement roofing tiles as shown in Table *4-7* and *Table 4-13*. As per the thermal properties, glass fibre reinforced fly ash-cement roofing tiles can be regarded as a good insulator due to the high specific heat and low thermal conductivity and diffusivity compared with Calicut clay tiles, asbestos fibre cement roofing corrugated sheets and non-asbestos fibre cement corrugated sheets. But clay tiles have this natural system to gradually lower the air temperature through the process of evaporation. Based on the 'bio air-conditioning', the porous surface acts as a heat exchange; it absorbs water from the inside and sends it to the outer surface. On contact with air, the water evaporates. It is important to note that there are other considerations which intervene the indoor thermal comfort in a house which are lapping between tiles/sheets, roof pitch, solar reflectance and thermal emittance. The reduction in thermal conductivity of the glass fibre reinforced fly ash-cement roofing tiles by means of CFA is probably related to the, the lower particle density, partly to the amorphous structure of CFA & AR glass fibres and due to the presence of cenospheres in CFA.

The long term durability of glass fibre reinforced fly ash-cement roofing tiles is satisfied. Considerable amount of leaching heavy metals from the tile was not observed.

Hence, glass fibre reinforced fly ash-cement roofing tiles is promising substitute for asbestos fibre cement roofing sheets in terms of transverse strength, density, water absorption, thermal properties and durability. However, the production cost of tiles can be reduced by lowering the AR glass fibre incorporation.

5 CONCLUSIONS

The following conclusions can be drawn from this research:

- All the compositions of glass fibre reinforced fly ash-cement (GFFC) roofing tiles complied with the transverse strength requirements (230 N) as specified in the standard SLS 1189 Part 2. Highest value was observed in tile including 2% AR fibres with the unprocessed CFA (1650 N) and the lowest from tile incorporated with the CFA below 45µm (1470 N). The characteristic transverse strengths of GFFC roofing tiles is in comparable with Calicut clay tiles (1000-2000N) in Sri Lanka.

- The water absorption of GFFC roofing tiles did not comply with the requirement (maximum 10%) whereas the observed maximum value was 20%. Nevertheless, asbestos and non-asbestos roofing sheets have much higher values which are 23% and 29%, respectively.

- The dry density of GFFC roofing tiles (1.63-1.68 g/cm3) is comparable with the dry density of asbestos sheet which is ≈1.65 g/cm3

- GFFC roofing tiles can be considered as a good thermal insulator due to the high specific heat (1296 J/kg.K), low thermal (0.278 W/m.K) conductivity and diffusivity (1.31×10-7 m2/s) compared with the asbestos, non-asbestos roofing sheets and Calicut clay tiles.

- The long term durability of glass fibre reinforced fly ash-cement roofing tiles is satisfied.

- Hence, the glass fibre reinforced fly ash-cement roofing tile is promising substitute for asbestos fibre cement roofing sheets in terms of transverse strength, density, water absorption, thermal properties and durability.

- GFFC roofing tile is a promising roofing material by the incorporation of CFA in both unprocessed and sieved form due to the comparable physical and mechanical properties with Calicut clay tile, asbestos fibre cement corrugates sheets and non-asbestos fibre cement corrugated sheets.

- The lowest particle density CFA fraction was obtained from the wet separation method indicating that it consisted of higher amount of cenospheres. The highest density was observed in the finest CFA fraction (<45µm) assuming that it consisted of solid or thick walled cenosphers or fine improved fly ash residues.

- The particle densities of all the CFA components may have contributed to the density of the unprocessed CFA but it can be said that, among them, carbon and coarse improved fly ash residue may have contributed majorly to the overall particle density reduction of the unprocessed CFA.

- The lowest strength was observed in the composites consisted of particles extracted from wet separation method so the strength reduction could be due to the higher cenospheres content. The finest CFA fraction ($<45\mu m$) has also delivered low strength. It could be due to the inherent property of the particular CFA where finer CFA does not contribute to the strength development or the presence of cenospheres.

6 RECOMMENDATIONS

- In order to come up with a more general correlation (on CFA produced out from Lakvijaya thermal power plant, Norochcholei, Sri Lanka) between the CFA particle size and strength behavior, different CFA samples have to be taken from the power plant , followed by size fraction, characterization and strength testing

- It is essential to experiment in which CFA particle size range the cenospheres concentration is higher in CFA available at Lakvijaya power plant, Sri Lanka which can be used to develop more thermally insulating and lightweight cement based products. For that, considerable amount of cenospheres needed to be extracted from wet separation/or dry separation method followed by particle size analysis, morphological analysis and chemical composition.

- The water: cement ratio can be further reduced (than 0.49) by using proper admixtures (eg: super plasticizers) and the cement content can be further replaced by introducing ultra-fine crushed rock particles

- Cost can be reduced by further reduced by lowering the AR glass fibre content.

- Pressing technique is recommended to cast roofing materials to get a homogeneous product.

- Use of suitable additives into the mix could further reduce the water absorption of the glass fibre reinforced fly ash-cement roofing materials.

REFERENCES

[1] FCPMA, Fibre Cement Products Manufacturers Association, "ශ්‍රී ලන්කාවේ ක්‍රිසෝටයිල් ෆයිබර් කර්මාන්තය පිළිබඳ විශ්ලේෂණය".

[2] "Steps to Ban Import of Asbestos Roofing Sheets by 2018," 2015. [Online]. Available: http://www.president.gov.lk/steps-to-ban-import-of-asbestos-roofing-sheets-by-2018/.

[3] F. C. P. M. A. FCPMA, Interviewee, *Meeting on Asbestos-Cement Roofing Sheet Industry held at National Building Research Organisation.* [Interview]. 21 October 2015.

[4] C. Jayasinghe, M.H.P.J De Silva, D.M.M.P Dissanayake and C.T.K.I Fernando, "Engineering Properties of Micro Concrete Roofing Tiles," in *Transactions 2006 Technical Papers The Institution of Engineers Sri Lanka*, Colombo, 2006.

[5] SLS 1189 : Part1: Specification for concrete roofing semi-sheets, tiles and fittings.Part 1: Requirements, SLSI, 1999.

[6] SLS 1189:Part 2: Specification for concrete roofing semi-sheets, tiles and fittings-Test Methods, SLSI, 1999.

[7] J. Chrishanthi, Interviewee, *Manufacturing of cement sand roofing tiles.* [Interview]. 5 10 2016.

[8] A. TAYAL, "A PROCESS FOR THE MANUFACTURE OF ASBESTOS FIBRE CEMENT AND FLYASH PRODUCTS". NEW DELHI, INDIA. Patent 212644, 10 December 2007.

[9] JAGADESH SUNKU, "ADVANTAGES OF USING FLY ASH AS SUPPLEMENTARY CEMENTING MATERIAL (SCM) IN FIBRE CEMENT SHEETS," in *10th international inorganic-bonded fibre composites conference*, São Paulo, 2006.

[10] BUREAU OF INDIAN STANDARDS, IS 459:1992 Corrugated and semi-corrugated asbestos cement sheets-specification, 1992.

[11] Bureau of Indian Standards, IS 5913:1989 Asbestos Cement Products - Methods of Test, Bureau of Indian Standards (BIS), 1989.

[12] Sarthak Kuila, "http://www.devalt.org/," [Online]. Available: http://www.devalt.org/newsletter/may12/of_3.htm. [Accessed 16 04 2017].

[13] G. Ramakrishna, T. Sundararajan and S. Kothandaraman, "STRENGTH OF CORRUGATIONS OF A ROOFING SHEETS REINFORCED WITH SISAL FIBRES," *ARPN Journal of Engineering and Applied Sciences,* vol. 6, no. 12, 2011.

[14] Pardon K. Kuipa, Cledwyn T. Mangunda,Olga Kuipa,Admire Chawatama, "Use of Pulverised Fuel Ash in the Manufacture of Concrete Roofing Tiles," *International Journal of ChemTech Research,* vol. 8, no. 3, pp. 1019-1025, 2015.

[15] M. Thomas, R. Jewell, R. Jones, "Coal fly ash as a pozzolan," in *Coal Combustion Products (CCP's)*, Elsevier Ltd, 2017, pp. 121-154.

[16] ROBERT BLISSETT, "COAL FLY ASH AND THE CIRCULAR ECONOMY," Birmingham, 2015.

[17] Annie S. Shoumkova, Tsenka I. Tsacheva, Valeria B. Stoyanova, Ivan N. Grancharov, Miko V. Marinov, "Physico-chemical and morphological properties of

coal fly ash from "Bobovdol" power plant,Bulgaria," *Ecology 2004, Scientific Articles,* 2004.

[18] M. Ahmaruzzaman, "A review on the utilization of fly ash," *Progress in Energy and Combustion Science,* vol. 36, p. 327–363, 2010.

[19] R.S. Blissett, N.A. Rowson, "A review of the multi-component utilisation of coal fly ash," *Fuel,* vol. 97, p. 1–23, 2012.

[20] V.M Malhottra, A.A Ramezanianpour, Fly ash in concrete, CANMET, 1985.

[21] ASTM International, ASTM C618 - 17a Standard Specification for Coal Fly Ash and Raw or Calcined Natural Pozzolan for Use in Concrete, ASTM International, 2017.

[22] Z.T. Yao, X.S. Ji, P.K. Sarker, J.H. Tang, L.Q. Ge, M.S. Xia, Y.Q. Xi, "A comprehensive review on the applications of coal fly ash," *Earth-Science Reviews,* vol. 141, p. 105–121, 2015.

[23] Mehta, P.K., "Testing and correlation of fly ash properties with respect to pozzolanic behavior," 1984.

[24] J.C. Hower, K.R. Henke, S. Dai, C.R. Ward, D. French, "Generation and nature of coal fly," in *Coal Combustion Products (CCP's)*, Elsevier Ltd., 2017, pp. 21-65.

[25] SLSI, SLS 107: Part 2 Specification for Ordinary Portland Cement: Test Methods, Sri Lanka Standards Institution.

[26] ASTM International, ASTM C204 - 17 Standard Test Methods for Fineness of Hydraulic Cement by Air-Permeability Apparatus, ASTM International, 2017.

[27] ASTM C188:Standard Test Method for Density of Hydraulic Cement, ASTM International, 2016.

[28] P.K. Kolay, D.N. Singh, "Physical, chemical, mineralogical, and thermal properties of cenospheres from an ash lagoon," *Cement and Concrete Research,* vol. 31, pp. 539-542, 2001.

[29] I. Acar, M.U. Atalay, "Recovery potentials of cenospheres from bituminous coal fly ashes," *Fuel,* vol. 180, pp. 97-105, 2016.

[30] Navid Ranjbar, Carsten Kuenzel, "Cenospheres: A review," *Fuel,* vol. 207, pp. 1-12, 2017.

[31] Asad Hanif, Zeyu Lu, Zongjin Li, "Utilization of fly ash cenosphere as lightweight filler in cement-based composites – A review," *Construction and Building Materials,* vol. 144, p. 373–384, 2017.

[32] Maciej Zyrkowski, Rui Costa Neto, Luis F. Santos, Karol Witkowski, "Characterization of fly-ash cenospheres from coal-fired power plant unit," *Fuel,* vol. 174, pp. 49-53, 2016.

[33] Nikhil Barbare, Arun Shukla, Arijit Bosea, "Uptake and loss of water in a cenosphere–concrete composite material," *Cement and Concrete Research,* vol. 33, p. 1681–1686, 2003.

[34] Joseph. K. V, Finjin Francis, Joyson Chacko, P.Das And G. Hebbar, "Fly Ash Cenosphere Waste Formation In Coal Fired Power Plants And Its Applicationas A Structural Material- A Review," *International Journal of Engineering Research & Technology (IJERT),* vol. 2, no. 8, 2013.

[35] Yong Huang, Rong Zhao, Jun Jiang, Ke-Yong Zhu, "Scattering and absorptive characteristics of a cenosphere," *International Journal of Thermal Sciences,* vol. 57, pp. 63-70, 2012.

[36] Prabir K. Kolay , Sudha Bhusal, "Recovery of hollow spherical particles with two different densities from coal fly ash and their characterization," *Fuel,* vol. 117, p. 118–124, 2014.

[37] Ling-ngee Ngu,Hongwei Wu ,Dong-ke Zhang, "Characterization of Ash Cenospheres in Fly Ash from Australian Power Stations," *Fuel,* vol. 21, no. 6, 2007.

[38] F. Blanco, P. Garcia, P. Mateos, J. Ayala, "Characteristics and properties of lightweight concrete manufactured with cenospheres," *Cement and Concrete Research,* vol. 30, pp. 1715-1722, 2000.

[39] "Physiochemical and engineering characteristics of cenosphere and its application as a lightweight construction material- A review".

[40] Yunpeng Wu, Jun-Yan Wang, Paulo J.M. Monteiro, Min-Hong Zhang, "Development of ultra-lightweight cement composites with low thermal conductivity and high specific strength for energy efficient buildings," *Construction and Building Materials,* vol. 87, p. 100–112, 2015.

[41] L.M.Manocha, K.A.Ram, S.M. Manocha, "Separation of Cenospheres from Fly Ashes by Floatation Method," *Eurasian ChemTech Journal,* vol. 13, pp. 89-95, 2011.

[42] Sarbajit Ghosal and Sidney A. Self, "Particle size-density relation and cenosphere content of coal fly ash," *Fuel,* vol. 74, pp. 522-529, 1995.

[43] Piotr Długosz, Paweł Darlak, Robert M. Purgert, Jerzy J. Sobczak, "SYNTHESIS OF LIGHT COMPOSITES REINFORCED WITH CENOSPHERES," *Composites,* vol. 11, no. 4, pp. 288-293, 2011.

[44] Tsuyoshi Hirajima, H.T.B.M. Petrus, Yuji Oosako, Moriyasu Nonaka, Keiko Sasaki, Takashi Ando, "Recovery of cenospheres from coal fly ash using a dry separation process: Separation estimation and potential application," *International Journal of Mineral Processing,* vol. 95, p. 18–24, 2010.

[45] Jun-Yan Wang, Yi Yang, Jat-Yuen Richard Liew, Min-Hong Zhang, "Method to determine mixture proportions of workable ultra lightweight cement composites to achieve target unit weights," *Cement & Concrete Composites,* vol. 53, pp. 178-186, 2014.

[46] Xuemei Liu, Min-Hong Zhang, Kok Seng Chia, Jiabao Yan, J.Y. Richard Liew, "Mechanical Properties of Ultra-lightweight Cement Composite at Low Temperatures of 0-to -60 oC," *Cement and Concrete Composites,* 2016.

[47] Asad Hanif, Zeyu Lu, Ming Sun, Pavithra Parthasarathy, Zongjin Li, "Green lightweight ferrocement incorporating fly ash cenosphere based fibrous mortar matrix," *Journal of Cleaner Production,* vol. 159, pp. 326-335, 2017.

[48] Xiaoyan Huang, Ravi Ranade, Qian Zhang, Wen Ni, Victor C. Li, "Mechanical and thermal properties of green lightweight engineered cementitious composites," *Construction and Building Materials,* vol. 48, p. 954–960, 2013.

[49] K. Senthamarai Kannan, L. Andal, and M. Shanmugasundaram, "An Investigation on Strength Development of Cement with Cenosphere and Silica Fume as Pozzolanic Replacement," *Advances in Materials Science and Engineering,* 2016.

[50] Asad Hanif, Zeyu Lu, Su Diao, Xiaohui Zeng, Zongjin Li, "Properties investigation of fiber reinforced cement-based composites incorporating cenosphere fillers," *Construction and Building Materials,* vol. 140, pp. 139-149, 2017.

[51] Miroslawa Losiewicz, t David P. Halsey, S. John Dews, Paul Olomaiye, Frank C. Harris, "An investigation into the properties of micro-sphere insulating concrete," *Construction and Building Materials,* vol. 10, pp. 583-588, 1996.

[52] BS 1377-Part 2:Methods of test for Soils for civil engineering purposes, BSI, 1990.

[53] BS EN 450-1: Fly ash for concrete. Definition, specifications,and conformity criteria., BSI, 2012.

[54] SLS 1144:Part 2:1996 Specification for Ready-Mixed Concrete Part 2: Test Methods, SLSI, 1996.

[55] Arnon Bentur, Sidney Mindess, Fibre Reinforced Cementitious Composites, E & FN Spon, 1990.

[56] ASTM C948-81 : Standard Test Method for Dry and Wet Bulk Density, Water Absorption, and Apparent Porosity of Thin Sections of Glass-Fiber Reinforced Concrete 1, 2009.

[57] ISO 10904:2011 (E): Fibre-cement corrugated sheets and fittings for roofing and cladding, 2011.

[58] William D. Callister, Jr.David G. Rethwisch, Materials Science and Engineering An Introduction, John Wiley & Sons, Inc., 2013.

[59] Sandra G. Lingbawan, "Thermal Properties of Fly Ash Bricks," 2009.

[60] Method 1311: Toxicity Characteristic Leaching Procedure, part of Test Methods for Evaluating Solid Waste, Physical/Chemical Methods, United States Environmental Protection Agency.

[61] International Organization for Standardization, ISO 2602:1980, Statistical interpretation of test results - Estimation of the mean - Confidence interval, ISO, 1980.

[62] SLS 2:1975 Specification for Clay Roofing Tiles, Sri Lanka Standard Institution, 1975.

[63] SLS 9:Part 2:2001 Specification for Asbestos-Cement Products;Part 2:Corrugated Sheets, Sri Lanka Standard Institution, 2001.

[64] Mohammed Aboustait, Taehwan Kim, M. Tyler Ley, Jeffrey M. Davis, "Physical and chemical characteristics of fly ash using automated scanning electron microscopy," *Construction and Building Materials,* vol. 106, pp. 1-10, 2016.

[65] Amir Fauzia, Muhd Fadhil Nuruddin, Ahmad B. Malkawi, Mohd Mustafa Al Bakri Abdullah, "Study of Fly Ash Characterization as a Cementitious Material," *Procedia Engineering,* vol. 148, pp. 487-493, 2016.

[66] Jianglong Yu, Xianchun Lib, David Fleming, Zhaoquan Meng,Dongmei Wangb, Arash Tahmasebi, "Analysis on Characteristics of Fly Ash from Coal Fired Power Stations," *Energy Procedia,* vol. 17, pp. 3-9, 2012.

[67] Stanislav V. Vassilev , Christina G. Vassileva, "Mineralogy of combustion wastes from coal-fired power stations," *Fuel Processing Technology,* vol. 47, pp. 261-280, 1996.

[68] James C. Hower, John G. Groppo, Uschi M. Graham, Colin R.Ward, Irena J. Kostova, Mercedes M. Maroto-Valer, Shifeng Dai, "Coal-derived unburned carbons in fly ash: A review," *International Journal of Coal Geology,* 2017.

[69] K. Erdoğdu, and P. Türker, "EFFECTS OF FLY ASH PARTICLE SIZE ON STRENGTH OF PORTLAND CEMENT FLY ASH MORTARS," vol. 28, pp. 1217–1222,, 1998.

[70] Kelly A, Strong solids, Oxford Clarendon Press, Oxford, 1966.

[71] C. Leiva, C. Arenas, L.F. Vilches, B. Alonso-Fariñas, M. Rodriguez-Galán, "Development of fly ash boards with thermal, acoustic and fire insulation properties," *Waste Management,* 2015.

[72] Noureddine Benichoun and Mohamed A. Sultan, "Thermal properties of lightweight-framed construction components at elevated temperatures," *FIRE AND MATERIAL,* p. 165–179, 05 January 2005.

[73] Ramazan Demirbog and Rustem Gul, "The effects of expanded perlite aggregate, silica fume and fly ash on the thermal conductivity of lightweight concrete," *Cement and Concrete Research,* vol. 33, p. 723–727, 2003.

[74] Matthew C. Wingert, Jianlin Zheng, Soonshin Kwon,Renkun Chen, "Thermal Transport in Amorphous Materials: A Review," *Semiconductor Science and Technology,* 2016.

[75] FIGEN BALO, AYNUR UCAR, HALIT LÜTFI YÜCEL, "DEVELOPMENT OF THE INSULATION MATERIALS FROM COAL FLY ASH, PERLITE, CLAY AND LINSEED OIL," *Ceramics,* pp. 182-191, 2010.

[76] Vishnu, G.Manavendra, "Experimental Investigation on Thermal Properties of Fly Ash Reinforced Epoxy Composite," *International Journal of Innovative Research in Science,Engineering and Technology,* vol. 5, no. 12, pp. 20723-20729, 2016.

[77] Pratik Shetty, Vinay Atgur, Manavendra.G, Padmayya Naik, "Experimental Evaluation of Specific Heat Carrying Capacity of Fly-ash Reinforced Aluminium 6061 Composite," *International Research Journal of Engineering and Technology,* vol. 2, no. 9, pp. 774-780, Dec 2015.

[78] Narrative Content Group, "Natural air conditioner cools with the power of terracotta and evaporation," 23 May 2018. [Online]. Available: https://www.treehugger.com/sustainable-product-design/natural-air-conditioner-terracotta-thibault-faverie.html. [Accessed 28 June 2019].

[79] Andrew Hunt, *Sustainable Green Building with Clay and Concrete Roof Tile,* 2015.

[80] USA gov, "Ground Water and Drinking Water.National Primary Drinking Water Regulations," [Online]. Available: https://www.epa.gov/ground-water-and-drinking-water/national-primary-drinking-water-regulations. [Accessed 23 04 2017].

[81] MICHAEL S. MAMLOUK , JOHN P. ZANIEWSKI, MATERIALS FOR CIVIL AND CONSTRUCTION ENGINEERS, THIRD EDITION, PEARSON, 2011, pp. 215-2016.

[82] Mònica Ardanuy, Josep Claramunt, Romildo Dias Toledo Filho, "Cellulosic fiber reinforced cement-based composites: A review of recent research," *Construction and Building Materials,* vol. 79, p. 115–128, 2015.

[83] R. N. Swamy and P. S. Mangat, "A THEORY FOR THE FLEXURAL STRENGTH OF STEEL FIBER REINFORCED CONCRETE," *CEMENT and CONCRETE RESEARCH,* vol. 4, pp. 313-325, 1974.

[84] Y. W. MAI, "Strength and fracture properties of asbestos-cement mortar composites," *JOURNAL OF MATERIALS SCIENCE,* vol. 14, pp. 2091--2102, 1974.

[85] Mohammed Razavi Nouri, Jalil Morshedian, "Tensile and flexural behaviour of fibre reinforced cementitious composites," *Iranian journal of polymer science and technology,* vol. 4, no. 1, pp. 56-63, 1995.

[86] A.J Majumdar, "Fibre cement and concrete-a review," in *Composites*, 1975, pp. 7-16.

[87] R. Ganeshalingam,P. Paramasivam and G. K. Nathan, "An evaluation of theories and a design method of fibre cement composites," *The International Journal of Cement Composites and Lightweight Concrete,* vol. 3, no. 2, May 1981.

[88] Chia KS, Zhang MH, Liew JYR, "High-strength ultra lightweight cement composite - material properties.," in *9th International Symposium on High Performance Concrete design, Verification and Utilization.*, 2011.

[89] Stanislav V. Vassilev,Christina G. Vassileva, "A new approach for the classification of coal fly ashes based on their origin, composition, properties, and behaviour," *Fuel,* vol. 86, no. 10-11, p. 1490–1512, 2007.

[90] BS EN 451-2:Method of testing fly ash. Determination of fineness by wet sieving, BSI, 1995.

[91] H.T.B.M. Petrus, Tsuyoshi Hirajima, Yuji Oosako, Moriyasu Nonaka, Keiko Sasaki, Takashi Ando, "Performance of dry-separation processes in the recovery of

cenospheres from fly ash and their implementation in a recovery unit," *International Journal of Mineral Processing,* vol. 95, pp. 15-23, 2011.

[92] J. Orlowsky, M. Raupach, H. Cuypers and J. Wastiels, "Durability modelling of glass fibre reinforcement in cementitious environment," *Materials and Structures,* pp. 155-162, March 2005.

[93] Kung Lo-shu, Su Man-qing, Shi Xing-sheng,Li Yun-xiu, "Research on several physico-mechanical properties of lightweight aggragte concrete," *The International Journal of Lightweight Concrete,* vol. 2, December 1980.

[94] "Concrete change: Making cement carbon-negative," GreenBiz Group Inc, 06 12 2018. [Online]. Available: https://www.greenbiz.com/article/concrete-change-making-cement-carbon-negative. [Accessed 27 12 2018].

[95] Barbara Lothenbach, Karen Scrivener, R.D. Hooton, "Supplementary cementitious materials," *Cement and Concrete Research,* vol. 41, p. 1244–1256, 2011.

[96] M. Mercedes Maroto-Valer,Darrell N. Taulbee, and James C. Hower, "Novel Separation of the Differing Forms of Unburned Carbon Present in Fly Ash Using Density Gradient Centrifugation," *Energy & Fuels,* vol. 13, pp. 947-953, 1999.